1

From Anion Recognition to Organocatalytic Chemical Reactions

Friedemann Dressler and Peter R. Schreiner

Justus Liebig University, Institute of Organic Chemistry, Heinrich-Buff-Ring 17, 35392 Giessen, Germany

1.1 Introduction and Background

Non-covalent organocatalysis [1–14] utilizes small organic molecules for the activation of substrates through hydrogen bonding ("*partial protonation*") to neutral or negatively charged (*anion-binding*) electron lone pairs. This catalytic concept mimics nature where non-covalent interactions (NCIs) are ubiquitous and essential for many processes essential to life [15], e.g., through catalyzing many biochemical reactions [16–18]. NCIs empower enzymes with the high selectivity in substrate recognition, activation, and the stereocontrol in biotransformations [19]. The reason why nature uses these bonding types in catalytic systems such as ribonucleases, antibodies, and enzymes is that the binding (recognition) of the substrates is associated with small changes in Gibbs free energies [20]. Crystal structure analyses, spectroscopic investigations [21, 22], and computational studies [23, 24] reveal that enzymes typically do not contain strong Lewis acidic sites [25, 26]. Binding to electron-deficient metal ions, which would be the obvious alternative for catalyzing chemical reactions, would result in strong enthalpic binding [1]. Copper, iron, or zinc ions in enzymes are considered "soft" in the Pearson HSAB sense, and they are embedded in large and polarizable structures, e.g., in carbonic anhydrase [27]. The recognition processes and the details of enzyme catalysis are difficult to deconvolute because there are multiple interactions, and each of them are necessary for high selectivity and high reactivity [15, 20, 28–31]. The dominant parts of these interactions are hydrogen bonding [32–37] and anion binding [38, 39], but also, NCIs such as aromatic π–π stacking [40, 41], van der Waals [42, 43], and dipole–dipole interactions [44, 45] are included in the enzyme's active site. Scheme 1.1 depicts four examples of enzymes using either hydrogen bonding or anion binding for substrate activation and reaction initiation in their active sites. Epoxide hydrolase (**1**) activates an epoxide for a nucleophilic opening reaction *via* double hydrogen bonding [46–48] similar to haloalcohol dehalogenase (**2**) that activates the same species for reversible ring opening with chloride [49]. Formate dehydrogenase (**3**) promotes the oxidation of formate, which binds *via* the

Anion-Binding Catalysis, First Edition. Edited by Olga García Mancheño.

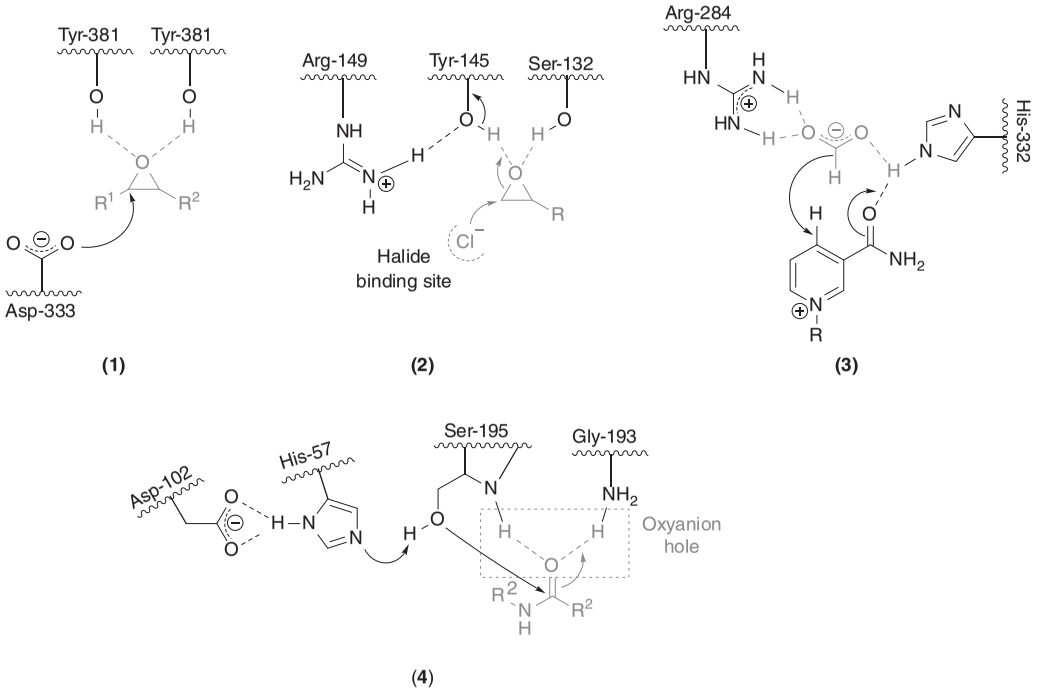

Scheme 1.1 Enzyme active sites utilizing either hydrogen bonding or anion binding for substrate recognition and activation: Epoxide hydrolase (**1**), halo alcohol dehydrogenase (**2**), format dehydrogenase (**3**), and serine protease (**4**).

guanidine function of an arginine residue [28, 50]. Serine protease (**4**) is an excellent example of multifunctional activation for the cleavage of amides. The protease binds the amide utilizing double hydrogen bonding, while at the same time, the imidazole moiety of a histidine moiety activates in concert with a carboxylic acid function of an aspartic acid motif, the hydroxy function of a serine, which cleaves the amide [51].

These examples show that (double) hydrogen bonding and anion binding in enzymes are very closely related. Catalysis by hydrogen-bonding enzymes shows no apparent product inhibition [52] but high turnover frequencies (TOFs), e.g., acetylcholinesterase with TOF = 25 000 s^{-1} [53], while operating in water and under aerobic conditions [54, 55]. These characteristics offer attractive perspectives for the development of metal-free artificial enzyme moieties [56], the so-called "*synzymes*" [57–61], which represent an alternative to traditional metal(-ion)-containing catalysts that are often toxic and sensitive to moisture and air [62]. *Synzymes* designed on the basis of Pauling's [63, 64] and related paradigms [26, 65] have the goal of imitating the complete enzyme architecture with its structurally complex protein backbone and active site(s). This design strategy leads to reaction mechanisms that follow general acid catalysis [44, 66–68] and Michaelis–Menten kinetics [69, 70] comparable to natural enzymes. The structural design of *small-molecule catalysts* such as (non)-covalent organocatalysts, however, builds on the idea that only the active site of an enzyme will be mimicked, resulting in small organic molecules with a minimum of complexity [28, 71] such as *explicit double hydrogen-bonding* and *anion-binding catalysts*. Scheme 1.2 depicts the reduction of nitro-olefins utilizing either enzyme catalysis (**5**) or organocatalysis (**6**). Enzymes from baker's yeast or the Old Yellow Enzyme (OYE) [72], which was termed a nitroalkene reductase, efficiently catalyze the NADPH-linked olefin reduction through activation of the nitroalkene by hydrogen bonding to His-191 and Asn-194. The hydride transfer to the β-position occurs from reduced flavin generated with NADPH, followed by proton transfer from the Tyr-196 hydroxyl to the α-position [73–75]. Zhang and Schreiner adapted this complex enzymatic arrangement to a simple organocatalytic system and utilized a thiourea moiety for nitro-olefin activation through hydrogen bonding and a Hantzsch ester as an NADPH analog.

The long success story of anion-binding chemistry using hydrogen bonding apparently started in 1940 when Bartlett and Dauben observed an increased acid

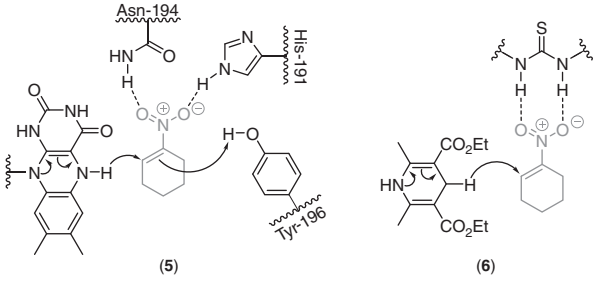

Scheme 1.2 Proposed models for the reduction of nitroalkenes utilizing enzyme catalysis (**5**) and the adapted thiourea-catalyzed biomimetic reduction (**6**).

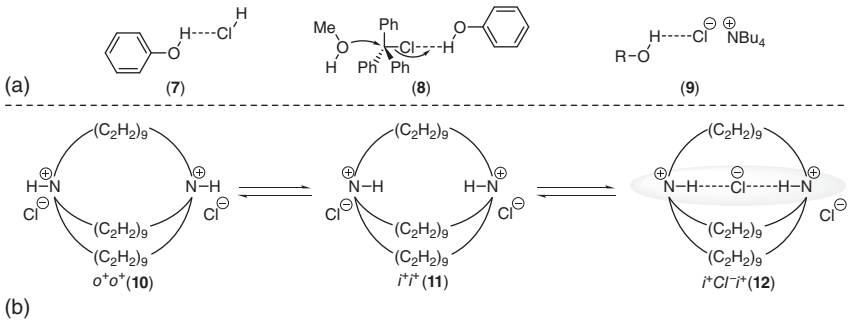

Scheme 1.3 (a) First examples of anion binding through hydrogen bonding and (b) isomerization of the first cage compound diazabicyclo[9.9.9]nonacosane dihydrochloride and the corresponding cage structure (**12**).

strength of hydrogen chloride in dioxane by the addition of alcohols [76]. They interpreted this by a hydrogen bond of the hydroxy function of the alcohols to the chlorine of hydrogen chloride (**7**) as depicted in Scheme 1.3 and found a correlation between the ability to form a hydrogen bond and the acid strength of phenol derivatives, except for ortho-substituted phenols that preferentially form intramolecular hydrogen bonds. In 1948, Swain investigated the kinetics of the S_N1 reaction of trityl chloride and alcohols in benzene with an excess of pyridine [77]. When methanol was used as the nucleophile, he found first-order kinetics for trityl chloride and second-order kinetics for methanol; the same result was obtained using phenol as the nucleophile, but the reaction was slower. When Swain used a 1 : 1 mixture of methanol and phenol as nucleophiles, the methyl ether formed seven times faster than the sum of the individual reaction rates, with first order in relation to trityl chloride, methanol, and phenol (**8**). Furthermore, only the methyl ether formed. He postulated a mechanism where one hydroxy group binds to the chloride *via* hydrogen bonding, thereby weakening the carbon–chlorine bond. Simultaneously, the second alcohol solvates the incipient carbocation. The reason why only methyl ether forms is the higher Brønsted acidity of phenol, causing a stronger hydrogen bond to chloride. These two examples derive from a strong intermolecular hydrogen bond to the *in situ* formed halide, even though the term "anion-binding" was not used. In 1958, Lund introduced the term "*hydrogen-bonding to an anion*" when he investigated the effect of quaternary ammonia halides on the O–H stretching frequency of various alcohols such as ethanol, phenol, and 2,2,2-trichloroethanol (**9**) [78]. He observed that Brønsted acidity and the strength of anion binding did not correlate and proposed to use Lewis acidity instead. Bufalini and Stern confirmed Lund's work and described the "*hydrogen bond formation to an anion*" as a solvation process [79]. In addition, they calculated the "*solvation enthalpy*" for the $n\mathrm{Bu}_4\mathrm{Br}$–MeOH system as $\Delta H = -6.7\,\mathrm{kcal\,mol^{-1}}$ in good agreement with the accepted value of $\sim 5\,\mathrm{kcal\,mol^{-1}}$ for the formation of the hydrogen bond in the water dimer [80, 81]. The determined entropy change of $\Delta S = -14.0\,\mathrm{cal\,K^{-1}\,mol^{-1}}$ matches the reported value of $\Delta S = -13.6\,\mathrm{cal\,K^{-1}\,mol^{-1}}$ closely [81]. In 1963, Schleyer and Allerhand investigated covalent and ionic halides as proton acceptors

in hydrogen-bonding complexes *via* IR spectroscopy [82]. They used butyl halides and $HgCl_2$ as covalent halides and observed small shifts of the O–H stretching frequencies of methanol and phenol as covalent halides are weak proton acceptors. However, quaternary ammonium halides are much better proton acceptors and lead to a larger hydrogen-bonding frequency shift. In addition, they observed that the magnitudes of these shifts significantly depend on extent on the halide anion, in the order $Cl^- > F^- > Br^- > I^-$; when ionic halides were used, for covalent halides, the order was $F^- < Cl^- < Br^- < I^-$, but in total much smaller. The variation of the cations made little difference for bromine and iodide but had a much bigger influence for chlorine. This effect was not investigated for fluoride because the synthesis of quaternary fluorides was laborious and only a few derivatives were described in the literature at that time. In 1968, Simmons and Park described a series of bridged macrobicyclic diamines **10** [83–85]. First, they investigated the *in–out*-isomerization of the bis-hydrochlorides and found that alkyl chains with even numbers of carbon atoms favor the *in–in*- and those with odd numbers the *out–out*-conformation. By treating diazabicyclo[9.9.9]nonacosane with HCl, the authors obtained crystals, which revealed the presence of only the *katapinate* (**12**) in the ^{1}H NMR (Scheme 1.3). A similar behavior was observed with HBr, which was less favorable than HCl; however, with iodide, no encapsulation in the cavity was observed. Simmons and Park also treated diazabicyclo[10.10.10]triacontane with NaCl in 50% aqueous trifluoroacetate and observed a high field shift of the α-CH_2 protons in the ^{1}H NMR, which indicated the formation of the in^+–Cl^-–in^+ conformer. Similar results were obtained using bromide and iodide salts. The authors concluded that the size of the cavity is an important factor in halide "*katapinosis*." A few years later, Marsh and coworkers confirmed the structure of the host–guest complex by X-ray single-crystal analysis [86].

The work of Simmons and Park arguably marks the beginning of the supramolecular chemistry of artificial organic host molecules with anions as guest molecules [87–90]. In the following years, the field of supramolecular anion recognition was applied to anion sensing [89, 91–94], extraction [95–97], anion transport [98–105], and self-assembling of molecular capsules [106–109]. Nevertheless, despite the large number of publications in the field of supramolecular chemistry, the selectivity of the host molecules for a given anion species was limited to a few examples. In the last years, especially "fluoride-only" receptors appeared, often containing boron because of its high affinity to fluoride [87, 110–112]. "Halide-only" hosts were also developed [113], but the differentiation between chloride and bromide is still a challenge [114]. The development of anion-binding (recognition) organocatalysts and their application in synthetic organic chemistry emerged from supramolecular chemistry and goes hand in hand with the introduction and improvement of explicit double hydrogen-bonding catalysts [1, 2]. Both catalysis types emerged at about the same time, and the mode of action is also similar: The catalyst coordinates and activates either a neutral substrate (hydrogen-bonding catalysis) or an anion substrate (anion-binding catalysis). This indicates that many hydrogen-bonding catalysts can also be used as anion-binding catalysts and vice versa, and so the anion-binding catalyst story cannot be told without the story of the double hydrogen-bonding catalyst

(Scheme 1.4). Hydrogen-bonding interactions have been known since the fundamental works of Errera and Mollet in 1936 [118], and, in particular, Wolf, Prahm, and Harms in 1937 [119]. Errera and Mollet measured the IR spectra of ethanol solutions in carbon tetrachloride (0.1 M) at different temperatures and observed a band at 3640 cm^{-1} (56% absorption) and a large band at 3350 cm^{-1} (94% absorption) at 0 °C [118]. At 70 °C, the authors observed the band at 3640 cm^{-1} with increased absorption (64%), whereas the band at 3350 cm^{-1} decreased to a low percentage. Errera and Mollet described the band at 3640 cm^{-1} as the O–H stretching vibration of "*isolated alcohol molecules*," and in contrast, the band at 3350 cm^{-1} "*to intermolecular actions, for example, the hydrogen atom of one molecule vibrating with the oxygen atom belonging to another one (hydrogen-bond, as interpreted by Sidgwick*) [120]." Wolf, Prahm, and Harms examined the mixing heat, density, dissociation, and solvation energy of various solvent mixtures of aliphatic alcohols (methanol, ethanol, and propanol), acetone, carbon tetrachloride, and hydrocarbons such as *n*-hexane and benzene. The authors described interactions between a ligand and a substrate and introduced the term supra- or supermolecule ("*Übermolekül*") [119].

Hine and coworkers investigated the double hydrogen bonding of 1,8-biphenylenediol **13** with hexamethylphosphoramide, 1,2,6-trimethyl-4-pyridone, and 2,6-dimethyl-γ-pyrone using cocrystals for X-ray crystal structure analysis (Scheme 1.4) [115]. They reported two simultaneous and identical strong hydrogen bonds of the almost coplanar adduct of 1,8-biphenylenediol **13** to the Lewis bases and reported the shortest intermolecular hydrogen bonds (2.548 Å) detected in an X-ray crystal structure analysis at that time. In 1985, the same group reported the aminolysis of phenyl glycidyl ether **24** with diethyl amine in butanone at 30 °C using phenol-based catalysts (Table 1.1) [116, 117]. In the absence of catalyst, they observed a small autocatalytic effect by the product and proposed that amino alcohol **25** catalyzed the reaction *via* hydrogen bonding to the epoxide oxygen. A Brønsted plot suggested a strong linear correlation between the catalysts pK_a values and the reaction rate, with two exceptions: first, catechol **30** catalyzed the reaction somewhat faster than expected from the Brønsted plot because hydrogen bonding can occur *via* two hydroxyl groups. This effect could easily be corrected by specifying the reaction rate per hydroxyl group of the catalyst. The second exception was 1,8-biphenylenediol, which was as efficient as would be expected for a phenol that was about 600 times as acidic, and catalyzed the reaction with a TOF of 0.1 h^{-1}. Catechol, whose hydroxyl groups did not form simultaneous double hydrogen activation to one substrate molecule, was less active, which indicates that both hydroxyl groups of **13** are involved in the epoxide activation. Further investigation of the ionization constants (pK_a values) using electron-rich and electron-poor 1,8-biphenylenediol derivatives indicated that the acidity of the hydroxyl functions correlates with the ability to double hydrogen bond formation. The most acidic 4,5-dinitro-1,8-biphenylenediol **14** (Scheme 1.4) was found to be the strongest double hydrogen bond donor [121–124].

In 1990, Kelly's group synthesized 3,6-dipropyl-4,5-dinitro-1,8-biphenylenediol **15**, which is more soluble in CD_2Cl_2, for the Diels–Alder reactions between various α,β-unsaturated aldehydes as well as ketones with cyclopentadiene at 55 °C and

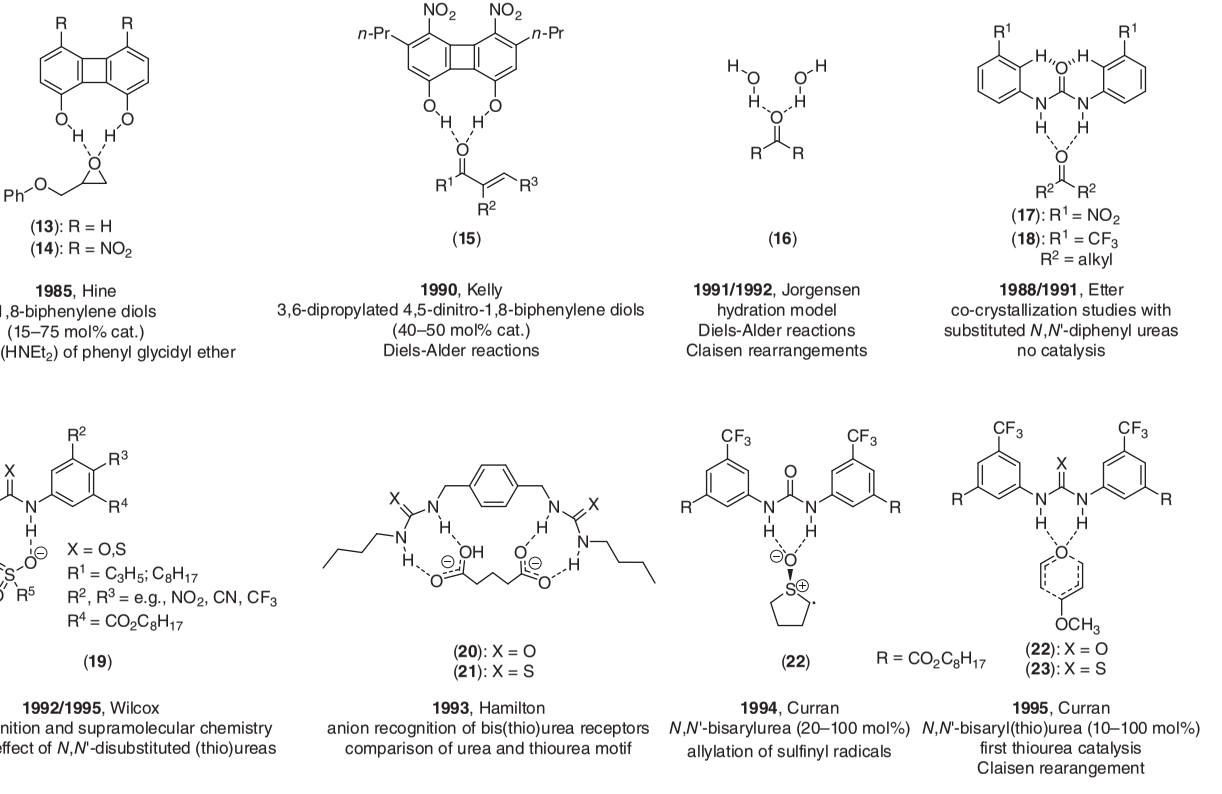

Scheme 1.4 Historic milestones on the way to hydrogen-bonding and anion-binding catalysts that display explicit double hydrogen bonding interactions for substrate recognition.

Table 1.1 Aminolysis of phenyl glycidyl ether **24** catalyzed by phenol-based derivatives. The reaction rates k_c are given relative to the uncatalyzed reaction.

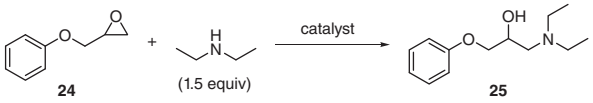

24 **25**

	26	**27**	**28**	**29**	**30**	**31**	**32**	**13**
								TOF = 0.1 h^{-1}
$10^5\,k_c/L^2\,mol^{-2}\,s^{-1}$	6.0	7.7	15.3	17.0	11.9	11.5	7.3	75
pK_a	9.99	9.14	7.97	7.15	9.36	8.64	9.15	8.01

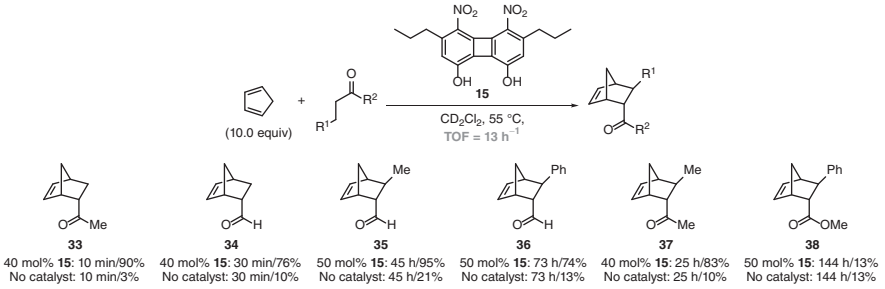

33 40 mol% **15**: 10 min/90%; No catalyst: 10 min/3%

34 40 mol% **15**: 30 min/76%; No catalyst: 30 min/10%

35 50 mol% **15**: 45 h/95%; No catalyst: 45 h/21%

36 50 mol% **15**: 73 h/74%; No catalyst: 73 h/13%

37 40 mol% **15**: 25 h/83%; No catalyst: 25 h/10%

38 50 mol% **15**: 144 h/13%; No catalyst: 144 h/13%

Scheme 1.5 Typical products of the 15-catalyzded Diels–Alder reaction of cyclopentadiene and α,β-unsaturated carbonyls.

40–50 mol% loading of **15** achieving a TOF of 13 h^{-1} (Scheme 1.5) [125]. They did not observe significant rate acceleration in the case of ester dienophiles, e.g., product **39**, which they explained by inhibition of complex formation as a consequence of repulsive interactions. The double hydrogen bond activation of dienophiles resulting in a substrate–catalyst complex as depicted in Scheme 1.4 was interpreted as the reason for the observed up to 30-fold rate enhancements. Monte Carlo simulations confirmed the catalyst–substrate association motif and the accelerating solvent effect of water compared to aprotic solvents in Diels–Alder reactions [126, 127] and Claisen rearrangements [128], for which Jorgensen and coworkers computed a 100-fold rate enhancement. They explained these results not by cooperative hydrogen-bonding effects but rather with an aqueous solvent effect described through clamp-like hydrogen-bonding interactions (**16**) of two water molecules to the carbonyl group leading to transition state stabilization [128].

From 1988 to 1991, Etter *et al.* investigated the cocrystallization of imides and *N,N′*-diphenyl ureas with Lewis bases such as triphenylphosphine oxide [129], ethers, nitro aryl species, ketones, and sulfoxides by X-ray structural analysis [130, 131]. The N–H urea protons act as partial proton donors (Lewis acid) with

the carbonyl oxygen as the proton acceptor (Lewis base), leading to intermolecular hydrogen-bonding interactions as observed in *N,N′*-bisphenylurea [132]. *N,N′*-bis(3-nitrophenyl) -urea **17** co-crystallizes with cyclohexanone in a 1 : 1 ratio through hydrogen bonding of the N–H protons and the carbonyl oxygen. Etter and coworkers found many receptors that are better hydrogen bond acceptors than the urea oxygen of **17** and termed this derivative an "*only intermolecular proton donor*" [130]. Urea derivatives with electron-withdrawing substituents in ortho- or para-positions or *meta*-alkyl substituents did not form cocrystals. In addition to **17**, *N,N′*-bis[(3-trifluoromethyl)phenyl]urea **18** cocrystallizes with carbonyl compounds, which was explained by the nearly planar urea conformation and short distances between the weakly acidic ortho protons and the carbonyl oxygen of 2.23–2.29 Å [130] that is below the limit for hydrogen-bonding interactions of about 2.4 Å [133, 134]. This distance is 2.49–2.66 Å in *N,N′*-bisphenylurea [132], therefore not leading to hydrogen-bonding interactions. Wilcox *et al.* examined the hydrogen-bonding recognition of sulfonates, phosphates, carboxylates, and zwitterionic 4-tributylammonium-1-butanesulfonate with *N*-allyl- [135] and *N*-octyl-*N′*-phenyl(thio)ureas **19** [136]. The host–guest complexes were investigated by ^{1}H NMR titration experiments *via* quantification of the downfield shifts of the N–H protons upon complexation. In addition, these studies confirmed the stronger double hydrogen bonding with anions, in particular, when electron-deficient substituents in meta- or para-position in the ureas were used, and that acidity can be considered a *useful parameter* of hydrogen-bonding strength [137]. In 1993, Hamilton's group examined the anion recognition of *N,N′′*-[1,4-phenylenebis(methylene)]bis[*N′*-butyl]urea **20** and the thiourea analog **21** to glutarate. They found a 15-fold increase in the binding constants for the thiourea derivative compared with the corresponding urea in accord with Wilcox' results that thiourea binding is stronger than that of the corresponding urea derivatives [138]. In 1994, Curran and Kuo used 20–100 mol% of urea catalyst **22** as the first double hydrogen bonding urea organocatalyst (or additive in the case of equimolar amounts) for the allylation of *α*-sulfinyl radicals generated from **39** with allyltributylstannane (Scheme 1.6) [140]. Instead of the well-established NO_2 groups, electron-withdrawing CF_3 substituents were incorporated in meta position in combination with lipophilic ester substituents to improve the solubility in common organic solvents. In the presence of the catalyst, Curran and Kuo observed small rate accelerations (TOF = 0.1 h^{-1}) and increased *cis*/*trans* selectivity.

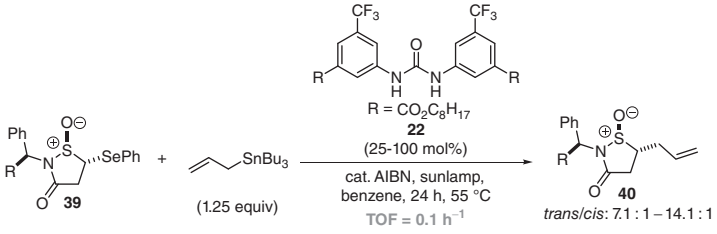

Scheme 1.6 Allylation of α-sulfinyl radicals catalyzed with **22**.

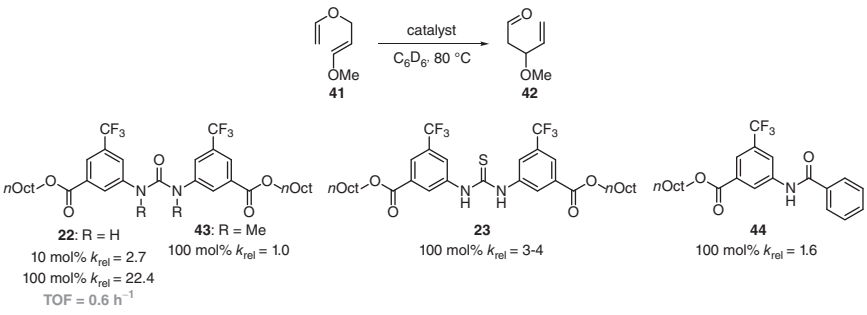

Scheme 1.7 Claisen rearrangement catalyzed by urea **22** and thiourea **23**.

The same group utilized urea **22** in the Claisen rearrangement of 1-methoxy-3-vinyloxy-propene **41**, where they observed with 10–50 mol% catalyst loading a rate acceleration enhancement by 1.7- to 5.0-fold; using 100 mol% gave 22-fold acceleration (Scheme 1.7) [139]. The authors probed the double hydrogen-bonding motif by using the *N,N′*-dimethyl derivative **43** ($k_{rel} = 1.0$), and a corresponding benzanilide **44** ($k_{rel} = 1.6$). These findings confirmed the work of Hine [115–117, 122] and Kelly [125] with **13** and **15** for epoxide and carbonyl activation, respectively, namely, that the double hydrogen-bonding motif is important for catalytic activity. Furthermore, Curran and Kuo examined thiourea analog **23** in the same reaction, and although slow decomposition was observed under the same reaction conditions, some rate acceleration was detected (at <10% decomposition: $k_{rel} = 3–4$) [139].

1.1.1 Evolution of Thiourea-Based Catalysts

Schreiner's group intensified the research on thiourea derivatives as organocatalysts starting in early 1997 (when this work was first presented, oddly at a conference geared toward organometallic chemistry ("OMCOS") in Göttingen where one of the authors was a local co-organizer) [141]. The idea was to bring hydrogen-bonding catalysis to the forefront of organic synthesis where it would be practical in the sense of ease of preparation of the catalysts, catalyst efficacy that was clearly rather limited at that time when one considers the high loadings (20–100 mol%), and the poor rate accelerations ($k_{rel} < 5$) and generality. One early consideration was that electron-deficient thiourea catalysts would be more practical than their urea analogs because of the following [142]:

(1) Thiourea derivatives are typically much more soluble in various organic solvents because of the lower tendency of the sulfur atom to serve as a hydrogen bond acceptor.
(2) Thiourea derivatives are easier to prepare (for instance, liquid thiophosgene is much easier to handle than gaseous phosgene).
(3) The acidity of thiourea ($p\mathrm{K_a} = 21.0$) is about six orders of magnitude higher than that of urea ($p\mathrm{K_a} = 26.9$) [138, 143], which should lead to stronger hydrogen-bonding and anion-binding interactions.

The strong hydrogen-bonding ability of thiourea derivatives became apparent in various areas such as supramolecular chemistry [144, 145], molecular anion recognition [146–148], crystal engineering [149, 150], herbicides [151, 152], and inclusion compounds [153–155]. Schreiner's group introduced the 3-(trifluoromethyl)phenyl (e.g., in **45**) and 3,5-bis(trifluoromethyl)phenyl (e.g., in **46**) motifs for thiourea catalysts with the idea that the ester function in Curran's **23** would obstruct the catalytic process by engaging in hydrogen-bonding interactions as well (Scheme 1.6) [156]. Early DFT computations (B3LYP/6-311+G(d,p)) suggested that **45** activates ketones through explicit double hydrogen-bonding interactions, which is conceptually similar to Jorgensen's realization of two water molecules acting as activators in aqueous Claisen rearrangements (Scheme 1.4) [156, 157]. Binding studies of catalyst **45** with the bidentate dienophiles *N*-acyloxazolidinone **52** revealed that **45** acts as a bidentate Lewis acid through explicit double hydrogen bonding (Scheme 1.8) [158].

This was confirmed experimentally by low-temperature IR measurements and comparison of the observed shifts of the carbonyl groups with computations on a reduced model system – assuming that **45** adopts a *syn*-conformation (*trans*/*trans* rotamer) as suggested by the crystal structure data of urea **17** [130, 134], other bisaryl-ureas [132, 159], and in particular structurally related thiourea **46** [1, 160]. Utilizing temperature-dependent ^{1}H NMR studies, it was found that **46** exhibits a large dimerization entropy ($\Delta S = -35.6\,\mathrm{cal\,K^{-1}\ mol^{-1}}$), which leads to free available catalyst at room temperature and consequently favored complexation with 1,3-diketone substrates ($\Delta S = -9.6\,\mathrm{cal\,K^{-1}\ mol^{-1}}$). The high diastereoselectivity of the Diels–Alder reaction between cyclopentadiene and *N*-acyloxazolidinone **52**

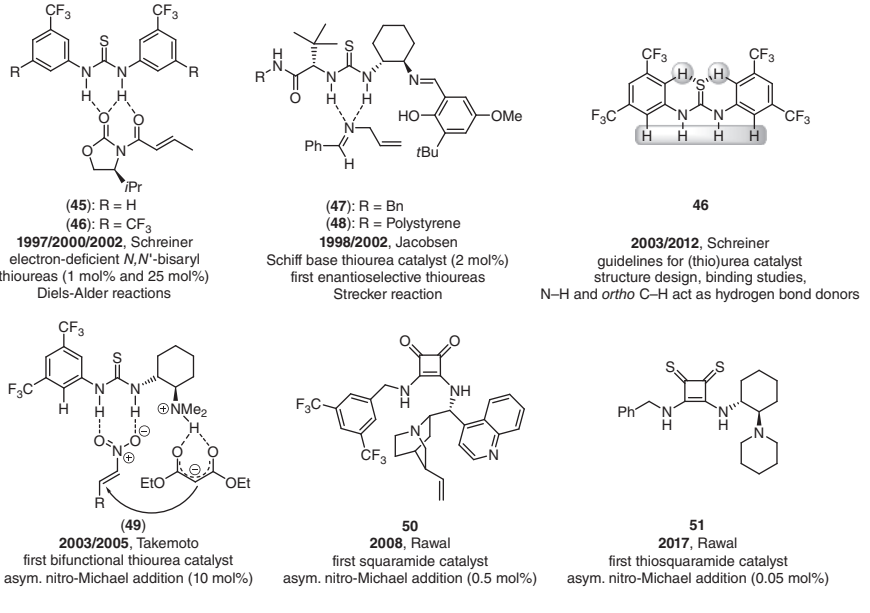

Scheme 1.8 Milestones in hydrogen-bonding thiourea catalysis of neutral and anionic Lewis basic sites with (thio)urea derivatives.

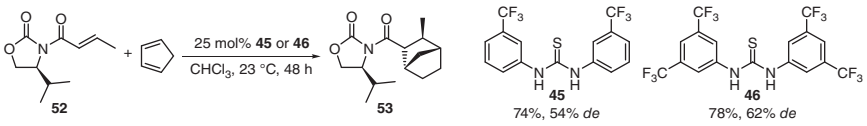

Scheme 1.9 Diastereoselective cycloaddition of *N*-acyloxazolidinone **52** and cyclopentadiene in the presence of **45** and **46**.

using 25 mol% of **45** supported the spectroscopic experiments and computational data [158]. More acidic **46** [143] eventually became a highly active privileged organocatalyst that activates neutral or anionic substrates through explicit double hydrogen bonding (Scheme 1.9) [142]. The 3,5-bis(trifluoromethyl)phenyl group became a very highly appreciated "privileged" anchor group in a large variety of organocatalysts not limited to hydrogen-bonding catalysis [158, 161–170] but also including, *inter alia*, proline [171, 172] and Brønsted acid catalysis [7, 173].

In pursuit of a tridentate chiral metal ligand in enantioselective Strecker reactions of *N*-allyl protected aldimines **54**, in 1998, Jacobsen's group identified in the course of high-throughput screening (HTS) of more than 130 tridentate Schiff bases thiourea catalysts [1] **47** and **48**, which were the first enantioselective thiourea organocatalysts (Scheme 1.10) [174]. Strecker products **55** were obtained as trifluoroacetyl-protected species (65–92%, 70–91% *ee*). Catalyst evolution and additional catalysts for asymmetric Strecker reactions are discussed in Section 1.2.2 including a detailed discussion of the substrate activation.

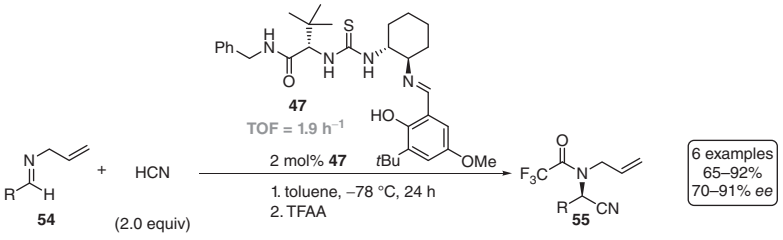

Scheme 1.10 Asymmetric Strecker reaction of aromatic and aliphatic *N*-allyl-protected aldimines catalyzed with **47**.

Structure–reactivity relationships of hydrogen-bonding catalysts in Diels–Alder reactions of cyclopentadiene and various dienophiles such as methyl vinyl ketones and (aza)chalcones, utilizing symmetrically *N,N′*-disubstituted thioureas with 1 mol% catalyst loading, were examined as early as 2003 [157]. The reaction rates determined by ^{1}H NMR qualitatively confirmed the conceptual ideas of Hine *et al.* for the aminolysis of epoxides (Table 1.1) [117], namely, that rigid

1 Jacobsen introduced the term "Schiff base catalyst" to demonstrate that the structure of this novel catalyst class originates from Schiff base ligands – originally developed for metal-based catalysis – and incorporates a Schiff base moiety. Notably, this term does not indicate that these catalysts operate as bases, but their high catalytic efficiencies result from the thiourea moiety as shown in Section 1.2.2. In the following, the scientifically established term "Schiff base (thio)urea" is used to describe this class of organocatalysts.

electron-withdrawing aromatic substituents lead to higher catalytic activity, as **45** (k_{rel} = 2–6; TOF = 52 h^{-1}) and **46** (k_{rel} = 5–8; TOF = 72 h^{-1}) were the most efficient catalysts, while dialkyl or electron-rich aromatic substituents are poorly activating (e.g., *N,N′*-diphenylthiourea **56**: k_{rel} = 1–2). Furthermore, product inhibition turned out to be very low because catalyst activity was still present even after 80% conversion. This emphasizes the entropy term in the formation of catalyst–substrate complexes and the weak enthalpic binding between the thiourea catalyst and the carbonyl group (~7 kcal mol^{-1} at rt in DCM) [158]. In addition, more conformationally flexible catalysts (e.g., **56** with a DFT (B3LYP/6-31G(d)) computed C_{aryl}–N rotational barrier of only ΔE_{rot} = 1.5 kcal mol^{-1}) perform poorly compared to conformationally more restricted derivative **46** (ΔE_{rot} = 3.4 kcal mol^{-1}) [157]. Moreover, electron-deficient substituents in meta- or para-position polarize the aromatic ortho-hydrogens, leading to intramolecular hydrogen-bonding interactions to the Lewis basic thiocarbonyl sulfur that hinders the rotation of the thiourea moiety and favors complexation entropically (Scheme 1.8). Substituents in ortho position, in contrast, lead to repulsive interactions with the thiocarbonyl group and the *syn–syn* conformation is entropically disfavored [130, 157]. Therefore, catalysts with substituents in meta- or para-position are more active than derivatives containing substituents in the ortho position. Schreiner's group highlighted the concept of thiourea organocatalysis at the very beginning of this research field and provided rough guidelines for (thio)urea catalyst design, which are still valid today and can readily be identified in every (thio)urea organocatalyst developed in the past 20 years [1]:

(1) The relative stabilization of the transition state must be larger than the stabilization of the starting material(s) and product(s);
(2) Bi- or multidentate catalyst–substrate complexes are favorable;
(3) There should be a balance between rigidity and flexibility in the catalyst structure to avoid entropy loss on the one hand and to retain adaptability to the substrate structure on the other hand;
(4) To prevent self-association, the catalyst should not incorporate strong hydrogen bond acceptors such as ester groups – the non-coordinating acidifying CF_3 group as in the 3,5-bis(trifluoromethyl)phenyl moiety of **46** appears to be ideal;
(5) To avoid product inhibition, the enthalpic binding interactions should be weak to allow low catalyst loadings;
(6) The catalyst should be water compatible or even catalytically active in water.

In 2003, Takemoto's group introduced the first bifunctional thiourea **49** for use in Michael addition reactions [161]. They postulated the simultaneous activation of the nitro olefins **57** by the N–H thiourea protons and malonates **58** by the amine (cf. Scheme 1.8), thereby obtaining α-chiral malonate derivatives **59** depicted in Scheme 1.11 (TOF = 0.7 h^{-1}) [175]. The authors performed kinetic studies on the Michael reaction and observed first-order kinetics for both reactants and the catalyst. Catalyst evolution and additional catalyst derivatives for asymmetric Michael reactions are discussed in Section 1.2.3, including a detailed discussion of the mode of substrate activation.

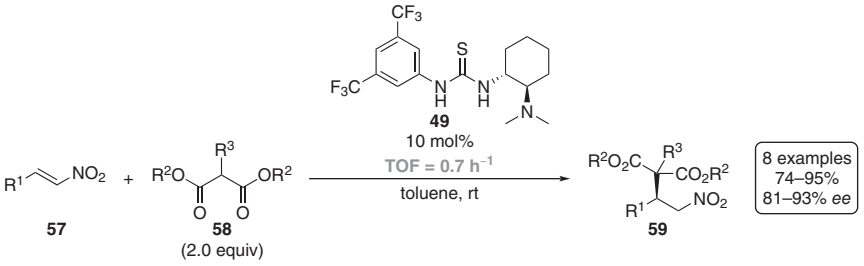

Scheme 1.11 Product range of the asymmetric Michael addition of dialkyl malonates to *trans*-β-nitrostyrenes catalyzed with **49**.

In 2006, Kotke and Schreiner applied the principle of anion-binding catalysis to high-yielding acid-free acetalizations [176]. They utilized various aromatic, aliphatic, unsaturated, and acid-labile aldehydes as well as ketones, which could be cleanly acetalized in the presence of 4.0–4.3 equivalents of methanol, ethanol, 1-propanol, 2-propanol, and 1,2-ethandiol as the alcohol components and as a solvent. The acetals were obtained in yields of 61–95% at low catalyst loading of only 0.01–1.0 mol% **46** – at that time the lowest catalyst loading in an organocatalytic reaction – at room temperature (Scheme 1.12). A limitation of the protocol, however, was the acetalization of electron-rich carbonyl compounds such as *p*-tolylaldehyde, cyclohexanone, and acetophenone **64** with long reaction times (92–250 h) and lower conversions (71–74%). In contrast, aldehydes were acetalized at much shorter reaction times (9–14 h) and in high yields (89–95%). Kotke and Schreiner proved the synthetic utility of this protocol when they isolated 67% of pure product from the acetalization of acid-labile TBS-protected *m*-hydroxybenzaldehyde **68** that was reported to react rather sluggishly under Brønsted [177] or Lewis acid catalysis [178]. Kotke and Schreiner found for the diethyl acetalization of *p*-chlorobenzaldehyde **65** and *n*-octanal TOFs of 632 h^{-1} or rather turn over number (TON) = 9800, and 577 h^{-1} (TON = 9700), respectively. These values are approximately ten times higher than those of previously reported thiourea-catalyzed reactions and were

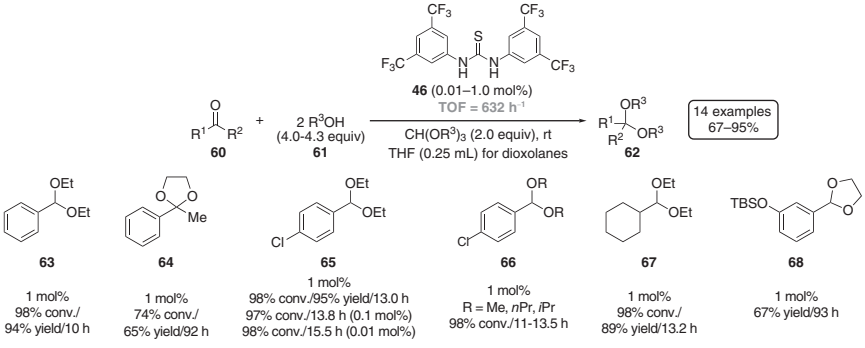

Scheme 1.12 Representative examples of the first anion-binding catalysis reaction described in the literature. Products was obtained under mild and acid-free conditions catalyzed by **46**.

significant, as the uncatalyzed reactions generally even after one week furnished <1% product. In addition, the authors found, on the one hand, no influence of the utilized alcohol but to the carbonyl component on the other hand. A competition experiment between benzaldehyde and acetophenone – using ethanol as well as triethyl orthoformate – resulted in a product mixture of 6.1 : 1 favoring the diethyl benzaldehyde acetal. This chemoselectivity is in line with the different reactivity of aldehydes and ketones under nucleophilic attack [176].

The initial working hypothesis was that the catalyst undergoes double hydrogen bonding to the carbonyl moiety – comparable to dienophile activation depicted in Scheme 1.8 – to increase the electrophilicity of the carbonyl carbon and, at the same time, to stabilize the increased negative charge on the carbonyl oxygen during the nucleophilic attack. However, utilizing thiols instead of alcohols in the presence of ethyl orthoester only provided the diethyl acetal, although thiols are much better nucleophiles [179]. Therefore, Kotke and Schreiner proposed a mechanism that starts with thiourea-assisted orthoester heterolysis, with **46** stabilizing multiple oxyanion intermediates. The stabilized alcoholate anion **69** rapidly undergoes nucleophilic attack onto the carbonyl compound and **46** binds the incipient hemiketal anion **70**. Subsequent nucleophilic addition provides the "double acetal **71**," which dissociates to alkyl formate **72**, the oxocarbenium ion **73**, and another **46**-stabilized alcoholate **69** that in turn attacks **73**, leading to the acetal product and releases the catalyst for subsequent turnover (Scheme 1.13). This mechanism is in in line with the well-established enzymatic mechanisms in which hydrogen-bonding interactions stabilize alkoxide intermediates [180].

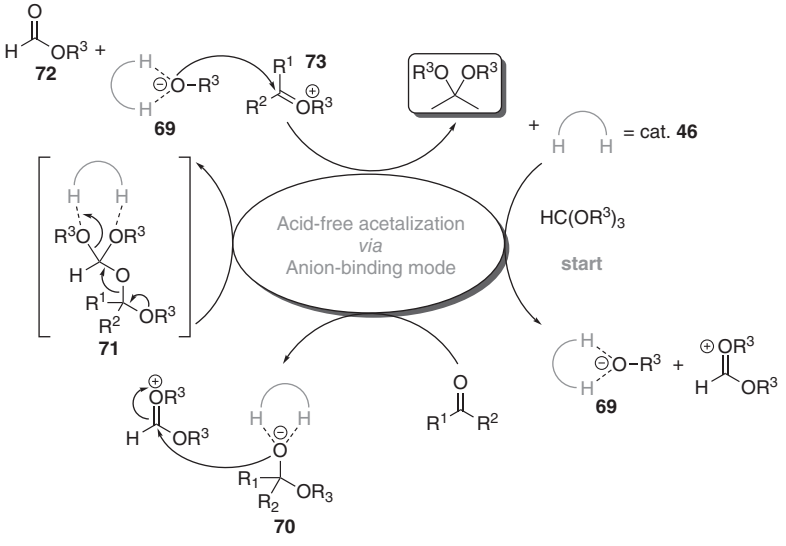

Scheme 1.13 Proposed acetalization mechanism catalyzed with **46** starting with thiourea-assisted heterolysis of an orthoester and subsequently multiple oxyanion stabilization through **46**-mediated anion binding.

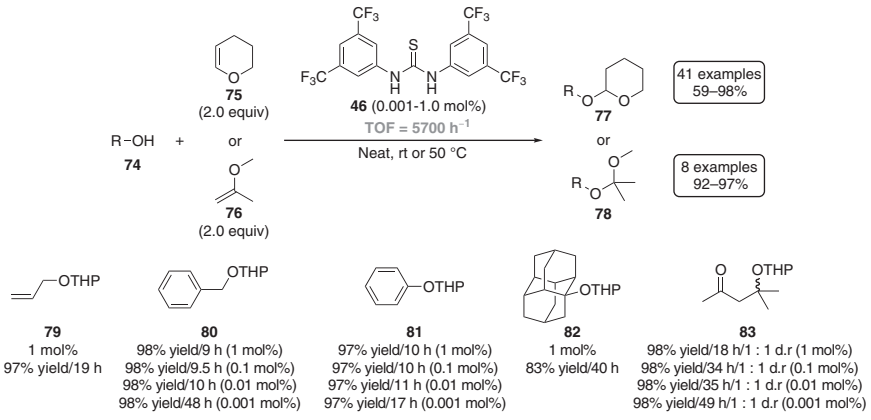

Scheme 1.14 Representative products of the THP and MOP protection of hydroxyl functionalities catalyzed with **46**.

In 2007, Kotke and Schreiner introduced the organocatalytic tetrahydropyran (THP) and 2-methoxypropene (MOP) protection of alcohols, phenols, and other hydroxyl containing substrates (Scheme 1.14) [182]. The tetrahydropyranylation catalyzed with **46** using 3,4-dihydro-2*H*-pyran **75** (DHP) as reactant and solvent was applicable to a broad spectrum of alcohols and furnished the corresponding tetrahydropyranyl ethers **77** under mild conditions and in yields of 59–98% at very low catalyst loading of only 0.001–1.0 mol% **46**. The THP protection of benzyl alcohol **80** at very low catalyst loadings down to 0.001 mol% emphasized the catalytic power of **46** and revealed a TON close to 100 000 and TOF of approximately 2000 h^{-1}. Phenol derivatives were also readily converted into the corresponding acetals at 50 °C. As shown for **81**, THP protection could be achieved with 0.001 mol% catalyst loading, resulting in 97% isolated product after 17 h. This indicates a TOF of approximately 5700 h^{-1}, which still marks the most efficient organocatalytic reaction utilizing hydrogen bonding to date. Scale-up experiments (50 mmol scale), e.g., in the case of phenol, also demonstrated that catalyst loadings of only 0.01–0.1 mol% are sufficient and feasible for preparative THP protection. Tertiary alcohols, which are generally difficult to protect as THP ethers due to steric hindrance and elimination as a common side reaction, could also be THP protected under these conditions. Remarkable is the tolerance of even most sterically hindered substrates diamantan-1-ol affording ether **82**. Because of the acid-free conditions, the protocol also tolerated acid-labile hydroxyl-functionalized substrates such as aldol reaction products (**83**; TOF = 2000 h^{-1}), β-hydroxy esters, epoxides, acetonides, cyanohydrins, oximes, and highly acid-sensitive TBS-protected alcohols without detectable side reactions in yields of 59–98%. Kotke and Schreiner applied their protocol to the alternative enol ether 2-methoxypropene **76** and prepared the corresponding MOP-ethers **78** in yields ranging from 92% to 97% at room temperature; it was noted that MOP is so reactive that the uncatalyzed reaction also proceeded albeit at lower rates (Scheme 1.14) [182].

A reasonable mechanistic entry into this reaction may start with the complexation of catalyst **46** with the alcohol substrate [182]. This double hydrogen-bonding-mediated coordination increases the alcohols' acidity as well as polarizability and

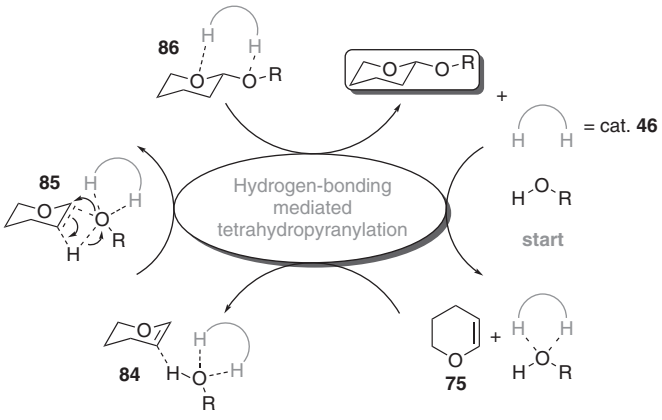

Scheme 1.15 Proposed mechanism for the **46**-mediated tetrahydropyranylation of alcohols.

hence its ability to form a subsequent ternary complex **84** with enol ether **75**. The catalyst remains attached during the polar addition through a highly polarized transition structure **85** and is finally released from the product complex **86** to initiate a new catalytic cycle (Scheme 1.15).

This mechanistic proposal indicates the departure from the often-implied concept of carbonyl or related functionalities such as nitroolefins activation through hydrogen bonding with (thio)urea derivatives and other hydrogen-bonding organocatalysts [3, 183]. Hence, this mechanistic alternative suggested either the hydrogen-bond-assisted generation of the free nucleophile (e.g., RO^- and CN^-) and subsequent anion binding or the stabilization of the active form of the nucleophile through hydrogen-bonding and polar interactions to the respective precursor (e.g., ROH, $HC(OR)_3$ [176], HCN, and TMSCN [184]). Kotke and Schreiner elucidated this mechanistic proposal utilizing DFT (B3LYP/6-31G(d,p)) and coupled cluster computations (CCSD(T)/cc-pVDZ,), which demonstrated that the catalyst preferentially stabilized the developing *oxyanion hole* in the transition state through double hydrogen-bonding without the formation of a charged alkoxide nucleophile. This conclusion was based on a comparative computational analysis of the uncatalyzed versus catalyzed model reaction of methanol with **75**. The stabilizing effect of **46** on the key transition structure was estimated to be 23 kcal mol^{-1}, resulting in a minimized barrier of only 17.7 kcal mol^{-1} (uncatalyzed: 45.2 kcal mol^{-1}): These values are in line with the experimentally found efficacy of **46** already at room temperature in contrast to the uncatalyzed THP protection, which showed no product formation under otherwise identical conditions. Additionally, the transition structure revealed that **46** helps pre-organizing the reactants and the overall geometric changes in going from the complexes to the transition structures; **46** is placed sideways and points away from the "R group" of the substrate making steric hindrance not a critical factor, as found experimentally [182]. Pápai, Varga, and coworkers reinvestigated the mechanism of the THP protection mechanisms utilizing DFT studies (ωB97X-D/6-311G(d,p)) and isotope labeling experiments [185]. In

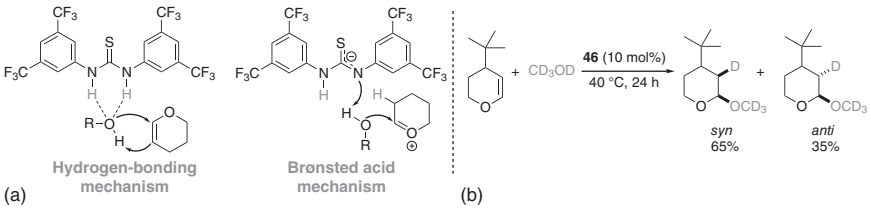

Scheme 1.16 (a) The two investigated possible mechanisms of the THP protection of alcohols and (b) isotope labeling experiment utilizing CD_3OD.

addition to the mechanism proposed by Schreiner and Kotke, the authors also examined an alternative reaction pathway with **46** acting as a Brønsted acid and protonating **75** (Scheme 1.16a). The computed transition structure for the Brønsted acid pathway was $\Delta\Delta G = 6.5\,\text{kcal mol}^{-1}$ lower in energy compared to the hydrogen-bonding mechanism. In isotope labeling experiments, utilizing CD_3OD and conformationally rigid DHP derivative 4-(*tert*-butyl)-3,4-dihydro-2*H*-pyran, a mixture of the *syn*- and *anti*-product was obtained in a 65 : 35 ratio, respectively, that supported a two-step mechanism *via* Brønsted acid mechanism (Scheme 1.16b). An additional hint for a Brønsted acid mechanism was obtained by utilizing 2-thiouracil that could not engage in double hydrogen bonding to the alcohol, however furnished THP-protected phenol **81** in similar yield (92% conversion, 12 h, 0.2 mol% catalyst loading) compared to **46** (100% conversion, 12 h, 1.0 mol% catalyst loading). In 2019, McGarrigle and coworkers utilized 2-thiouracil in the stereoselective glycosylation of galactals and proposed a mechanism where thiourea or 2-thiouracil engaged *via* general acid/base catalysis – similar to the mechanisms proposed by Pápai, Varga, and coworkers – but excluded a "simple" acid-catalyzed mechanism [186]. Utilizing acids with similar pK_a values such as Meldrum's acid, $Et_3N{\cdot}HCl$, or 4-nitrobenzoic acid does not lead to product formation [185–187].

In 2011, Schreiner and coworkers developed a cooperative catalyst system for the enantioselective cyanosilylation of aldehydes **87** (Scheme 1.17) [170]. They utilized thiourea **89** as the catalyst, benzoic acid as the cocatalyst, and TMSCN as the cyanide source and obtained acetyl-protected chiral cyanohydrins **88** in yields of 57–90% and *ee*-values of 8–88% utilizing 10 mol% **89** and cocatalyst each (TOF = $0.6\,\text{h}^{-1}$).

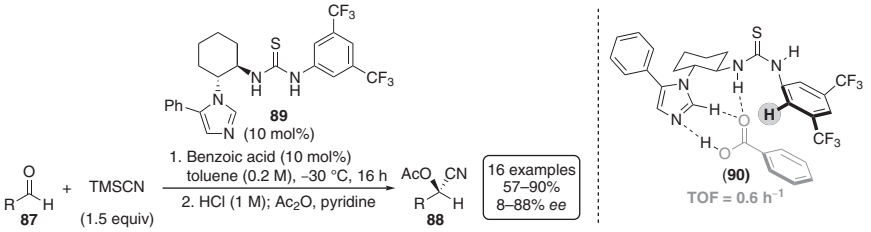

Scheme 1.17 Enantioselective cyanosilylation of aldehydes catalyzed utilizing the *in situ* formed cooperative catalyst (**90**).

The authors utilized a combination of NMR and ESI-MS techniques for mechanistic studies that reveal the presence of a hydrogen-bonded complex of **89** and benzoic acid that was also supported by DFT computations (M06/6-31G(d,p)). The complex (**90**) formed a well-defined chiral hydrogen-bonding environment, where one N–H proton coordinated the benzoic acid, whereas the second N–H proton formed hydrogen bonding to the aldehyde. Furthermore, the strong fixation of the aromatic aldehyde occurred *via* T-shaped π–π stacking interactions of the acidified ortho protons of the 3,5-bis(trifluoromethyl)phenyl moiety with the phenyl ring, which was supported by downfield shift of the ortho-protons in NMR experiments. This interplay of hydrogen bonding and π–π stacking interactions supported the formation of a chiral ternary complex preferring the observed stereoinduction of cyanide addition and emphasized the importance of the catalysts ortho-protons for substrate activation [170].

In 2012, Schreiner's group measured the pK_a values of various (thio)urea derivatives in dimethyl sulfoxide (DMSO) to examine the influence of CF_3 groups on the N–H protons' acidity (Scheme 1.18) [143]. The reason for choosing DMSO and not water as the solvent was that most organic reactions are carried out in organic solvents; the aqueous pK_a values are not useful because the differences to non-aqueous pK_a values are large and not even qualitatively meaningful [188]. The authors found that the pK_a values correlate well with the overall number of CF_3 groups attached to the aromatic rings; each CF_3 group decreases the pK_a by approximately 1.2 pK_a units (cf. **49** vs. **97**), and the combined effect of the four CF_3 groups in thiourea **46** resulted in a pK_a value of 8.5, which allows its deprotonation by organic amine bases such as *N*,*N*-diisopropylethylamine (DIPEA) [189]. Additionally, the pK_a values of thioureas were approximately 5 pK_a units lower compared to the corresponding urea derivatives (**94** vs. **46**).

The influence of the electron-withdrawing substituents on the ortho-protons and their engagement in substrate binding was investigated more closely by Schreiner's group in 2012, utilizing a combination of low-temperature IR spectroscopy, 2D NMR techniques, MS investigations, and DFT computations (M06/6-31+G(d,p)) [190]. The authors found strong evidence of **46** binding to δ-valerolactone both through the N–H protons and the ortho-proton. The IR spectra of a 1 : 1 mixture revealed a small

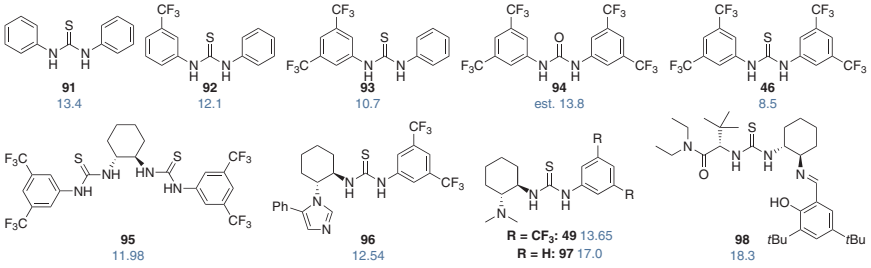

Scheme 1.18 Substituent effects on a selection of (thio)urea derivative pK_a values in DMSO. The pK_a value of **94** was estimated because of solubility issues. The pK_a value of **98** is an apparent value, a result of the similar acidity of the thiourea moiety and the phenolic OH.

$\nu_{C=O}$ band of free lactone and a large red-shifted band ($\Delta\nu = 32\,cm^{-1}$), indicating a hydrogen-bonding complex. In addition, ^{19}F-^{1}H HOESY experiments showed a cross-peak between the fluorine of the CF_3 group and the δ-methylene protons of the lactone, and the binary complex could also be identified by ESI-MS. [143]. As a further development of the thiourea catalysts, Rawal and coworkers introduced chiral cinchona-based squaramide derivatives as alternative (thio)carbonyl organocatalysts in 2008 (Scheme 1.19) [191]. Utilizing squaramide **50**, the authors performed the Michael addition of β-nitrostyrenes **99** and 2,4-pentanediones **100** – similar to the substrates used by Takemoto *et al.* in 2003 [161] – and obtained the products **101** in yields ranging from 65% to 98% and *ee*-values of 88–98%. Low catalyst loading of 0.5 mol% resulted in TOF = $24\,h^{-1}$, a 30 times higher value as compared to Takemoto's approach (TOF = $0.7\,h^{-1}$; cf. Scheme 1.11).

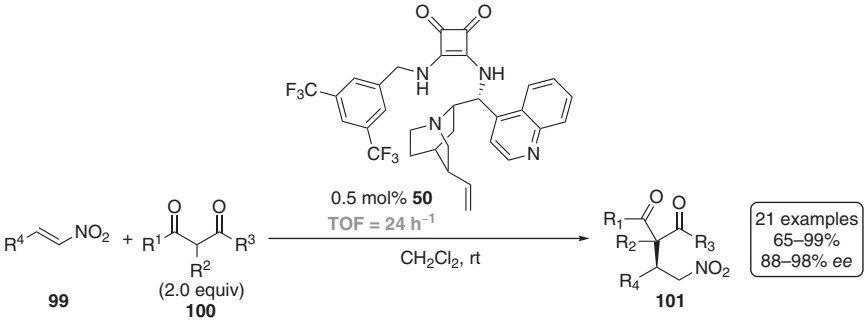

Scheme 1.19 Nitro Michael addition of 2,4-pentadienones to *trans*-β-nitroolefins catalyzed with squaramide **50**.

Four reasons for the higher catalytic activity of squaramides as compared to thioureas for this particular reaction were provided (Scheme 1.20) [192–194]:

(1) The nitrogen lone pairs are delocalized in both derivatives, restricting C–N bond rotation. The delocalization in squaramides takes place through the aromatic cyclobutenedione moiety; hence, the N–H acidity of squaramides is higher as compared to that of thioureas [143, 195].
(2) The squaramide scaffold is more rigid, which leads to reduced conformational flexibility [196].
(3) The squaramide moiety forms stronger hydrogen bonds due to the geometric structure of the cyclobutenedione ring that results in a larger distance and

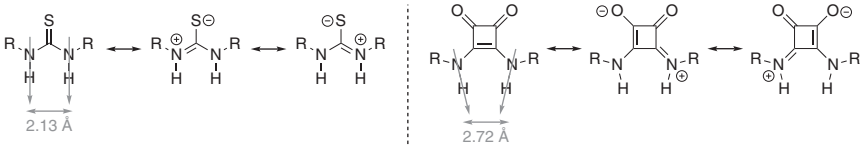

Scheme 1.20 Comparison of thiourea and squaramide skeletons regarding the zwitterionic species, the N–H-proton distance, and the orientation of the N–H-protons in thioureas (parallel) and squaramides (convergent).

convergent orientation of the N–H-protons with a larger H···X···H angle (X = Lewis base) [191, 192].

(4) Squaramides exhibit dual functionality because the carbonyl oxygens may act as Lewis bases [197–199].

Subsequently, squaramides were used in various organocatalyzed transformations, driving on concepts of double hydrogen bonding of neutral and anion-binding Lewis basic sites [192, 193, 200]. Almost ten years later, Rawal's group synthesized chiral thiosquaramide **51** and examined this derivate in Michael addition reactions of β-nitrostyrene derivatives **102** and barbiturates **103** (Scheme 1.21) [201]. Catalyst **51** provided Michael adducts **104** in ranges of 88–99% and *ee*-values of 72–98% at a catalyst loading of only 0.05 mol%. Similar to ureas and thioureas, thiosquaramides are more acidic than squaramides [202–204], which can be easily identified using TOF values: Compared to squaramide **50**, the TOF value of **51** (3960 h^{-1}) is about 160 times higher and is in the order of the TOF value of **46** in the THP protection of alcohols (cf. Scheme 1.14) [182].

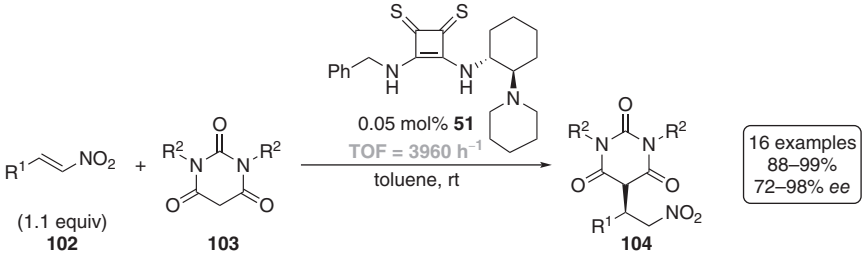

Scheme 1.21 Asymmetric Michael addition of barbituric acids to *trans*-β-nitroolefins catalyzed with **51**.

In 2017, Pittelkow's group introduced croconamides, the higher analogs of squaramides, as a new dual hydrogen-bonding motif for anion recognition and organocatalysis [205]. The authors tested the ability of croconamides in anion binding utilizing derivative **215** as a catalyst in the THP protection of phenol derivatives and measured rate constants for a series of substrates (Scheme 1.22).

At the same time Ho, Jolliffe, and coworkers employed quantum mechanical computations (G3(MP2)) to predict the pK_a values of several (thio)ureas, (thio)deltamides, (thio)squaramides, and croconamides [206]. Because many pK_a values of these hydrogen-bonding donors are known from the literature [195], the authors compared the computed values with the experimental data and observed differences of approximately 1.5 pK_a units. The croconamides were identified as the most acidic oxo-species; however, thiosquaramides were slightly more acidic (~2 pK_a units), but no investigations of thiocroconamides – which have not yet been reported – were made. Additionally, Jolliffe's group introduced deltamides as anion receptors [206]. The authors investigated the chloride-binding affinities and observed an unusual trend for the croconamide series: the binding affinities for *N*,*N*′-bisalkylcroconamides were higher than for *N*,*N*′-bisaryl derivatives. These results were explained by the high acidity of aryl-substituted derivatives that exist as

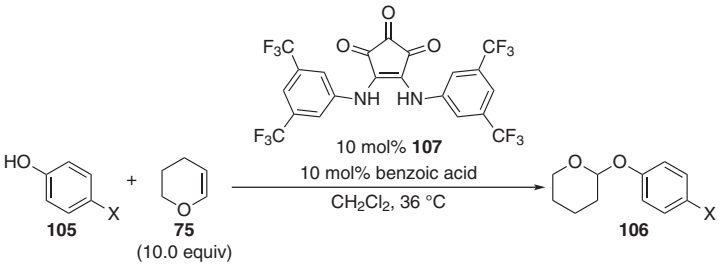

Scheme 1.22 THP protection of a series of phenols catalyzed with **215**.

partially deprotonated at neutral pH, thereby reducing their ability to bind anions. Because deltamides are less acidic than squaramides, but more acidic than ureas, *N*,*N*′-bisaryl derivatives resulted in higher affinities than *N*,*N*′-bisalkyl derivatives, and attachment of phenyl groups decreased the pK_a value and increased the anion affinity. Moreover, deltamides displayed lower chloride affinities than ureas and squaramides, whereas the affinities of all three species to the coplanar acetate anion are similar. In contrast to ureas and squaramides, where the anion-binding affinity correlates with anion basicity, deltamides also revealed higher affinities for tetrahedral $H_2PO_4^-$ than for coplanar carboxylates. The authors explained these results by the different structures of deltamides, where the DFT-computed distance of the N–H protons is approximately 3.5 Å and is therefore significantly larger than in ureas (2.13 Å) and squaramides (2.72 Å, Scheme 1.20). These results emphasize the strong correlation between the N–H geometry and the anion-binding affinity [206].

1.1.2 Evolution of Triazole-Based Catalysts

Non-covalent interactions involving C–H hydrogen bond donors have been known since the fundamental work by Kumler in 1935 [207], which took place at the same time when Pauling described "*traditional*" N–H and O–H hydrogen bond donors [181]. However, C–H hydrogen bonding was mentioned only occasionally in the following 30 years until Sutor utilized X-ray single-crystal analysis of 1,3,7,9-tetramethyluric acid **108** and described an intramolecular C–H···O hydrogen bond (Scheme 1.23) [209–211]. Sutor argued that the distance of 3.00 Å between the methyl group (C_{11}) and the oxygen atom (O_{12}) was much shorter than the sum of the van der Waals radii of a methyl group and an oxygen atom (3.40 Å) [211]. In 1982, Taylor and Kennard investigated the crystal structures of 113 organic compounds (many of them are amino acid and nucleoside derivatives) with respect to C–H···O hydrogen bonding and found strong evidence for this kind of NCI [133]. In 2008, a number of seminal studies on anion binding *via* C–H bonds emerged [208, 212–218]. In parallel, the 1,2,3-triazole unit was introduced in macrocyclic receptors, e.g., in the triazolophane **109** (Scheme 1.23) [208]. The C–H-mediated hydrogen-bonding motif was comprehensively reviewed [219–225], as where the triazoles utilized in anion recognition processes [226, 227].

Mancheño's group employed 1,2,3-triazol-based catalysts as alternative hydrogen-bonding donors in anion-binding catalysis [228] and carried out halide

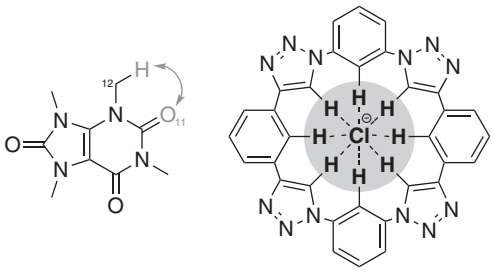

108 **109**

Scheme 1.23 C–H Hydrogen bonding in **108** and triazolophane-bound chloride anion in **109**.

anion-binding affinity and activity studies of a series of bis-triazole derivatives (Scheme 1.24) [229]. The authors synthesized a series of derivatives **110–120** with variation of the triazole substituent and the bridged phenyl moiety. Mancheño *et al*. performed chloride-binding studies and measured the highest chloride affinity for **114** that was substituted by the well-established 3,5-bis(trifluoromethyl)-phenyl moiety [190] as a triazole substituent and the 2-(methoxy-propan-2-yl)acetylene group as the substituent in *para* position for the phenyl unit [229, 230]. The importance of the ortho-protons of the 3,5-bis(trifluoromethyl)-phenyl moiety was also supported by the finding that the corresponding pentafluorophenyl derivative **113** bound chloride much less effectively than **114**. Furthermore, the authors observed a high preference for chloride binding ($k_{THF} = 1417\,M^{-1}$) as compared to bromide ($k_{THF} = 438\,M^{-1}$) and iodide ($k_{THF} = 319\,M^{-1}$). This was explained with the limited space inside the spherical binding pocket, which was further supported by the low binding affinity for the small, but linear cyanide ion ($k_{THF} = 394\,M^{-1}$).

Thereafter, Mancheño's group utilized bis-triazole **114** for alkylation of primary and secondary amines as well as thiophenol **127** and phenol **128** with 4-dimethylamino-*N*-triphenylmethyl-pyridinium chloride **121** (12–85%; 10 mol% catalyst loading; TOF = $0.12\,h^{-1}$) by binding of the counteranion and therefore activation of the electrophile (Scheme 1.25) [229, 230]. The high chloride affinity of the catalyst and the anion-binding mechanism were confirmed by anion selectivity studies utilizing each 10 mol% **114** and thiourea **46** in the presence of 20 mol% tetrabutylammonium bromide. The conversion dropped from 79% to 51% and from 82% to 37% for **114** and **46**, respectively (48 h).

In 2014, Mancheño and coworkers introduced the first helical triazole-based anion-binding catalyst with four triazole subunits and chiral 1,2-diaminocyclohexane backbone in a Reissert-type reaction of indole derivatives with silyl ketene acetals as nucleophiles [231–236] and in the dearomatization of pyrylium derivatives [237]. The evolution of the helical design and catalyst application are discussed in Section 1.2.3. The concept of triazole-based anion catalysis was applied to switchable catalysts as well [238]. In 2020, Dorel and Feringa reported a switchable stilbene-based catalyst with helical chirality that incorporates four triazole units [239]. This first-generation molecular motor-based [240] catalyst was utilized in

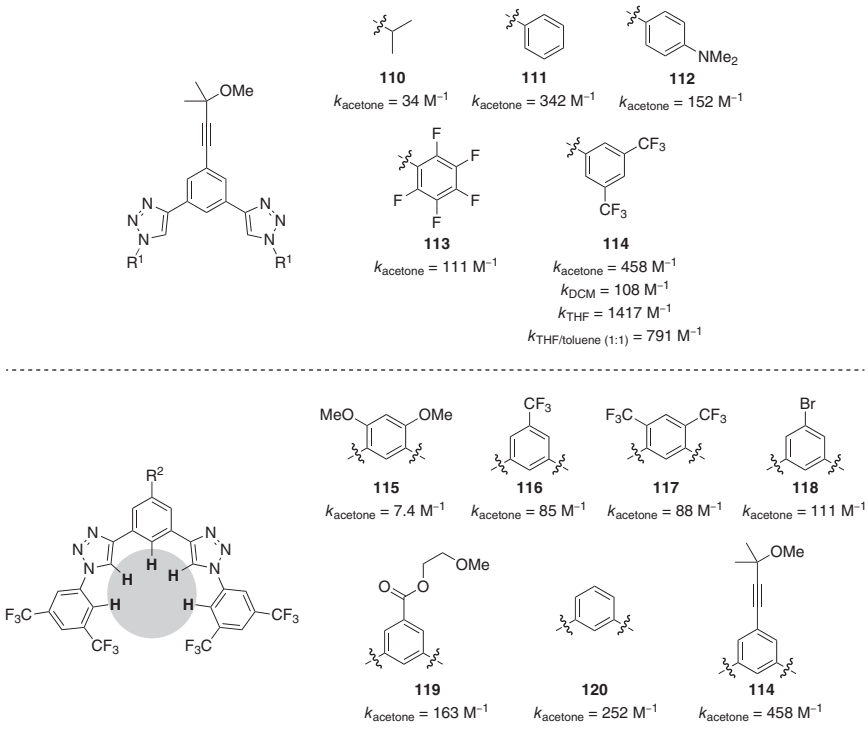

Scheme 1.24 Various 1,2,3-triazole-based catalysts and the corresponding chloride-binding affinity. The blue cycle indicates the spherical anion recognition pocket.

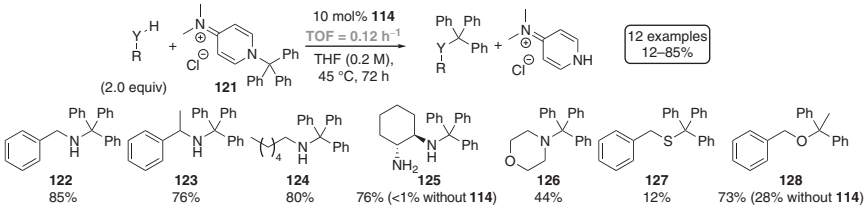

Scheme 1.25 Bistriazole **114**-catalyzed alkylation utilizing DMAP-derived alkylation reagent **121**.

the stereodivergent addition of silyl ketene acetals to oxocarbenium ions through chloride abstraction and binding with 10 mol% catalyst loading. The chirality of the catalyst was switched through light- and heat-driven rotation around the stilbene moiety, resulting in reversal of the enantiomeric ratio of the products. While Dorel and Feringa obtained a racemic mixture in the presence of the *trans* state, the (*M,M*)-*cis* and (*P,P*)-*cis* states gave up to 80 : 20 *e.r.* and 9 : 91 *e.r.*, respectively, of the opposite enantiomers, which means an Δ*ee* of 142%. Although the enantioselectivities were lower than those reported for non-switchable thiourea organocatalyst **223** (Section 1.2.3, Scheme 1.54, 92% *ee*; 0.1 mol% catalyst loading) [242], this work provided an exciting proof of concept [239].

1.1.3 Progress on Halogen-Binding-Based Catalysts

A novel kind of anion-binding catalysis utilizes halogen bonding instead of hydrogen bonding. The basic interaction dates back about 200 years when Colin reported an ammonia–iodine complex during his investigations of nitrogen iodine compounds such as NI_3 in 1814, only about two years after iodine was accidentally discovered and isolated [243, 244]. Because Colin did not reported a formula of the complex, Bineau investigated the formation of this complex further and reported a composition of the complex of three ammonia and one iodine molecule in 1844 [245]. About 20 years later, Guthrie reported this complex (**129**) as a 1 : 1 mixture during his study of the reaction with mercury, where he observed only nitrogen and mercury(I)-iodide in a 1 : 2 ratio [246], and it was not until 1950 that Mulliken described the compound as a charge transfer complex (Scheme 1.26) [247, 248]. Notwithstanding this realization, Benesi and Hildebrand examined the interaction between iodide and benzene and its alkyl-substituted derivatives in 1949. They reported a 1 : 1 complex of benzene and iodine (**130**) that formed in non-polar solvents such as carbon tetrachloride or *n*-heptane and determined the thermodynamic data of the complex [249]. Beginning in the 1950s, Hassel and coworkers published a series of X-ray structure analyses of halogen-bonding adducts, describing a linear orientation of the heteroatoms, e.g., in the adduct between dioxane and bromine (**131**) [250–254]. In the following years, the interest in this kind of non-covalent interactions considerably waned until Paolo and Sandorfy described complexes between fluorinated iodoalkanes and amines (such as **132**) [255]. In the 1970s and 1980s, Dumas introduced the term "halogen-bonding" during his research on the interactions between aliphatic halides and organic bases [256, 257].

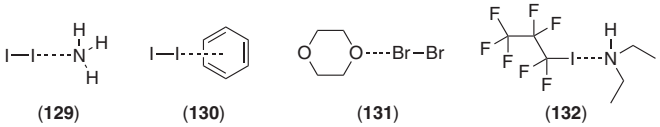

Scheme 1.26 Some adducts of milestones in halogen-bonding adducts.

The concept of "halogen-bonding interactions" based on the σ-hole, which is well known for atoms of group 14 (tetrels), 15 (pnictogens), 16 (chalcogens), and 17 (halogens) elements when covalently bonded to electron-withdrawing substituents [258]. The electronic density of these atoms is not equally distributed but rather anisotropic. The σ-hole describes the region of positive molecular electrostatic potential (MEP) and is placed collinearly on the opposite side relative to the substituent. Because of σ-holes, in principle, "negatively charged" anions act as if they were "positively charged" [259, 260]. In the last few years, the concept of halogen bonding and σ-hole interactions has been comprehensively reviewed [243, 258, 259, 261–271]. In 2011, Huber's group reported the first anion-binding additive utilizing double halogen bond donor species in a Ritter-type solvolysis of benzhydryl bromide **133** in acetonitrile (Scheme 1.27) [272]. The authors synthesized a series of bis-imidazolium derivatives and observed that only the double

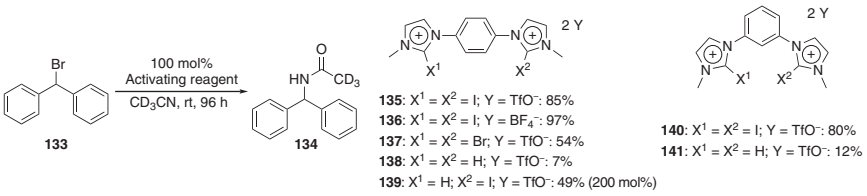

Scheme 1.27 First anion-binding activation induced by charged halogen-bonding catalysts.

halogen bond donors **135**, **136**, and **140** – attached with two iodine substituents in 2-position of the imidazole moiety – accelerated the reaction well (>80% yield; 100 mol% loading), whereby the *para*-substituted derivative showed a slightly higher activity (**135** = 85%; **136** = 80%). The corresponding bromine derivative **137** gave only 54% yield, which indicated the importance of the halogen species. Hydrogen-bonding donors **138** and **141** did not provide significant conversion, and single halogen-bonding donor **139** only gave 49% conversion utilizing 200 mol% of the additive. Additionally, Huber and coworkers observed a slight influence of the counterion (**135** = TfO^- = 85%; **136** = BF_4^- = 97%). These results indicated the role that halogen-bonding plays in abstracting and binding the bromide, as also confirmed by isothermal calorimetric titrations [273].

In 2013, Huber's group synthesized a series of neutral halogen-bonding donors based on bridged 2,6-diiodo-3,4,5-trifluorophenyl moieties such as the tridentate variant **146** and utilized them as catalysts for substitution reactions between 1-chloroisochroman **142** with various silyl ketene acetals (10 mol% catalyst loading; TOF = 0.76^{-1}) [274]. The tridentate catalyst **146** (91%) was much more active than the fluorinated derivative **147** (<5%) or the bidentate derivatives **144** (37%; TOF = 0.31^{-1}) and **145** (14%; TOF = 0.12^{-1}), and also the well-established thiourea catalyst **46** resulted in significant lower product formation (12% at −78 °C; 28% at −40 °C). Because **144** should provide a better basis for possible future catalyst development, the authors tested the activity at −40 °C and obtained 52% of the product (Scheme 1.28). To prove the anion-binding mode in this reaction, the authors ran a reaction with 10 mol% **146** in the presence of 20 mol% TBACl and observed no conversion. This was the first anion-binding catalysis utilizing a neutral halogen-bonding donor catalyst and indicated that the number of iodine substituents is relevant for catalyst activity [274].

1.1.4 Miscellaneous Anion-Binding Catalysts

One of the most recent motifs for anion-binding catalysis is anion–π binding. Anion–π interactions are defined as favorable NCIs between anions and arenes' π-acidic faces [275–277] and were first proposed in 2002 based on gas-phase computations [278–280]. In 2013, again Matile's group described a series of π-acidic naphthalenediimides for anion-π-binding Kemp-type elimination [281]. A general base deprotonates 5-nitro-1,2-benzisoxazole **148** in the key step yielding *ortho*-hydroxybenzonitrile **149** as the product (Scheme 1.29). Utilizing tetrabutyl-ammonium hydroxide (TBAOH) as a base, up to 7606-fold rate

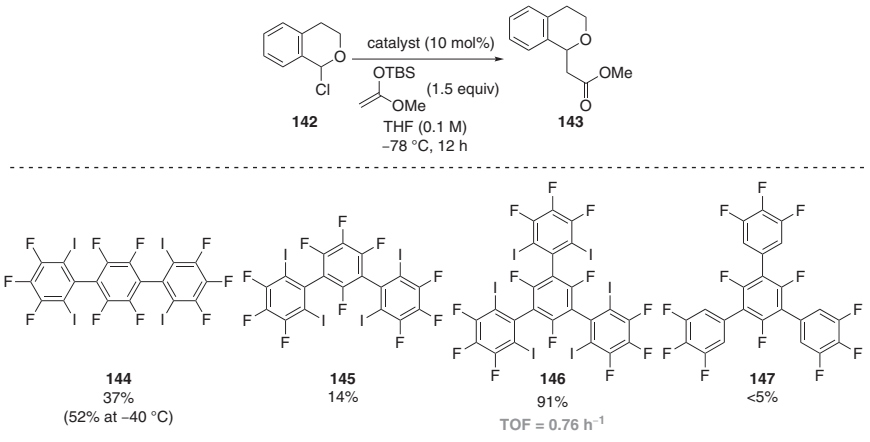

Scheme 1.28 Screening of neutral halogen-bonding derivatives in anion-binding catalysis through chlorine abstraction.

enhancements were observed, corresponding to a transition state stabilization by the naphthalenediimides derivatives of approximately 30 kJ mol^{-1}. Additionally, the authors investigated perylenediimides as a less π-acidic catalyst because of the expanded π-system to examine the π–π interactions in the reaction. The initial rates at high dilution utilizing perylenediimides were significantly lower and indicated the nearly irrelevant contributions of π–π interactions to anion–π catalysis.

Computational investigations using DFT methods (IEFPCM/M06-2X/def2-TZVP/-/IEFPCM/B97-D/6-311G(d,p)) as well as the independence of ground-state stabilization on increasing π-acidity supported this finding [282]. However, in 2014, a theoretical investigation by Lu and Wheeler (CM-M062X/def2-TZVP//PCM-B97-D/6-311g(d,p)) investigated the role of the anion–π interactions utilizing a smaller model system by omitting the linker to the carboxylic acid (**151**; Scheme 1.29c) [283]. The authors concluded that naphthalenediimides stabilizes the substrate complex **150·148** by anion–π binding at least as well as the transition structure, which even leads to a slightly increased activation barrier ($\Delta\Delta G = 0.3$ kcal mol^{-1}) and that additional dispersion interactions such as π–π stacking stabilize **150·148** and furnish the high rate acceleration. In the following years, recent examples of anion–π-binding catalysis [284] and the application of non-covalent π–π-interactions for catalyst design were discussed [285].

In 2014, Berkessel *et al.* presented a pyridinium-based catalyst **153·BPh$_4$** for the alkylation of 1-chloroisochroman (48–92% yield) for which an X-ray structure analysis revealed an anion–π interaction, and an NMR titration indicated a 1 : 1 complex with a binding energy of $\Delta G = 13$ kJ mol^{-1} [286]. Using low catalyst loadings of 2–10 mol% resulted in TOF = 3.7 h^{-1}. The authors described that a non-coordinating anion is important for catalytic activity; otherwise, no anion abstraction was observed. Berkessel's group proposed a mechanism starting with the abstraction of chloride and formation of an ion pair **160**. Without the addition of silyl ketene acetal, this ion pair was observed after 24 h as crystalline species suitable for X-ray analysis, confirming the anion-binding mode of the reaction. By the addition of silyl ketene acetal, C–C bond formation occurred, and after

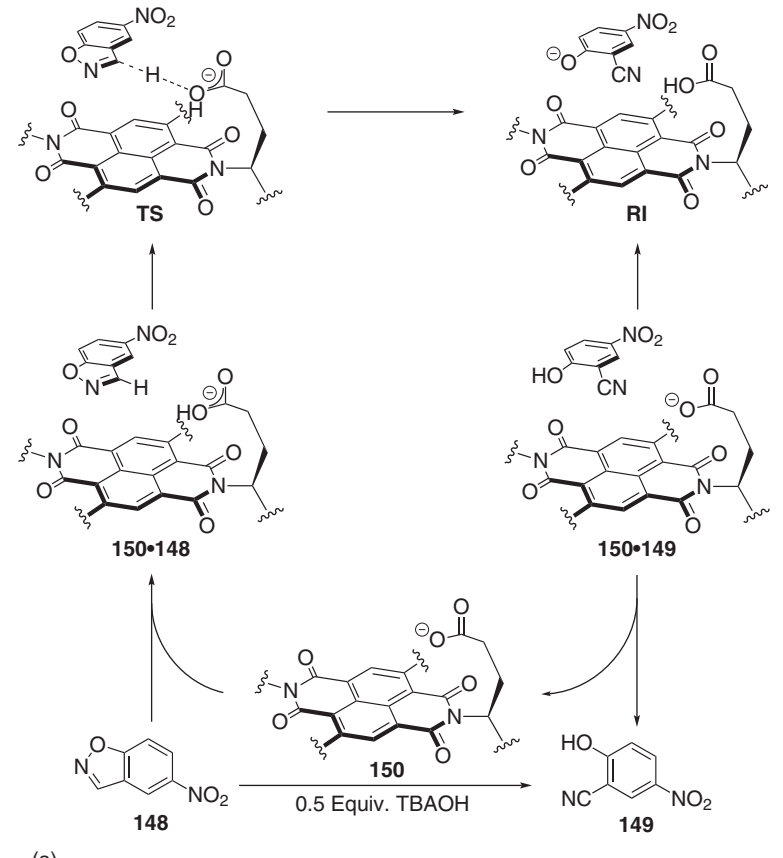

Scheme 1.29 (a) Anion–π-binding mediated Kemp-type elimination of 5-nitro-1,2-benzisoxazole **148**, (b) structure of the most active anion–π catalyst **150**, and (c) reduced model system used for computational investigations by Lu and Wheeler.

desilylation of intermediate **161**, the product and free catalyst were obtained (Scheme 1.30) [286].

For the sake of completeness, we must also mention that 1,1'-binaphthyl-based silanediol [287–289] and thiophosphoramide-based catalysts [290] have been utilized for anion-binding catalysis *via* hydrogen bonding. In 2013, the group of Mattson introduced silanediol **165** for anion-binding-mediated enantioselective acyl Mannich reactions of isoquinolines (Scheme 1.31). The authors proposed an anion abstraction mechanism and nucleophilic attack of silyl ketene acetals to the chiral ion pair and supported this suggestion by crystal structure analysis of the ion pair between **165** and isoquinoline hydrochloride, where **165** binds the chloride and forms a supramolecular complex [287]. Two years later, the same group synthesized derivative **166** that carries four phenyl substituents and showed higher activity (60% *ee* vs. 28% *ee*). Furthermore, Mattson's group suggested that NCIs such as π–π and π–cation interactions contribute to the stabilization of the transition state, which explained the higher stereoinduction of **166** compared to **165** [288].

In 2013, based on the work of Schreiner and coworkers from 2008, where the authors introduced the concept of cooperative catalysis of a Brønsted acid (mandelic acid) and thiourea **46** for Brønsted acid enhancement [291], Nagorny and coworkers utilized a similar catalytic system in [4+2] cycloadditions under mild reaction conditions [290] as compared to previous methods based on the use of highly ionic media, such as lithium perchlorate [292]. In catalyst screening utilizing cyclopentadiene and acrolein acetal **167** as a test reaction, thiophosphoramide **170** was found to be superior to the related thiourea **46** and squaramide **169** in terms of activity (Scheme 1.32). The authors utilized *para*-toluenesulfonic acid that supposedly forms a tetrahedral anion, which explains the high activity of **170** with its ability to form three strong hydrogen bonds to the anion, thus leading to a more stable complex than using **46** or **169**. This effect was support by NMR titration experiments and by the lower activation of HCl that was also activated by the thiourea derivative. With the optimized conditions in hand (6 mol% **170** + 3 mol% *p*-TSA), the authors obtained Diels–Alder products in yields ranging from 57% to 92% (Scheme 1.32). The anion-binding mode in this reaction differs from previously reported reactions in this chapter, where either the nucleophile or the electrophile is activated through anion binding [290].

The sheer number of reactions mirror that anion-binding catalysis, especially utilizing hydrogen-bonding catalysts such as (thio)urea derivatives, is an essential concept in organocatalysis. Moreover, the long known topic *organocatalysis* that had begun in 1832 with the report by Liebig and Wöhler about the well-known cyanide-catalyzed benzoin addition [293] has been very extensively reviewed over the past two decades. We emphasize this because the term "organocatalysis" is a translation of the old and neglected concept "organic catalysts" ("*die organischen Katalysatoren*"), coined by Langenbeck, who recognized the importance of "organic catalysts" and their relationship with the enzymes, with the first authoritative review on this topic as early as 1927 [294–301]. In section 1.2, we present the different modes of substrate activation in anion-binding catalysis. Selected examples from the literature will be used to demonstrate catalyst design concepts; experimental

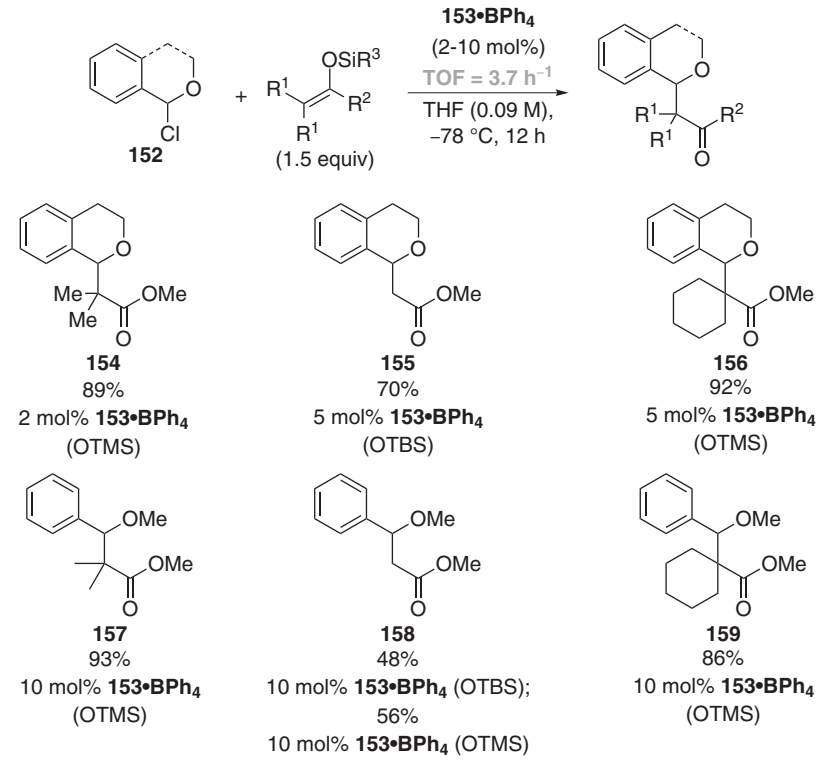

(a)

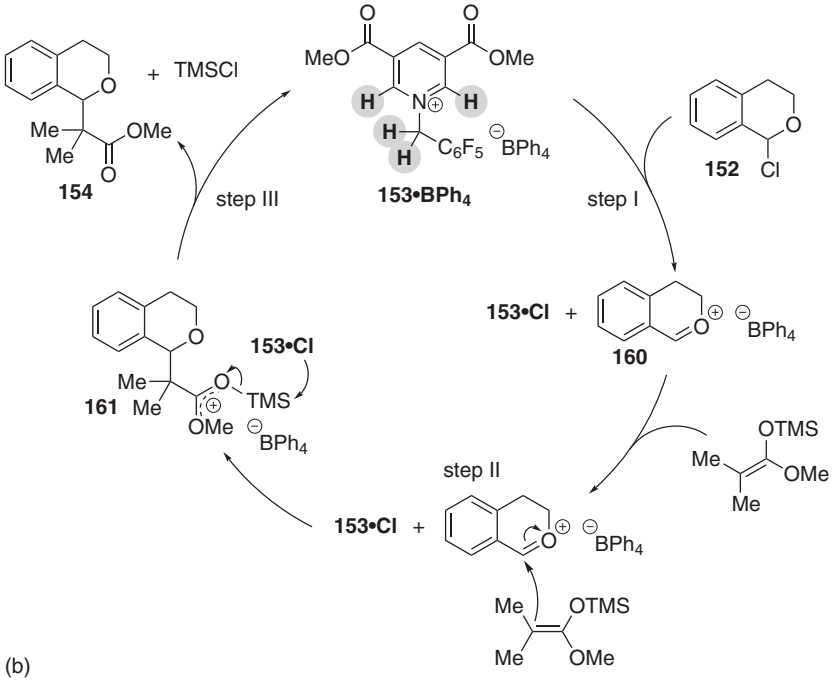

(b)

Scheme 1.30 (a) Products of the **153**·BPh_4-catalyzed substitution reaction; (b) proposed catalytic cycle with formation of the oxocarbenium ion **160,** followed by nucleophilic attack of the silyl ketene acetal. The important protons for anion recognition are highlighted.

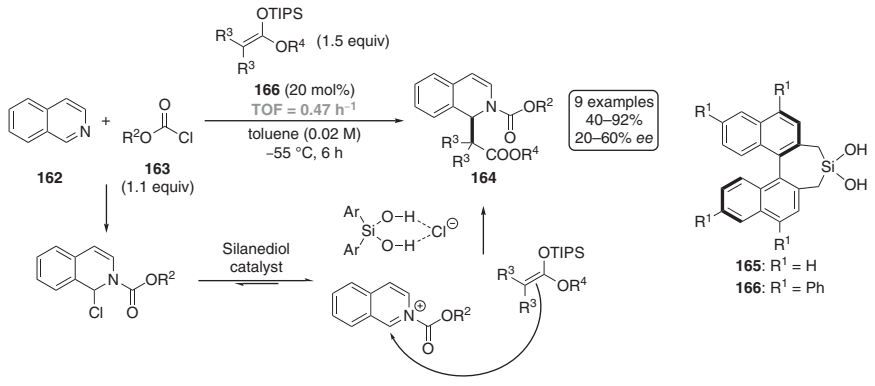

Scheme 1.31 The **166**-catalyed acyl-Mannich reaction utilizing silyl-ketene acetals as a nucleophile.

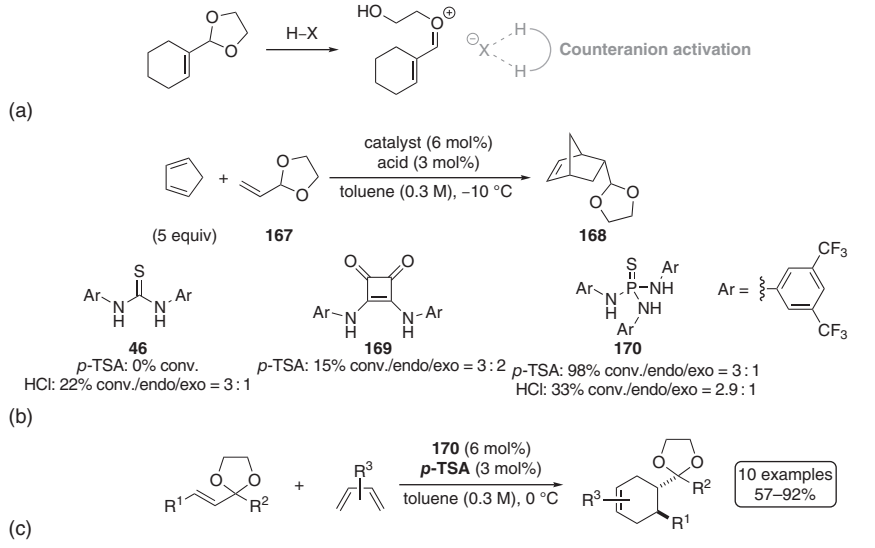

Scheme 1.32 (a) Proposed activation of the oxocarbenium ion in [4+2] cycloadditions *via* Brønsted acid enhancement; (b) comparison of three different hydrogen-bonding catalysts in the activation of the dienophile; and (c) [4+2] cycloadditions catalyzed with the **170**·*p*-TSA system.

details such as structure optimization studies, screening conditions, reaction conditions, and the typical substrate and product spectrum of the representative procedure; and some selected mechanistic studies.

1.2 Concepts in Anion-Binding Catalysis

1.2.1 Introduction

Controlling the stereochemistry of a chemical reaction through charged reagents or catalysts is the goal in asymmetric organic synthesis [302, 303] as every chemical

reaction takes place with changes in polarization or charge [304–306]. Asymmetric induction using chiral catalysts is beneficial from economic and ecological viewpoints because the catalyst is utilized in a sub-stoichiometric amount (even though this is not a requirement for catalysis) [307, 308] and is reusable. Nature also catalyzes reactions this way when using enzymes [309]. Catalysts can be distinguished into metal-based or metal-free catalysts ("organocatalysts"). Further, the organocatalysis field can be divided into two main directions: (i) covalent organocatalysis, where the catalyst interacts with the substrate(s) because of covalent bonding, and (ii) non-covalent organocatalysis, where the catalyst interacts through NCIs such as anion-binding, hydrogen-bonding, halogen-bonding, chalcogenide-bonding, and/or dispersion interactions [310]. As anion-binding catalysis is part of non-covalent organocatalysis, this section will not review the field of covalent organocatalysis as it has been comprehensively reviewed elsewhere [311–319]. The two main parts in non-covalent organocatalysis are on the one hand hydrogen-bonding catalysis [6, 157], where the catalyst activates a neutral electrophile, and on the other hand ion pair catalysis, which is characterized by charged catalyst–substrate species. Furthermore, ion pair catalysis is classified into ion-binding catalysis and counterion-directed catalysis and is additionally sub-classified into anionic type and cationic type (Scheme 1.33) [9].

In 1926, Bjerrum introduced the physical principle of ion pairing, in which ion-pairing catalysis rests on and which derives directly from Coulomb's law [320, 321]. Based on his work, Anslyn and Dougherty defined that an ion pair is present when the electrostatic attraction is greater than the thermal energy $k_B T$ (k_B = Boltzmann constant; T = absolute temperature in K) that would be required for separation [322] because of Brownian motion [323]. The distance λ_B (Bjerrum length) defines the gap between two oppositely charged ions (q_1 and q_2), where the electrostatic interaction is inversely related to the dielectric constant of the medium (ε_r), the vacuum permittivity (ε_0), and the thermal energy $k_B T$. Utilizing Eq. (1.1), the distance where electrostatic interactions matter in catalysis can easily be calculated [321]. Therefore, solvation effects are important in ion pair catalysis.

$$\text{Bjerrum length}: \lambda_B = \frac{q_1 q_2}{4\pi\varepsilon_0\varepsilon_e}\frac{1}{k_B T} \tag{1.1}$$

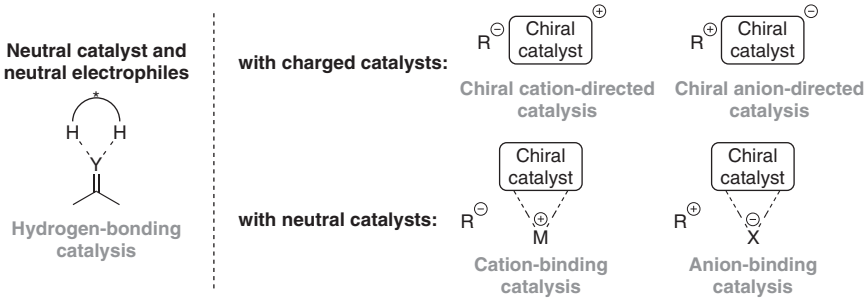

Scheme 1.33 General activation modes of hydrogen-bonding catalysis (left) and ion pair catalysis (right) with counterion-directed catalysis above and counterion-binding catalysis below. Source: Brak and Jacobsen [9].

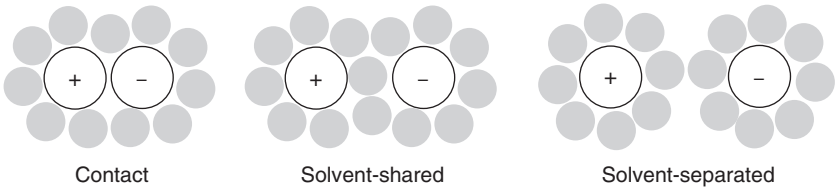

Scheme 1.34 Schematic presentation of different ion pairs . Source: Marcus [324].

Ion pairs are divided into three types that describe the association of the ions and the solvent molecules with one another [324, 325]. A *contact ion pair* exists if both anion and cation share one solvation shell without solvent molecules between them. If solvent molecules are present between the ions, there are two different terms: (i) *solvent shared*, if they share the same solvent shell but are separated through solvent molecules, and (ii) *solvent separated*, if each of the ions has its own solvent shell (Scheme 1.34). Consequently, in ion pair catalysis, the solvent has a significant influence on what type of ion pair exists. Generally, non-polar solvents favor *contact ion pairs* [326, 327], and therefore, in many (enantio)selective reactions, where the selectivity is directed largely by the catalyst, non-polar solvents are usually used.

The synthetic chemist's goal is utilizing small molecules as catalysts compared to nature's catalytic systems, e.g., enzymes [1]. Several intermolecular interactions between the catalyst and the substrate control the selectivity of a reaction, and highly directed catalyst–substrate interactions are required to provide transition-state stabilization. Generally, a distinction is made between four types of interactions as depicted in Scheme 1.35 [9]. Covalent catalysis such as iminium-based catalysis [328, 329] or metal-based Lewis acid catalysis [330, 331] has successfully been utilized for carbonyl activation in enantioselective addition reactions, and both rely on strong and directional interactions. Organic-based Lewis acid catalysis and Brønsted acid catalysis are based on weaker and less-directional interactions between the substrate and the catalyst [1, 11]. While these three types of catalytic systems obviously work well in enantioselective catalysis, ion-paring catalysis is the best strategy for enantioselective transformations when charged intermediates are present. Because ion pairing interactions are inherently less directional, the design of (an)ion-binding catalyst for (enantio)selective reactions combined with low catalyst loadings is a real

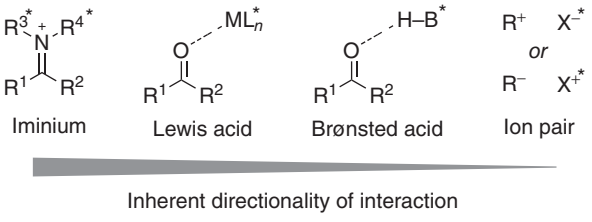

Scheme 1.35 Trend of directionality in common asymmetric catalyst–substrate interactions (L_n^* = chiral ligand; B*H = chiral Brønsted acid, X* = chiral counterion) [9]. Source: Based on Brak and Jacobsen [9].

challenge [9, 10]. However, in the past years, a large number of small molecules were described that operate through the general mechanism depicted in Scheme 1.33.

Note that the concepts of anion-binding catalysis and counterion-directed catalysis are quite different: in anion-binding catalysis, the catalyst binds the anion resulting in a supramolecular complex. In counterion-directed catalysis, such as the well-known asymmetric counterion-directed catalysis (ACDC) [12], the catalyst is an ion pair, e.g., **174**. In ACDC, the chiral counteranion of the catalyst induces stereochemistry, e.g., in the reduction of α,β-unsaturated aldehyde **175** depicted in Scheme 1.36 [332]. First, the formation of a chiral iminium–phosphoric acid ion pair occurs, followed by reduction with Hantzsch ester and formation of **176**. In contrast, the neutral (or positively charged) catalyst conveys the stereoinduction in asymmetric anion-binding catalysis, which is depicted for the Strecker reaction of aldimine **172**. Catalyst **171** binds the cyanide anion in a supramolecular complex. Moreover, catalyst and cyanide ion bind the aldimine *via* hydrogen-bonding interactions, and product **173** forms after nucleophilic attack (Scheme 1.36) [184].

One important characteristic of anion-binding catalysis is that the anion-binding motif of the catalyst only participates in the anion recognition process and does not engage in protonation or deprotonation, which distinguishes anion-binding catalysis from, e.g., guanidinium catalysis. Scheme 1.37 depicts an example of a guanidine-catalyzed asymmetric Strecker reaction utilizing C_2-symmetric **177** that emphasizes these differences [333]. Corey and Grogan postulated a mechanism that starts with the catalyst's coordination (**177**·**HCN**) and deprotonation of HCN, while coordination of imine **178** gives complex (**179**). After nucleophilic attack of the cyanide, the catalyst reprotonates the imine to furnish product **180**, however, not with the HCN proton but rather with the catalyst's proton. The mechanism was supported by computational studies using DFT methods (B3LYP/6-31G(d)) by Han and coworkers [334].

Most asymmetric anion-binding catalysts bear additional structural elements for substrate activation, e.g., dispersion interaction donors/acceptors [335, 336] or additional hydrogen bond donors/acceptors, and not only the "*anion recognition motif*." In the following sections, the catalyst applications are categorized by their mode of activation, and the evolution of the catalysts regarding conversion and stereoinduction will be discussed with some representative examples. The main activation modes in anion-binding catalysis can be separated into five mechanisms (Scheme 1.38):

(1) *Addition reaction catalyzed via anion binding* [176, 184]: The electrophile **E** is activated *via* a Lewis acid – formally the "leaving group" **M** of the nucleophile $\mathbf{Nu}^-$ – and the catalyst binds the nucleophile. Additionally, NCIs such as, e.g., a π-cation [337], and hydrogen-bonding [184] interactions take place between the catalyst and the electrophile. The nucleophilic attack occurs directly in the supramolecular complex (Scheme 1.38a).
(2) *Catalysis of S_N1-type reactions via anion abstraction and delivery of a cationic species* [242, 338]: The catalyst binds to the leaving group ($\mathbf{X}^-$) and intermolecular nucleophilic attack occurs (Scheme 1.38b). A similar activation mode takes

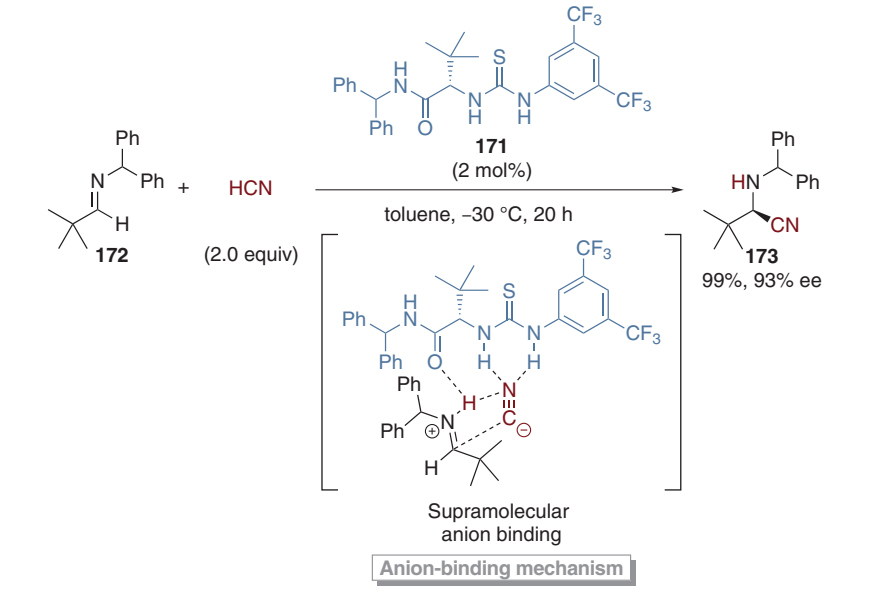

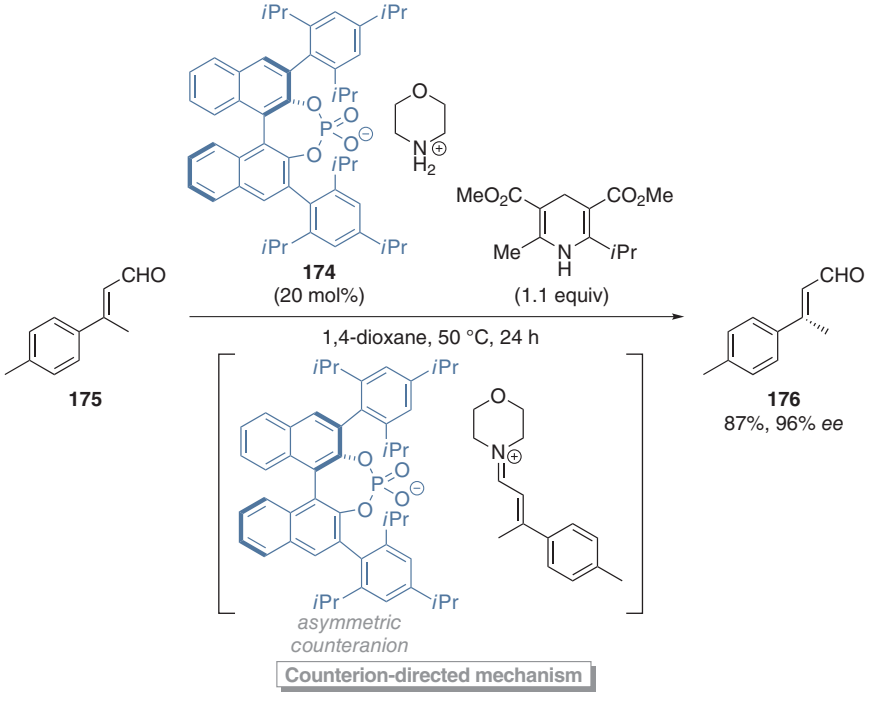

Scheme 1.36 Comparison of the anion-binding mode and the counterion-directed mechanism in asymmetric catalysis. The catalysts are shown in blue and the atoms of the HCN molecule in red for visualization of the anion-binding mode.

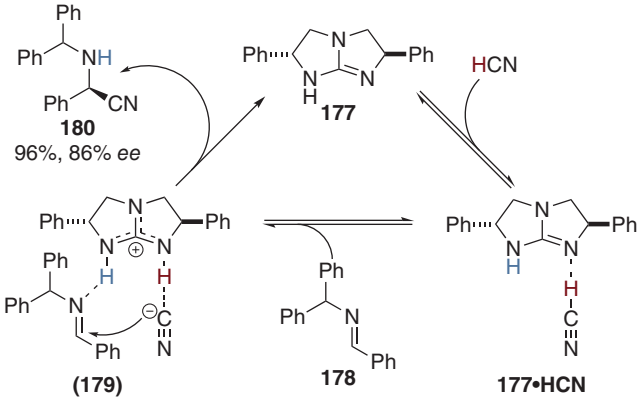

Scheme 1.37 Asymmetric Strecker reaction catalyzed by C_2-symmetric guanidine **177**.

place in the cationic cyclization of iminium [339] or allyl cations [340] *via* anion abstraction.

(3) *Cooperative catalysis with an achiral nucleophilic* ***cocatalyst*** [341]: The **cocatalyst** activates the electrophile **E** and the anion-binding catalyst recognizes the leaving group $\mathbf{X}^-$. Two mechanisms are described: either the direct nucleophilic attack that furnishes the product and the catalyst [342] or an anion exchange from $\mathbf{X}^-$ to $\mathbf{Nu}^-$ with subsequent nucleophilic attack on the electrophile (Scheme 1.38c) [337, 343].

(4) *Lewis acid enhancement catalysis by recognition of a Lewis base* [344, 345]: An initial Lewis acid $\mathbf{LB–LA_1}$ – typically trialkylsilyl triflates – dissociates and the anion-binding catalyst binds the Lewis basic part "LB" (triflate) as well as the Lewis acidic part "$\mathbf{LA_1}$" (trialkylsilyl), leading to an enhanced Lewis acid. The catalyst binds the electrophile, which also possesses a Lewis acidic part "$\mathbf{LA_2}$" – similar to "LA_1" – by NCIs. After the nucleophilic attack, the product and the enhanced Lewis acid catalyst – containing Lewis acidic part "$\mathbf{LA_2}$" – form (Scheme 1.38d).

(5) *Phase transfer catalysis via anion delivery*: The catalyst binds an anion $\mathbf{X}^-$ that derives from a soluble and an insoluble salt (in organic solvents) such as cesium fluoride [346, 347] or potassium fluoride [348] and forms a soluble ion pair. Additionally, the catalyst binds the electrophile through NCIs and the nucleophilic attack occurs directly in the supramolecular complex (Scheme 1.38e).

1.2.2 Anion-Binding Catalysis in Addition Reactions

In 1998, Sigman and Jacobsen utilized a library of polystyrene-bound Schiff bases and high-throughput screening (HTS) in the asymmetric Strecker reaction of *N*-allyl benzaldimine with TBSCN as the cyanide source and described the first asymmetric thiourea organocatalyst (Scheme 1.10) [174]. The basic goal of this research work was to find a new tridentate ligand for a chiral organometallic catalytic system; therefore, the authors used solid-phase synthesis and systematic structure

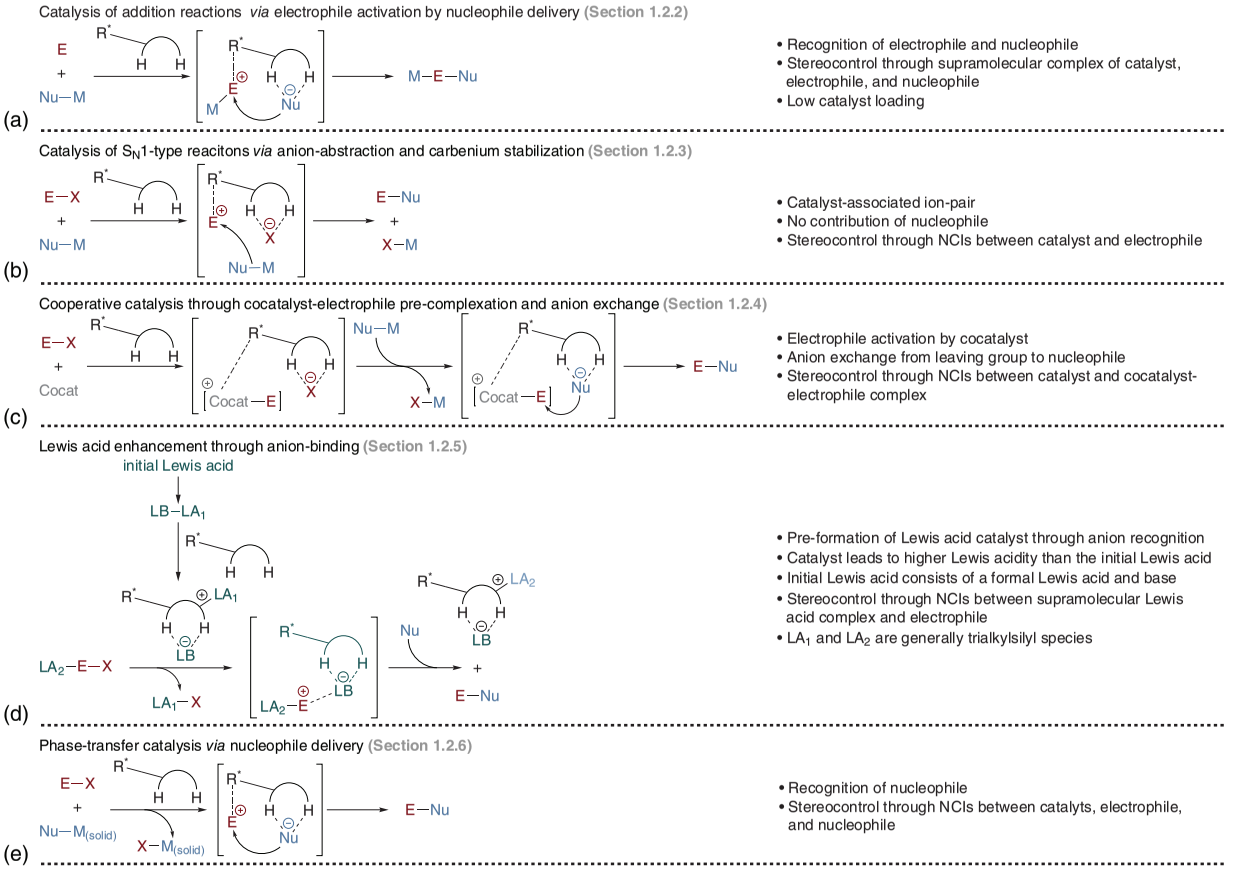

Scheme 1.38 The five different activation modes in asymmetric anion-binding catalysis: (a) Addition reactions *via* binding of the anionic nucleophile, (b) S_N1-type reactions by anion abstraction, (c) cooperative catalysis with anion exchange from the counterion to the nucleophile, (d) binding of a Lewis base and formation of a Lewis acid with enhanced acidity, and (e) phase transfer catalysis *via* nucleophile delivery.

optimization variations leading to high diversity of potential catalysts. The core structure of the tridentate ligand was based on a chiral amino alcohol and a salicylaldehyde derivative, which coordinates a metal ion. In order to implement the idea of solid-phase synthesis, the amino alcohol was replaced with chiral 1,2-diamines ((*R,R*)-1,2-diaminocyclohexane or (*R,R*)-1,2-diphenyl-ethylendiamine), which could be attached *via* a linker to a solid support. In addition, a second chiral element, an amino acid, was incorporated and linked *via* caproic acid (linker 1) to the polystyrene support and *via* a (thio)urea or a guanidine group (linker 2) to the chiral diamine (Scheme 1.39) [174].

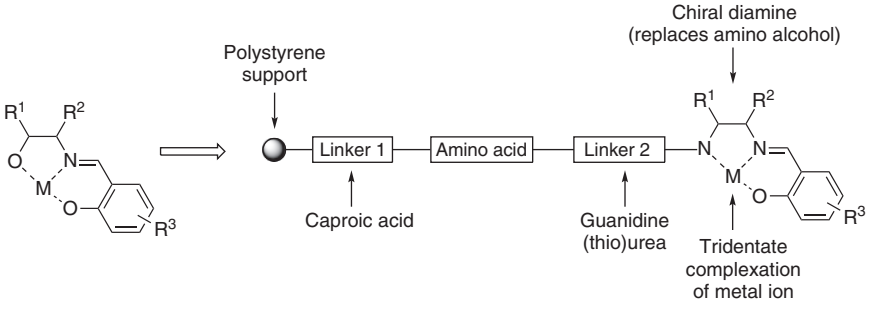

Scheme 1.39 Initial work stream for HTS optimization to identify chiral metal ligand for enantioselective metal-based Strecker reaction.

Sigman and Jacobsen performed iterative HTS optimization of the Strecker reaction enantioselectivity with three libraries consisting of 12 (library 1), 48 (library 2), and 132 (library 3) polymer-bound catalyst candidates. Library 1 (variation of the metal ion) led to the highest enantioselectivity when the pure, metal-free organocatalytic system (19% *ee*) was utilized rather than in the presence of a metal ion (11 complexes tested, highest enantioselectivity: Ru = 13% *ee*). In Library 2, the general influence of both linkers, the relative stereochemistry of the amino acid compared to the diamine, the amino acid unit, and the substitution pattern of the salicylaldehyde derivative were investigated. The authors found that linker 1 (caproic acid) leads to an unspecified background side reaction and was therefore removed, leading to the amino acid unit coupled directly to the polystyrene support. Furthermore, Sigman and Jacobsen observed the highest *ee*-values with the 3-*tert*-butyl-substituted salicylaldehyde and leucine as amino acid. The relative stereochemistry of the catalyst was important for enantioselectivity; with (*R,R*)-diamine derivatives and L-leucine (32% *ee*), the enantioselectivity was much higher than with D-leucine (5% *ee*). Linker 2 was also found to be crucial for enantioselectivity, and thiourea derivatives (55% *ee*) turned out to be superior to either urea-based systems (45% *ee*) or guanidine derivatives (21% *ee*). The focus of library 3 was on different non-polar amino acids, 1,2-diamino derivatives, and the substitution pattern of the salicylaldehyde unit. Sigman and Jacobsen found bulky L-*tert*-leucine and 3-*tert*-butyl-5-methoxysalicylaldehyde to provide the best results. Moreover, (*R,R*)-1,2-diaminocyclohexane was found to be slightly superior to (*R,R*)-1,2-diphenyl-ethylendiamine, and finally, Schiff base thiourea **48** was

determined as the most efficient catalyst in terms of enantioselectivity [174]. The corresponding Schiff base thiourea **47** incorporating the important units of the polystyrene-bound derivative **48** was synthesized independently in solution and tested in the asymmetric Strecker reaction of aromatic as well as aliphatic *N*-allyl-imine derivatives. Utilizing 2 mol% of catalyst **47** and HCN as a cyanide source, trifluoroacetylated Strecker adducts were formed in the range from 65% to 92% yield and *ee*-values of 70–91% (cf. Scheme 1.10) [174]. Based on the core structure of catalyst **47**, Jacobsen and coworkers constructed a new optimization library of 70 polymer-bound Schiff bases incorporating seven amino acids with large α-substituents and ten new salicylaldehyde derivatives in 2000 [349]. After evaluating each library member in HCN [350] by adding to the *N*-allyl imine of pivaldehyde at 23 °C, polymer-bound 5-pivaloyl-substituded derivative **181** was found as the most efficient catalyst. Furthermore, Jacobsen's group synthesized the urea derivative **182** because of the higher solubility and easier preparation and observed comparable catalyst efficiency and utilized **182** in the asymmetric Strecker reaction of various aliphatic as well as aromatic aldimines and ketoimines (Scheme 1.40).

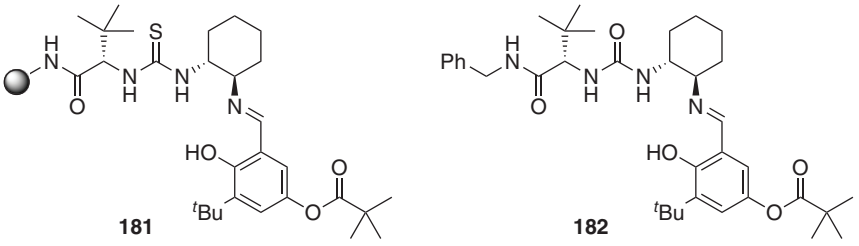

Scheme 1.40 More active Schiff base catalyst **181** found by HTS and the polymer-free urea derivative **182**.

In 2002, Vachal and Jacobsen utilized NMR spectroscopy, kinetic structure–activity relationships, and DFT studies (at the uncorrected B3LYP/6-31G(d,p) level of theory on a much simplified system to model the catalyst–imine and catalyst–product complexes in the gas phase) to elucidate the activation mode of Schiff base **182** [351]. Based on NOESY and ROESY NMR, the authors found that **182** exists in a well-defined secondary structure with the urea moiety in a *syn–syn* conformation. The kinetics of the hydrocyanation followed Michaelis–Menten kinetics, with first-order dependence on **182** and HCN, and saturation kinetics with respect to the imine substrate. Through alkylation of the urea nitrogens, or replacement of the urea moiety by a carbamate unit, the authors found that both urea N–H protons bind the imine substrate, similar to proposals by Wittkopp and Schreiner [158, 352]. Based on multiple NOE interactions between **182** and a series of *Z*-imines, such as 3,4-dihydroisoquinoline, Vachal and Jacobsen determined the orientation between the substrate and the catalyst. Cross-peaks of the catalyst in the free and bound state were essentially invariant and indicated that no significant change in conformation results from binding the substrate. The authors describe a clamp-like hydrogen-bonding interaction of both urea N–H to the imine-nitrogen, with the substrate being twisted. Furthermore, titration of the catalyst with *Z*-imines

results in up-field shifts of the two urea protons to similar degrees, supporting this proposal. The gas-phase DFT studies underscored the results of the NMR measurements, even though the computed structure of the catalyst–product complex only provided one hydrogen bond as the most energetically favorable complex. The bridging interaction in the catalyst–substrate complex was found stronger (8.5 kcal mol^{-1} for urea; 10.0 kcal mol^{-1} for thiourea) than the single hydrogen bond event (5.0 and 6.3 kcal mol^{-1}, respectively). Based on these results, the authors describe the reversible formation of an imine–catalyst complex with **182** binding the imine through hydrogen bonding (cf. Scheme 1.8), with approximately 80% formation of the complex found in NMR experiments. Furthermore, the model of the catalyst–substrate complex provided information about the observed scope and stereoselectivity of the Schiff base (thio)urea-catalyzed Strecker reaction:

(1) The large group on the imine carbon is directed away from the catalyst and into the solvent. This explains why the Schiff base catalyst promoted hydrocyanations with high *ee*-values, regardless of the steric and electronic properties of the substrate.
(2) The small group (H for aldimines and Me for methylketoimines) is directed toward the catalyst, which indicates that ketoimines bearing larger substituents are poor substrates for the reaction, presumably because they could not adopt the optimal geometry.
(3) The N-substituent is also directed away from the catalyst. However, its size is restricted as a result of the requirement to access the *Z*-isomer of the imine.
(4) On the basis of the observed trend of stereoinduction, addition of HCN takes place over the diaminocyclohexane portion of the catalyst and away from the amino acid/amide portion.

Following the work of Kotke and Schreiner in anion-binding catalysis in 2006 (cf. Schemes 1.12 and 1.13 [176]), Zuend and Jacobsen re-examined the cyanide addition to imines utilizing computations, Hammett analyses, catalyst structure/activity relationships, and isotope labeling studies and concluded that non-covalent interactions are crucial for stereoinduction [184]. The authors utilized modified (thio)urea derivatives of catalyst **182** and instead of the diaminocyclohexane moiety various phenyl substituents were incorporated, especially the well-established 3,5-bis(trifluoromethyl)phenyl group [190]. Similar to the work of Vachal and Jacobsen in 2002, Zuend and Jacobsen observed first-order kinetics for imine and HCN; however, the value of 0.8 for the catalyst is different from the previous work utilizing **182** (*vide supra*). Utilizing "same excess" experiments, the authors excluded deactivation of the catalyst and that product inhibition was negligible. After the authors excluded the competitive uncatalyzed background reaction due to the high *ee*-values and the slow initial rate of approximately 5% compared to the catalyzed reaction, they proposed a small degree of catalyst dimerization that was also observed in previous work [353, 354]. A Hammett analysis for distinguishing the two possible reaction pathways that could be started by protonation of the imine (Scheme 1.41a) or by addition of cyanide to the imine (Scheme 1.41b) provided strong evidence for the former because negative ρ-values were obtained

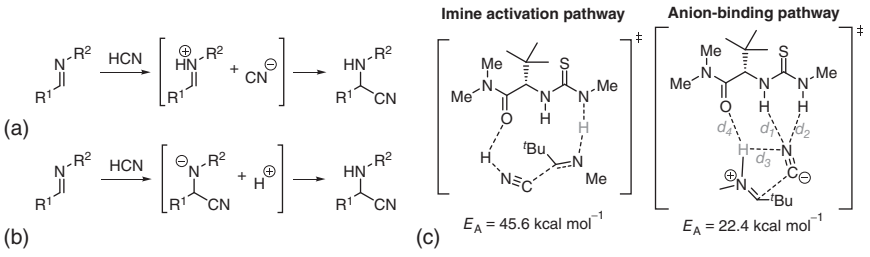

Scheme 1.41 Two possible mechanistic pathways of (thio)urea-catalyzed Strecker reaction *via* (a) an iminium ion or (b) an α-aminonitrile anion and (c) computed activation energies for both reaction pathways.

($\rho_{\text{thiourea}} = -2.7$; $\rho_{\text{urea}} = -2.5$). Additionally, utilizing uncorrected DFT gas-phase computations (B3LYP/6-31G(d)) on a reduced model system (cf. Scheme 1.41c) at 0 K, the authors found that the activation barrier for the iminium activation pathway was approximately 23 kcal mol^{-1} higher in energy than the anion-binding pathway and that the activation energy using urea catalyst is about 5.6 kcal mol^{-1} higher than that of the thiourea catalyst [184].

Based on these result, Zuend and Jacobsen investigated a mechanism based on the thiourea binding the cyanide and forming an ion pair complex with the iminium ion utilizing isotope labeling experiments [184]. The authors utilized DCN and obtained the N-deuterated Strecker product, which indicated that the N–H protons of the (thio)urea moiety do not acts as Brønsted acids as would be required in pathway **B** (Scheme 1.41c). Based on the computations noted above, the authors proposed a reaction pathway that includes proton transfer of HCN (or HNC) to the imine, and generation of a thiourea-bound cyanide–iminium ion pair (Scheme 1.41c). The experimental energy differences (ΔG) between the HCN and HNC protonation pathways were too low to be distinguished. Nevertheless, the outcome is the same, as the HNC protonation pathway convert into the HCN protonation pathway because of rearrangement of the cyanide ion during the reaction. This proposed mechanism was supported by the strong correlation between the experimental and the computed enantioselectivities for eight different thiourea catalysts. To elucidate the stereoinduction, correlation plots were constructed for different bond lengths vs. enantioselectivity. No trend was observed when plotting the sum of the computed thiourea–cyanide bond lengths ($d_1 + d_2$) vs. enantioselectivity, implying that the enantioselectivity cannot result from the stabilization of the cyanide. In contrast, a positive correlation was observed between the enantioselectivities and the computed imine N–H hydrogen bond distances to the cyanide anion and amide carbonyl ($d_3 + d_4$) (Scheme 1.41c). Therefore, the enantioselectivity can be ascribed to the stabilization of the iminium cation in the diastereomeric transition states of the ion pair rearrangement [184]. All in all, the authors showed that secondary design elements for the formation of NCIs are crucial for stereoinduction. Simultaneously, Jacobsen's group utilized thiourea **183** (2 mol%) in Strecker reactions of various imines and obtained the products **185** in yields ranging from 96% to 99% and *ee*-values of 73% to 99% [355]. Compared to the previously utilized Schiff base **182**,

the catalyst loading was slightly higher, but the yields and *ee*-values significantly increased. The authors developed two different methods for the *in situ* generation of HCN utilizing KCN + AcOH or TMSCN + MeOH. The KCN/AcOH method gave the products with slightly decreased enantioselectivities at higher reaction temperatures, concentrations, and reaction rates (Scheme 1.42). Additionally, solid KCN is more practical than liquid TMSCN, and starting with the imine of pivaldehyde, Jacobsen's group obtained (*R*)-Boc-*tert*-leucine in 62–65% yield of crystalline product and 98–99% *ee* over four steps [355].

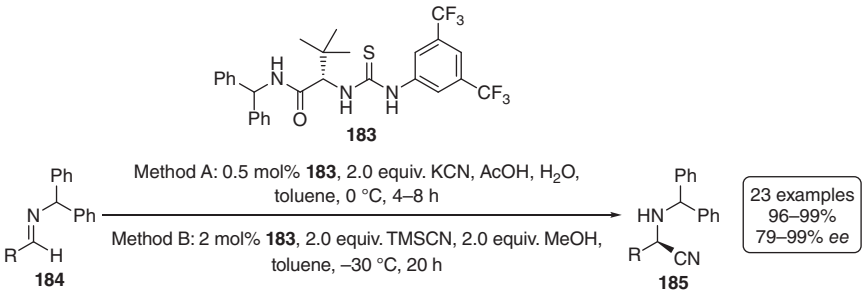

Scheme 1.42 The improved Strecker reaction of various aldimines with thiourea **183** with two different HCN sources.

In addition to the Strecker reaction, the Michael addition is a common and often used reaction in organic synthesis [356–358]. In 2003, Takemoto and coworkers introduced bifunctional catalyst **49** for the use in this kind of addition reaction (cf. Scheme 1.11) [161]. Takemoto's group synthesized a series of diaminocyclohexane-based thioureas (e.g., **49** and **189–192**) and screened them in the model Michael addition of diethyl malonate **186** to *trans*-β-nitrostyrene **187** at room temperature (Scheme 1.43). The authors identified tertiary amine-functionalized **49** as the most efficient catalyst in terms of catalytic activity (86% yield; 24 h) and enantioinduction (83% *ee*). Utilizing the chiral amine **189** that lacks the thiourea moiety, Takemoto's group obtained **188** in only 14% yield (24 h) and 35% *ee*. With achiral **190** lacking the tertiary amine group (requiring addition of 10 mol% triethylamine), the authors provided **188** in only 57% yield after 24 h. Using bulkier tertiary amine **191** and longer reaction time (48 h), the yield decreased (76%; 48 h) and the *ee*-value was slightly lower (87%). Comparing **49** and **192**, which lacks the two CF_3 groups, the advantage of the 3,5-bis(trifluoromethyl)phenyl motif was well recognized [157, 158, 190], as **192** provided the Michael adduct in only 58% yield and 80% *ee* within 48 h (Scheme 1.43) [161].

In 2005, Takemoto's group investigated the mechanism of the **49**-catalyzed Michael addition utilizing NMR kinetic studies and NMR titrations and postulated a reaction mechanism that starts with the deprotonation of the C–H-acidic 1,3-dicarbonyl compound by the tertiary amine and formation of complex (**193**), in which the six-membered enol of **187** is stabilized through interactions with the protonated tertiary amine group of **54** [175]. Subsequently, thiourea's N–H protons coordinate with the Michael acceptor through hydrogen-bonding interactions

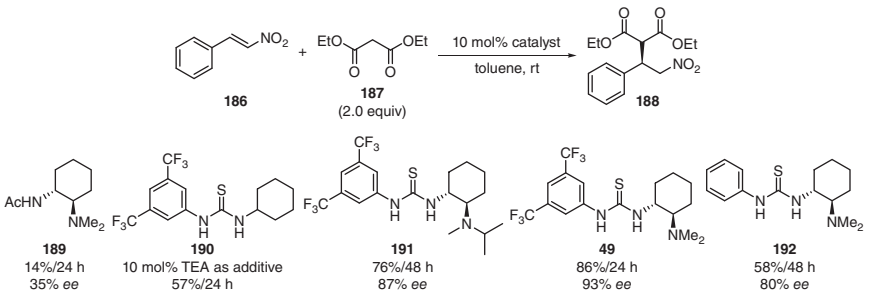

Scheme 1.43 Catalyst screening using chiral 1,2-diaminocyclohexane **413** and various thiourea derivatives in asymmetric Michael addition of diethyl malonate to *trans*-β-nitrostyrene.

resulting in the organized ternary complex (**194**) and a relative orientation that allows nucleophilic attack in an (*R*)-favored mode leading to complex (**195**). After final protonation, the catalyst–product complex dissociates and furnishes free catalyst and **188** (Scheme 1.44). Based on this proposed mechanism, Liu and coworkers performed DFT computations (B3LYP/6-31G(d)), utilizing diethyl malonate and simplified nitroethene as well as the corresponding urea of **49**

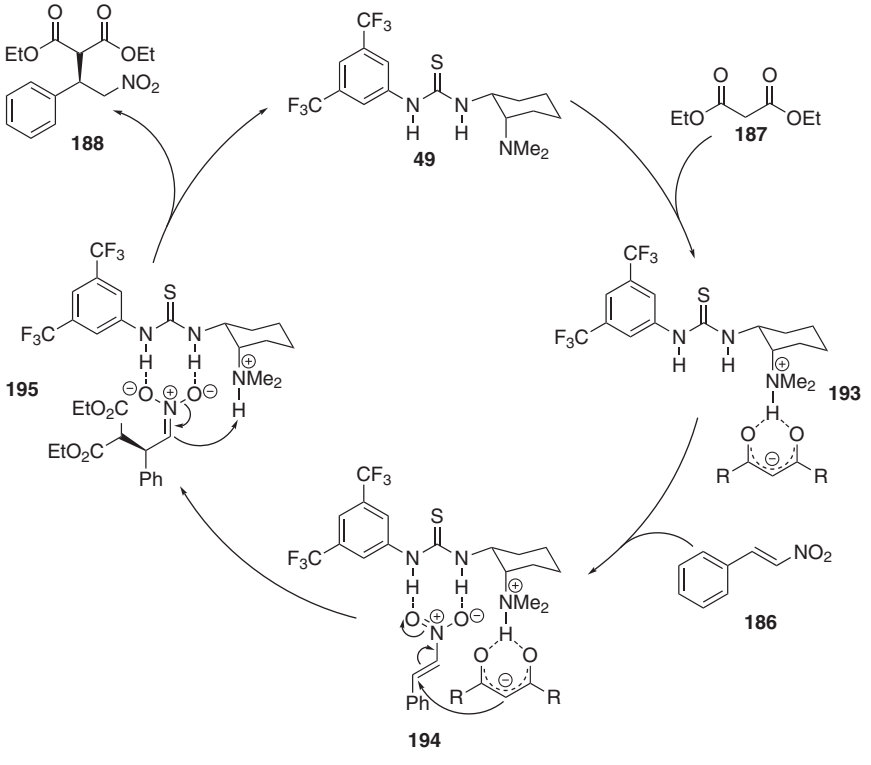

Scheme 1.44 Postulated mechanism of the enantioselective Michael addition between *trans*-β-nitrostyrene **186** and diethyl malonate **187** promoted by bifunctional **49**.

unfortunately lacking the 3,5-bis(trifluoromethyl)phenyl substituent, and proposed that the C–C bond formation step from **194** to **195** is enantiodetermining, while the reprotonation from catalyst's amine to the α-carbon in complex **195** was identified as the rate-determining step [359].

In the following years, thiourea **49** and its derivatives were well established in organic synthesis and were utilized in many asymmetric reactions [4, 360–363]. The synergetic activation of nucleophile and electrophile, leading to high conversion and enantioselectivity, was generally accepted. In 2006, Soós, Pápai, and coworkers reinvestigated the mechanism of the **49**-catalyzed Michael addition utilizing DFT methods (B3LYP/6-311++G(d,p)//B3LYP/6-31G(d)), with β-nitrostyrene as Michael acceptor and 2,4-pentadienone as Michael donor [364]. The authors investigated in addition to Takemoto's mechanism (hydrogen-bonding activation; pathway A) an alternative mechanism *via* anion binding of the enolate (pathway B). Both mechanisms afford the (*R*)-configured product; nevertheless, the transition structure for pathway B is preferred by $\Delta\Delta G = 2.7\,\mathrm{kcal\,mol^{-1}}$ compared to pathway A because of the higher number of NCIs. This theoretical study reveals the alternative mechanism of the **49**-catalyzed Michael addition and provides strong evidence for the anion-binding mode. In 2019, Hirschi, Vetticatt, and coworkers utilized a combination of experimental ^{13}C kinetic isotope effects (KIEs) and DFT computations (B3LYP/6-31+G(d,p)/PCM (toluene)) for mechanistic investigations on the **49**-catalyzed Michael addition of diethyl malonate to β-nitrostyrene [365]. The authors found the lowest lying transition structure **196**, which is very similar to that described in previous work [366]. Moreover, the lowest lying transition structure **197** of the opposite enantiomer was $\Delta\Delta G = 2.4\,\mathrm{kcal\,mol^{-1}}$ higher in energy because of the lack of the stabilizing hydrogen bond between the ortho C–H and the carbonyl oxygen. Furthermore, a similar transition structure **198** to that postulated by Takemoto's group (hydrogen bond activation of the nitroolefin) [175], but incorporating an additional hydrogen bond between ortho C–H and the carbonyl oxygen, was computed and found to be $\Delta\Delta G = 4.7\,\mathrm{kcal\,mol^{-1}}$ higher in energy (Scheme 1.45). The authors also computed the transition structures for the deprotonation of the diethyl malonate and the reprotonation of the nitronate, and the corresponding KIEs for the key carbon atoms of the reactants for all computed transition structures. The authors found that the C–C bond forming step is the rate-determining as well as the enantiodetermining step of this reaction, which was inconsistent to the proposed mechanism by Liu and coworkers [359], who postulated the reprotonation of the nitronate as the rate-determining step. The work by Hirschi, Vetticatt, and coworkers confirmed the anion-binding mode of the **49**-catalyzed Michael addition.

1.2.3 Anion-Binding Catalysis in Substitution Reactions

(Thio)ureas are well known as potent halide-binding hosts in supramolecular chemistry, and the corresponding supramolecular complexes could be easily investigated *via* ^{1}H NMR and IR spectroscopy [82, 367]. Therefore, over the years, many halide-binding approaches utilizing (thio)ureas were developed, in particular,

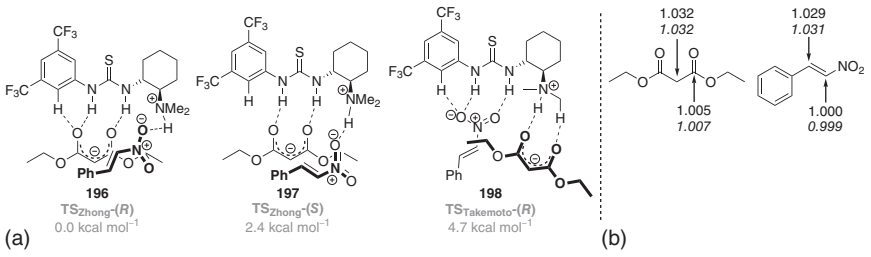

Scheme 1.45 (a) Three computed transition structures for the Michael addition of diethyl malonate and β-nitrostyrene with Δ*G* values related to **196** and (b) experimental KIE and computed (italics) KIE for C–C bond forming step as the rate-determining step.

for halide abstraction and substitution reactions [2, 9, 10]. In 2002, Wenzel and Jacobsen used a Schiff base catalyst in asymmetric Mannich reactions for the synthesis of β-aryl-β-amino acids and proposed an activation of the utilized *N*-Boc aldimines through hydrogen bonding [368], similar to the proposed activation mode in Strecker reactions by Vachal and Jacobsen (*vide supra*) [351]. In 2004, based on the work of Wenzel and Jacobsen, Taylor and Jacobsen presented the cyclization of indole derivatives **200** because of an asymmetric acetyl Pictet–Spengler reaction and suggested a similar activation mode [338]. The authors screened various thiourea derivatives, such as Schiff base **182** (cf. Scheme 1.40). Utilizing acetic anhydride, Taylor and Jacobsen did not observe product formation, even at high temperatures (Pictet–Spengler conditions). Switching to acetyl chloride as the acetylation reagent, the authors obtained the product in 65% and 59% *ee* catalyzed with 10 mol% **182**. After structure optimization of the catalyst, **199** was described as the most active one, bearing 2-methyl-5-phenylpyrrole moiety instead of the salicylaldehyde unit in **182** (70% yield; 93% *ee*). The authors described activation of the acyl-iminium ion by the thiourea's N–H protons and obtained Pictet–Spengler products **201** in yields ranging from 65% to 81% and *ee*-values of 86–95%, utilizing 5 or 10 mol% catalyst loading, whereby the imine substrate was generated *in situ* by condensation of the tryptamine derivatives with the corresponding aldehyde (Scheme 1.46). Furthermore, the products could be easily converted to tetrahydro-β-carbolines that are core structure elements in natural compounds [369, 370].

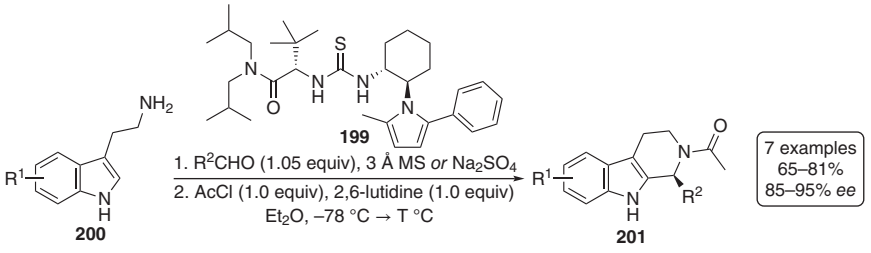

Scheme 1.46 Asymmetric acetyl Pictet–Spengler reaction catalyzed with 5 or 10 mol% **199**.

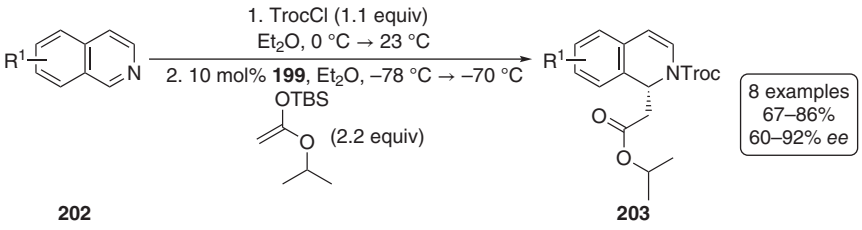

Scheme 1.47 Enantioselective acyl-Mannich reactions utilizing various substituted isoquinolines catalyzed with **199**.

In 2005, the same group utilized **199** in asymmetric acyl-Mannich reactions of isoquinolines **202** and obtained substituted dihydroisoquinolines **203** in yields ranging from 67% to 86% and *ee*-values of 60–92%, utilizing 10 mol% catalyst loading (Scheme 1.47) [371]. Additionally, Jacobsen's group observed in the acyl-Mannich as well as in the acyl Pictet–Spengler reactions a pronounced solvent effect, with diethyl ether providing the highest *ee*-values. The authors pointed out that the nature of the acyl-imine adduct is important in the reaction and deemed TrocCl the best acylation reagent, with *tert*-butyldimethylsilyl ketene acetal being the most reactive nucleophile. Bose, Spiegelman, and Manhas observed in the acylation of benzylimine with various acyl chlorides the formation of a covalent chloroamide in non-polar solvents, such as carbon tetrachloride [372]. Based on this work, and because of the strong leaving group effect of the acylation reagent and the high enantioinduction in non-polar solvents, such as diethyl ether, Jacobsen's group postulated the presence of the chloroamide structure, rather than the *N*-acylium chloride structure of the acyl-imine adduct [371].

In 2007, Jacobsen's group presented the enantioselective Pictet–Spengler-type cyclization of β-indolyl ethyl hydroxy lactams **205** utilizing TMSCl as a dehydrating agent to form *in situ* and irreversibly the corresponding chloride derivatives [373]. The hydroxy lactam substrates were synthesized either by imide reduction utilizing $NaBH_4$ or by imide alkylation with organolithium reagents. The authors obtained the cyclization products **206** in yields ranging from 51% to 94% and *ee*-values of 81–99%, utilizing pyrrole-based catalyst **204** (Scheme 1.48), which is the *N*-methylpentyl amide derivative of **199** (cf. Scheme 1.46) [373].

Jacobsen's group also investigated the mechanism using substituent-, counterion-, solvent-, and kinetic isotope effects and variable temperature ^{1}H NMR studies and

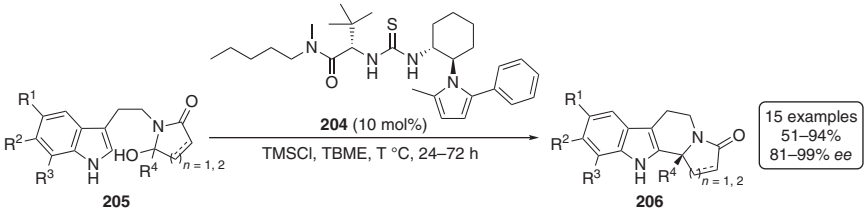

Scheme 1.48 Asymmetric Pictet–Spengler-type cyclization of hydroxy lactams *via in situ* generation of iminium ions catalyzed with **204**.

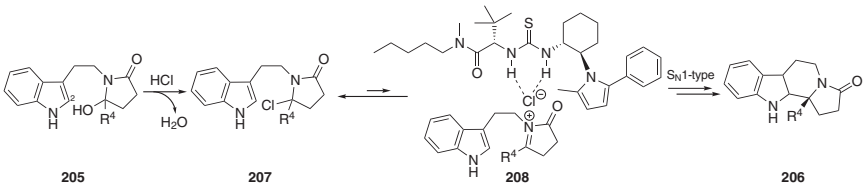

Scheme 1.49 Proposed mechanism for the enantioselective Pictet–Spengler-type cyclization of β-indolyl ethyl hydroxy lactams **205** with thiourea **204**.

suggested that the reaction starts with the TMSCl-induced formation of a chlorolactam, comparable to the chloroamides in the acyl Mannich reaction (cf. Scheme 1.47). Subsequently, the product forms through either an S_N2-type mechanism or a stepwise S_N1 route involving coordination of the chloride to the thiourea. Multiple observations indicate the stepwise mechanism (Scheme 1.49):

(1) The reaction rate was much higher with substituents stabilizing positive charge in the α-position.
(2) There is a strong enantioselectivity dependence on the counteranion (Cl, 97% *ee*; Br, 68% *ee*; I <5% *ee*), supporting the stepwise mechanisms *via* anion binding.
(3) No KIE was observed in reactions utilizing indole with deuterated C_2, ruling out the possibility of a rate-limiting deprotonation/rearomatization step.
(4) NMR experiments of mixtures of the catalyst with tetrabutylammonium chloride (TBAC) resulted in a downfield shift of 0.56 ppm of thiourea N–H protons, while bromide as well as iodide counterions appear at lower downfield shifts. These results indicate the anion-binding mode [373].

This reaction is the second reported example for anion-binding catalysis utilizing hydrogen-bonding organocatalysts, after Kotke's and Schreiner's fundamental work (cf. Schemes 1.12 and 1.13) [176]. Nevertheless, this is the first mechanistic proposal that suggests that a hydrogen-bonding organocatalyst binds an anion in an enantioselective reaction [373], whereby it is generally excepted that also the acetyl Pictet–Spengler (Scheme 1.46) as well as the acyl-Mannich reactions (Scheme 1.47) are catalyzed by anion-binding interactions [9, 10]. A similar chloride-binding concept was applied in many other anion-binding catalyzed reactions [2, 9, 10], e.g., Jacobsen and coworkers utilized a similar activation mode in the biomimetic cyclization of hydroxy lactams [339], which is based on the polycyclization of *N*-acyliminium ions of Dijkink and Speckamp of the 1970s [374, 375]. The idea was to convert the hydroxy lactams *in situ* into the corresponding chlorolactams and to use a bifunctional catalyst that activates the chlorolactams by anion abstraction while stabilizing the cationic intermediates **211** [339]. The authors utilized HCl for the *in situ* formation of the chlorolactams and 4 Å molecular sieve for water removal. Using **209** as a model substrate and starting from thiourea **212** (10%, 9% *ee*), the authors performed catalyst optimization and introduced a conformationally rigid pyrrolidine substituent with an additional stereogenic center (Scheme 1.50).

Catalyst **213** afforded product **210** in a slightly higher yield and increased enantioinduction (12%, 25% *ee*). Changing the phenyl-substituent to 1- and 2-naphthyl substituents, increased catalyst reactivity and stereoselectivity were observed

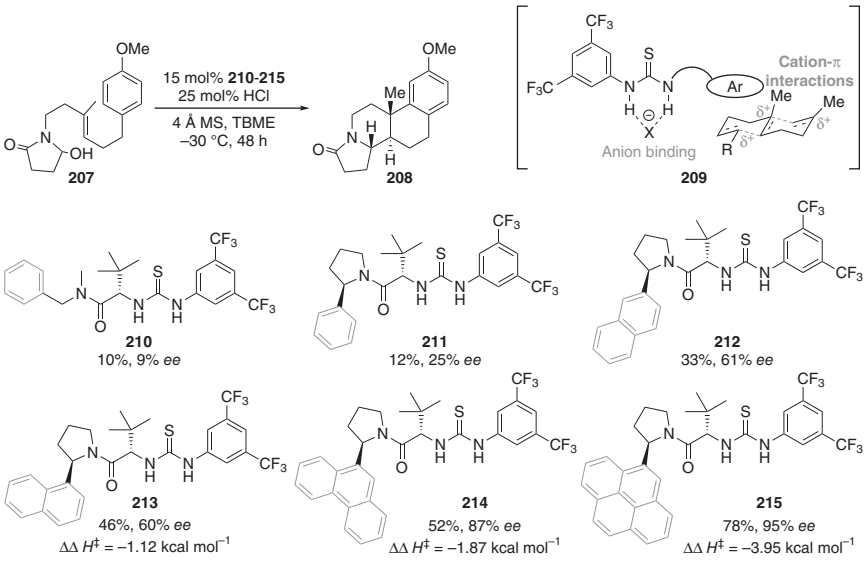

Scheme 1.50 Catalyst optimization for hydroxy lactam polycyclization and stabilization of the cationic intermediate **211**. For catalysts **215—217**, different activation enthalpies are given.

(46%, 60% *ee*; 33%, 61% *ee*, respectively). The 9-phenanthryl-substituted derivative **216** furnished **210** with a slightly decreased yield (52%) but increased enantioselectivity (87% *ee*). In the last optimization step, Jacobsen's group introduced the 4-pyrenyl substituent and obtained **210** with a good yield (78%) and a high *ee*-value (95% *ee*). Notably, the authors observed with all catalysts depicted in Scheme 1.50 the formation of one single diastereomer of 210, whereas performing the reaction without thiourea catalyst only monocyclic products were obtained [339].

With the optimized catalyst in hand, Jacobsen's group synthesized tetracyclic products **219** in yields ranging from 51% to 77% and *ee*-values of 89–94% and a typical TOF value of 0.07 h^{-1} (Scheme 1.51) [339]. The fact that the enantioinduction depends strongly on catalyst size, the authors noted that stabilizing cation–π interactions might play a key role in the intermediate as well as transition structure

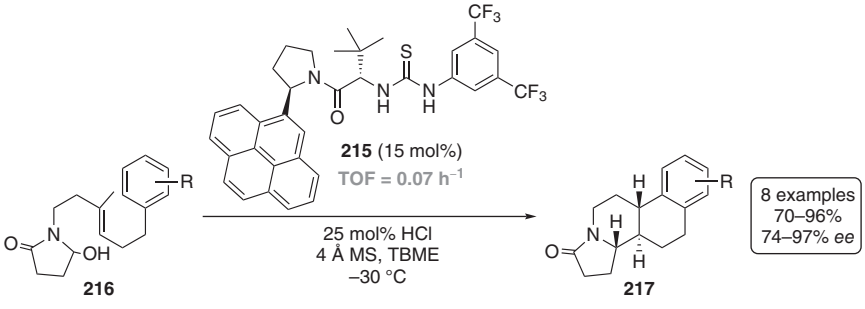

Scheme 1.51 Polycyclization of hydroxy lactams *via in situ* generation of the cationic intermediate catalyzed with **217**.

stabilization. Because catalysts **215–217** displayed a linear correlation between ln(*e.r.*) and reciprocal temperature over a 70 °C range, an Eyring analysis of the enantioselectivity revealed that the enantioselectivity was enthalpically controlled. Furthermore, the differential enthalpy increased obviously as the catalyst arene increased in size and was only attenuated slightly by increased differential entropy terms. These data support the importance of cation–π stabilization as the essential component in the mechanism [339].

Another example utilizing the *in situ* generation of an electrophile through chloride abstraction is the enantioselective addition to oxocarbenium ions generated from 1-chloroisochromans **220** [242]. Reisman, Doyle, and Jacobsen utilized 10 mol% of thiourea **223** and various silyl ketene acetals **221** as nucleophiles and obtained **222** in yields ranging from 70% to 96%, *ee*-values of 74–95%, and TOF = 1.45 h^{-1} (Scheme 1.52). The corresponding 1-chloroisochromans were prepared in a one-pot, two-stage procedure from the corresponding methyl acetals [242].

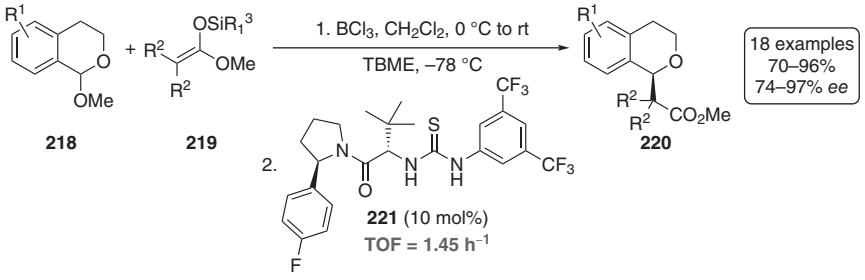

Scheme 1.52 Addition from various silyl ketene acetals to *in situ* generated oxocarbenium ions catalyzed with **223**.

In 2016, Jacobsen's group investigated the activation mode of the **223**-catalyzed chloride abstraction reaction [241, 376–378]. In "same-excess" experiments in the alkylation of 1-chloroisochroman, the authors did not observe catalyst deactivation through decomposition pathways or by product inhibition [376]. Additionally, the catalyst's reaction rate at high loading (>5 mol%) was found to be first order, while non-linear behavior was observed at low catalyst loading, and a positive non-linear relationship between product *ee* and catalyst *ee* was identified. The authors observed three head-to-tail catalyst dimers in 2D NOESY NMR studies, where each thiourea moiety forms hydrogen bonds to the amide oxygen, and that this agglomeration leads to an "off-cycle aggregation" event [376]. Furthermore, the authors obtained single crystals of dimeric catalyst complexes of $[(Z\text{-}\mathbf{223})_2\cdot\mathbf{Cl}]_2^-$ by addition of tetramethylammonium chloride. The X-ray single-crystal analysis shows the formation of a 4H–anion-binding mode with the four N–H protons of the thiourea moiety, and the authors suggested a cooperative and structurally similar chloride abstraction through two catalyst molecules *via* 4H–anion binding (Scheme 1.53) [376].

Jacobsen's group described pairwise catalyst combinations leading to four transition structures (*ZZ*–TS, *EE*–TS, *ZE*–TS, and *EZ*–TS) that apparently all make contributions to the overall reaction rate and enantioselectivity [241]. To suppress the (*Z*)-(*E*)-amide isomerization, the authors performed computational

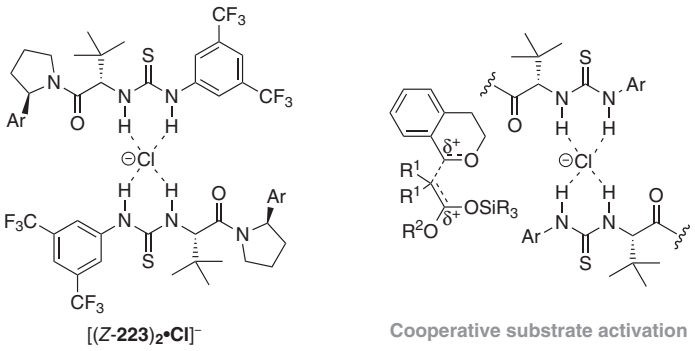

Scheme 1.53 Structures of the bis-thiourea coordinated chloride found in X-ray single-crystal analysis and the cooperative activation *via* the 4H–anion-binding mode.

analyses at the B3LYP/6-31G+(d,p)//B3LYP/6-31G(d) level (at 0 K, not taking zero-point vibrational energy corrections or dispersion interactions into account) of the relative energies of thiourea rotamers bearing a variety of substituents on the pyrrolidine moiety and identified the 2-aryl-2-methylpyrrolidine-derived thiourea **224** as a promising candidate. Jacobsen *et al.* identified in ^{1}H, ^{13}C, and 2D NOESY NMR experiments only the (*Z*)-amide rotamer and showed the improved activity compared to **224** with **223** in the oxocarbenium alkylation, where both yield and enantioselectivity increased (Scheme 1.54) [241]. Based on these results – the 4H–anion-binding mode and the benefit of the conformationally rigid 2-aryl-2-methyl-pyrrolidine moiety – Jacobsen's group synthesized bis-thiourea **225** that showed strict first-order behavior, high rate acceleration compared to **223**, and also a linear relationship between product *ee* and catalyst *ee* [378]. These results provided strong clues for a monocatalyst activation process of **225**, and much higher activity was shown in the formation of **226**, utilizing 0.1 mol% **225** (at 100 times lower catalyst loading, cf. Scheme 1.52), eight times shorter reaction time, and five times higher concentration (Scheme 1.54) [378].

In 2017, Jacobsen's group published the stereospecific β-glycosylation of various sugars catalyzed with thiourea derivatives [379]. The idea was to mimic the glycosyltransferase-catalyzed glycosylation [380]. As depicted in Scheme 1.55, the *cis*-1,2-*O*-glycosylation of α-mannosyl chloride **229** was utilized as a model reaction because the β-glycosidic linkage is strongly disfavored both sterically and electronically [381].

The glycosylation utilizing benzyl alcohol in the absence of any catalyst furnished the α-product predominantly (84 : 16 α:β) with very low yield (0.1%), whereas with 5 mol% **223** slightly higher reactivity, but no selectivity was observed (1%, 52 : 48 α:β). Nevertheless, this result showed that the thiourea catalyst could invert the selectivity, and bis-thiourea **231** leads to a very moderate yield and β-selectivity (15%, 20 : 80 α:β). To improve both the reactivity and selectivity, Jacobsen's group synthesized macrocyclic derivate **232** that forms **230** in good yield and β-selectivity (68%, 12 : 82 α:β). The introduction of a 2,3-dihydroindole instead of the pyrrolidine moiety

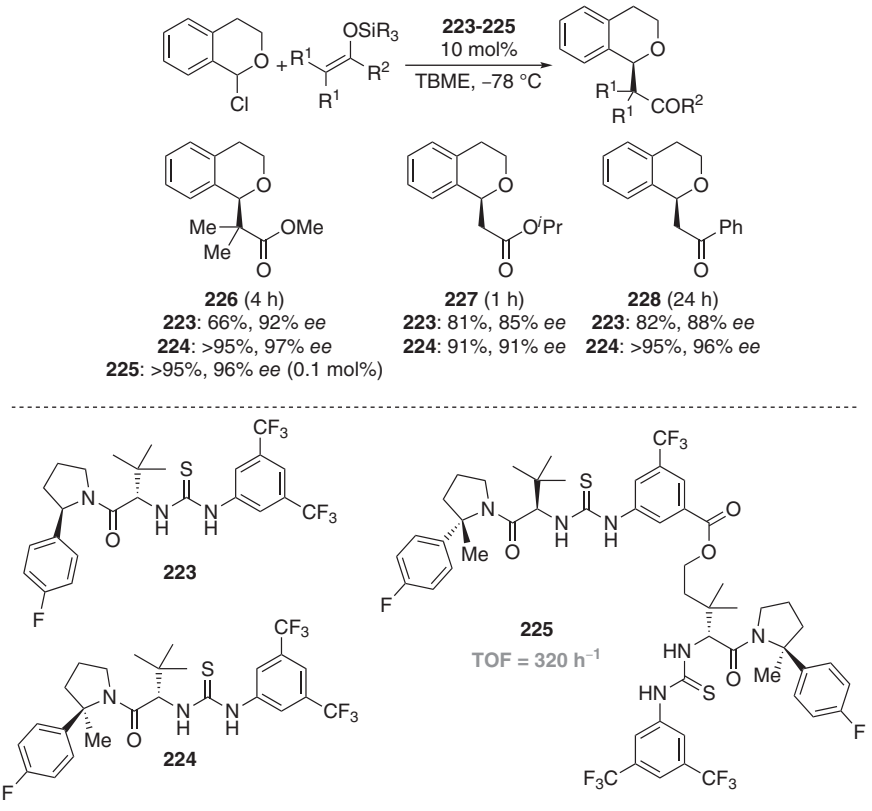

Scheme 1.54 Comparison of the enantioselective oxocarbenium alkylations utilizing thiourea **223**, conformational rigid **224**, and improved bis-thiourea **225**.

resulted in catalyst **233** that furnished the product in high yield as well as high β-selectivity (88%, 8 : 92 α:β) [379].

With the optimized catalysts in hand, the authors synthesized various disaccharides utilizing α-glycosyl chlorides **234** and obtained **235**–**240** in yields ranging from 64% to 88% and as predominantly β-linked products (Scheme 1.56) [379]. The thiourea activation of the leaving group (chloride) promotes both the S_N1 and S_N2 pathways, but nucleophile activation would exclusively support the S_N2 pathway. Overall, Jacobsen's group suggested an S_N2 mechanism based on the following observations:

(1) The products were obtained with a high degree of inversion.
(2) The reaction was insensitive to relative catalyst–substrate as well as nucleophile–electrophile stereochemical relationships.
(3) No limitations concerning the substrate scope could be observed.

The authors assumed an activation of the nucleophile by the catalyst's amide oxygen that acts as a Lewis base and found in DFT studies (M06-2X/6-31G(d) with PCM:benzene solvent inclusion, no temperature given) on the concerted

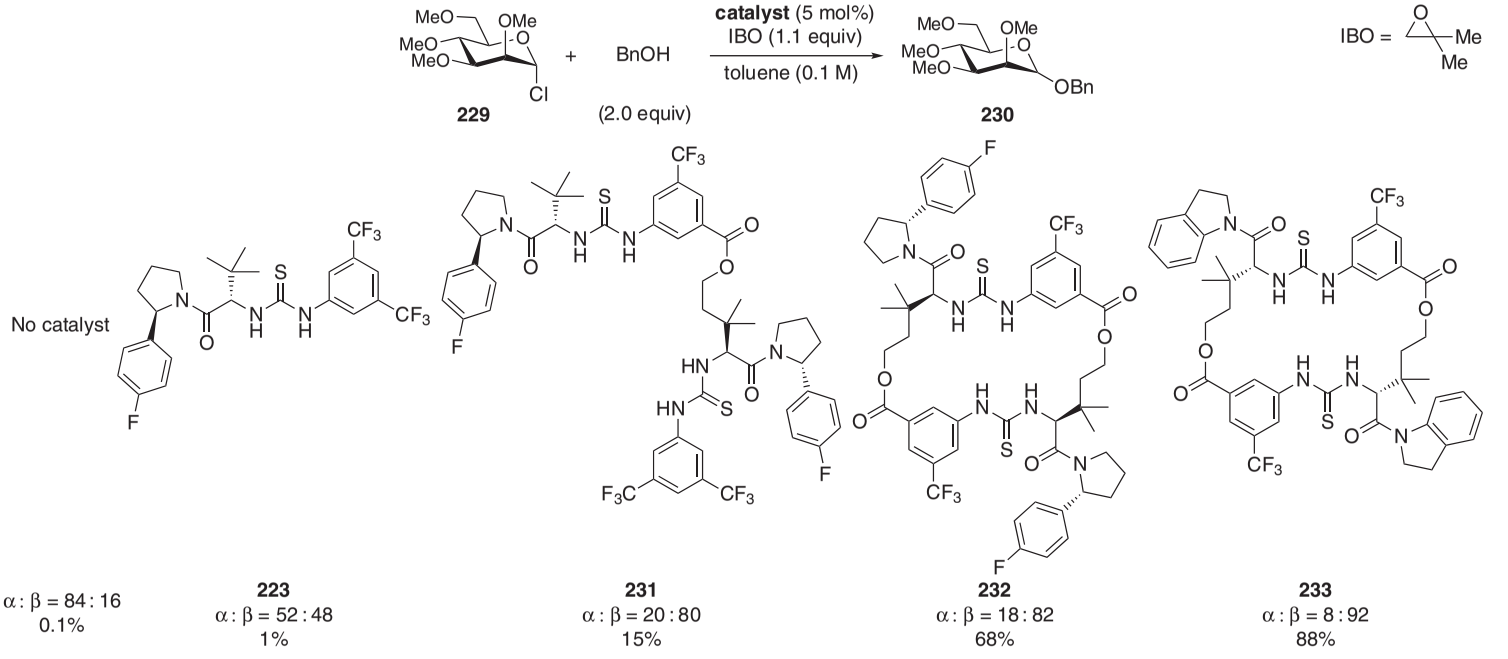

Scheme 1.55 Evolution of thiourea catalysts for the *cis*-1,2-*O*-glycosylation of mannosyl chloride utilizing benzyl alcohol as nucleophile and IBO as the HCl trapping agent.

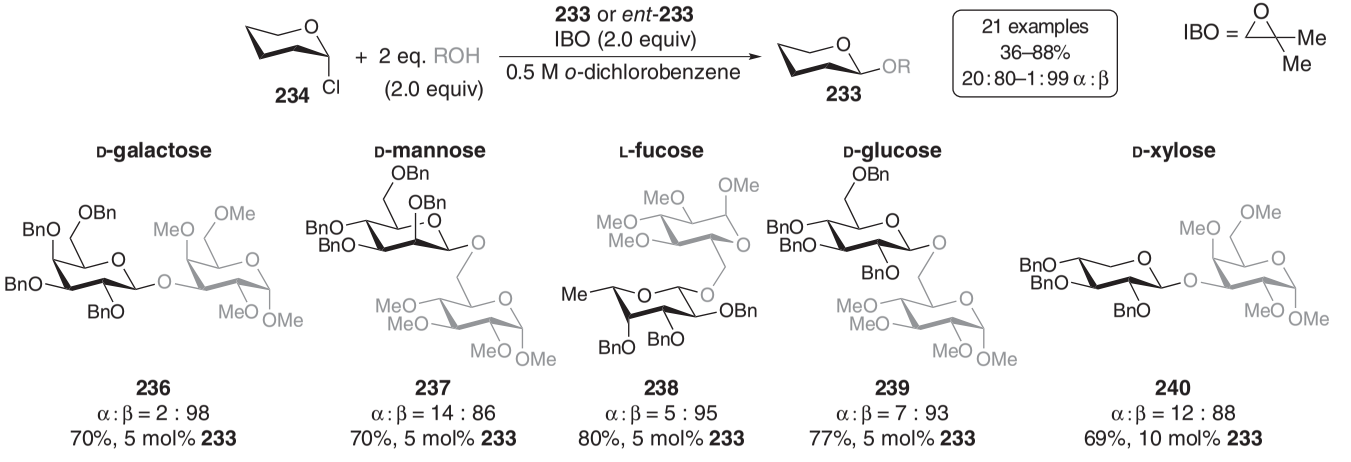

Scheme 1.56 Typical glycosylation products with high β-selectivity utilizing macrocyclic bis-thioureas **233** or *ent*-**233**.

glycosylation of glucosyl chloride by methanol a loose and asynchronous transition structure with hydrogen-bonding interactions between the methanol O–H and the amide oxygen that supported the S_N2 mechanism by both leaving group as well as nucleophile activation [379].

In 2014, on expanding from achiral triazole-based anion-binding catalyst **114** (Scheme 1.25) [229, 230], Mancheño's group introduced helical chiral derivatives with a chiral 1,2-diaminocyclohexane backbone [231]. The idea was to synthesize a flexible catalyst structure that in the "non-active mode" will be present in an equilibrium between linear and helical conformations, and that in the complexation mode to a chloride anion, the helical system is the dominant species. The authors synthesized a series of helical triazole-based anion-binding catalysts **243–247** and tested them in the Reissert-type reaction of quinolone **241** utilizing silyl ketene acetals as nucleophiles. Using bis-triazole-based catalyst **243** that cannot adopt helical chirality upon chloride binding, the observed enantioinduction was low (18% *ee*). Going on to tetra-triazole-based catalysts such as **243–247**, Mancheño's group obtained product **242** with increased *ee*-values (62–92% *ee*) and observed that the substitution pattern of the central phenyl ring was important with the 2-(methoxy-propan-2-yl)acetylene substituent as the most active one. The difference between catalysts **246** and **247**, where the connection of the phenyl groups by the triazole units was slightly changed, was marginal (90% *ee* and 92% *ee*, respectively) [231]. To validate the anion-binding mode of **247**, the authors performed NMR titration experiments with Troc-quinolinium chloride and observed that the eight hydrogens, which are highlighted in Scheme 1.57, form hydrogen bonds to the chloride [231]. Additionally, circular dichroism (CD) titration of **247** with TBAC showed conformational changes in the folding behavior of the flexible oligomer. Increased absorption bands as 250 and 265–280 nm in the positive as well as negative regions of the UV spectrum indicated catalysts' chloride binding and the formation of the helical chiral form. Furthermore, the authors synthesized a series of Reissert-type products utilizing 5 mol% of **247** and obtained products in yields ranging from 54% to 96% and *ee*-values of 44–96% [231].

1.2.4 Anion Binding in Cooperative Catalysis

Besides the high ability to coordinate with chloride (cf. Section 1.2.3), (thio)ureas are well-known receptors for Y-shaped anions, such as carboxylates [135, 138, 382, 383]. The topology of these coplanar anions allows a bidentate hydrogen-bonding mode with an N–H···O angle of approximately 170–175° that leads to anion stabilization [384, 385]. Dual thiourea/carboxylic acid catalyst systems have been utilized in many anion-binding mode-catalyzed reactions, e.g., the alcoholysis of styrene oxides [291], protio Pictet–Spengler reactions [169, 386, 387], [5+2] cycloadditions [388], and, in particular, kinetic resolution of primary amines [342, 343, 389–393], a topic that was reviewed by Seidel in 2014 [341]. The general concept of dual-catalyst kinetic resolution is based on the *in situ* formation of a chiral acylating reagent and consists of three components: a pyridinium species (most reactions use 4-dimethylaminopyridine (DMAP) [393] or its derivatives, e.g.,

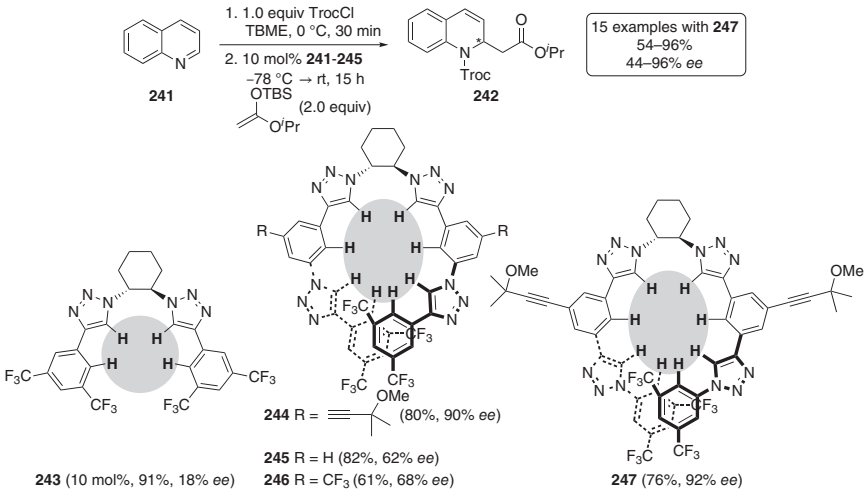

Scheme 1.57 Optimization of helical chiral catalyst structure in Reissert-type reactions. Hydrogens coordinating the chloride are highlighted.

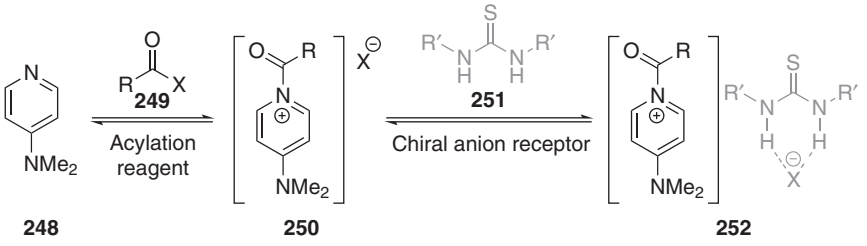

Scheme 1.58 Anion-binding concept for formation of chiral supramolecular ion pairs that serve as chiral acyl transfer species.

4-(pyrrolidino)pyridine (PPY) [390]), an achiral acylating reagent, and a chiral anion-binding/hydrogen-bonding catalyst. Mixtures of DMAP **248** and acylating reagents **249** exist in equilibrium with the corresponding achiral acylpyridinium salt **250** [394]. Chiral catalyst **251** binds the anion, leading to supramolecular chiral ion pair formation that affects the equilibrium between DMAP and its acylpyridinium salt because the supramolecular ion **252** is generally more soluble in organic solvents. Consequently, the substrates should rather react with the chiral supramolecular ion pair than with the acylpyridinium salt (Scheme 1.58).

Because the nature of the chiral supramolecular ion complex was at that time unknown, Seidel, Schreiner, and coworkers investigated the mechanism of the dual-catalysis anion-binding approach in the kinetic resolution of amines utilizing both experimental and computational approaches [393]. Based on the original study by Seidel's group in 2009 [342], Seidel, Schreiner, and coworkers utilized 1-phenylethylamine *rac*-**253** as a model substrate, DMAP as pyridinium species, and tested a series of chiral catalysts. Starting catalyst evolution with the "original" bis-thiourea **256** (s-factor = 8.5), amide–thiourea catalyst **257** (s-factor = 13.0),

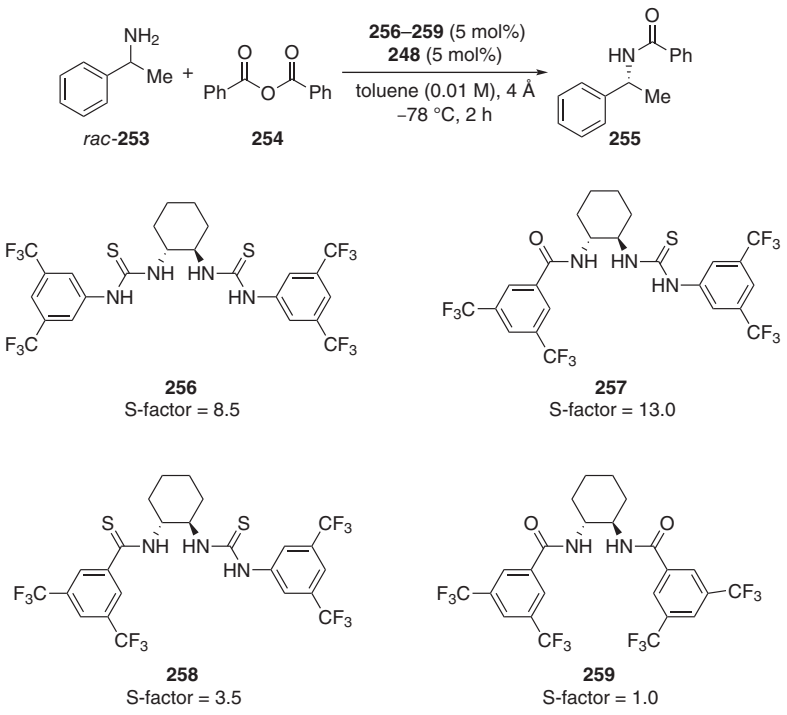

Scheme 1.59 Catalyst evolution for kinetic resolution of 1-phenylethanamine utilizing various catalysts with DMAP as cocatalyst.

which was also utilized in kinetic resolution of primary amines [341], was found to be the most selective catalyst. In the catalyst evolution study, Seidel, Schreiner, and coworkers found that the thiourea as well as the amide moieties are crucial for high selectivity because the corresponding thioamide–thiourea **258** (s-factor = 3.5) and diamide **259** (s-factor = 1.0) were much less selective (Scheme 1.59) [393]. Using various acylating reagents, the authors obtained the highest selectivities with benzoic anhydride but could not identify a trend regarding the electronic nature utilizing substituted benzoic anhydride derivatives ($(4\text{-}CF_3\text{–}PhCO)_2O$ s-factor = 7.5; $(4\text{-Me–PhCO})_2O$ s-factor = 12.8; $(4\text{-MeO–PhCO})_2O$ s-factor = 4.8) [393]. Because the catalyst–substrate ion pairing is obviously crucial for the selectivity, toluene (s-factor = 13.0) was found as the solvent that furnished the highest *s*-value, as it favors (contact) ion pairs, whereas more polar solvents, such as ethyl acetate (s-factor = 1.5), resulted in solvent-shared or solvent-separated ion pairs (cf. Section 1.2.1) [326, 327].

Because deprotonation of the thiourea moiety would lead to an alternative ion pair, the authors performed deprotonation studies and identified hydrogen-bonding interactions between the catalyst's N–Hs and various amines, such as DMAP, Hünig's base, and 1-phenylethylamine in ^{1}H NMR experiments, but could not observe a deprotonated catalyst species, which should be easily identifiable by shifts in the ^{13}C NMR spectrum [143, 189]. These findings confirm the structure

of supramolecular ion pair **252**. Only when the stronger base BEMP was utilized, the deprotonated catalyst could be identified in the ^{1}H and ^{13}C NMR spectra. Using DFT-based computations (ΔH_0, D_0, and ΔG values at M06/6-31G(d,p) including PCM solvent corrections for toluene at various temperatures), Seidel, Schreiner, and coworkers obtained for the ion pair of DMAP and benzoic anhydride substantial and negative dissociation energy ($D_0 = -6.8\,\text{kcal mol}^{-1}$; $D_{298} = -22.2\,\text{kcal mol}^{-1}$), which is consistent with the absence of NOE signals in NMR experiments; however, this could also be due to long proton–proton distances and fast exchange. Nevertheless, DOSY NMR spectroscopy equally did not reveal evidence of ion pair formation. Utilizing bis-thiourea **256**, the authors obtained a positive dissociation energy for ternary complex **252** (Scheme 1.58) in the gas-phase ($D_{195} = +10.4\,\text{kcal mol}^{-1}$) as well as in solution (toluene, $D_{195} = +3.6\,\text{kcal mol}^{-1}$), with **256** displaying (*Z,Z*)-oriented N–H protons. Additionally, Seidel, Schreiner, and coworkers identified that the benzoyl group is fixed in the ternary complex through π–π stacking with one of the thiourea aryl rings. Adding the (*R*)-configured amine, the lowest lying quaternary complex was found to coordinate the benzoate through double hydrogen bonding by one thiourea moiety, whereas the second thiourea unit coordinates the first thiourea moiety also through hydrogen bonding. Simultaneously, benzoate binds to the ortho and meta protons of the pyridinium cation. In this quaternary complex, the authors found threefold π–π stacking of one thiourea aryl, DMAP's pyridine, and the 1-phenylethylamine ring. Accordingly, quaternary complex formation was observed at −78 °C ($D_{195} = +19.0\,\text{kcal mol}^{-1}$; $D_{298} = +3.1\,\text{kcal mol}^{-1}$), whereas with the (*S*)-configured amine, the quaternary complex was less favorable ($D_{298} = +0.7\,\text{kcal mol}^{-1}$). Utilizing amide–thiourea catalyst **257**, the authors also found a (*Z,Z*)-oriented thiourea unit that binds the benzoate through double hydrogen bonding. Additionally, the acidified ortho-proton of the 3,5-bis(trifluoromethyl)phenyl moiety forms a hydrogen bond to one of the benzoate oxygens [190], and, similar to **256**, the amide binds *via* an N–H···S interaction to the thiourea. Benzoate forms hydrogen-bonds to DMAP's ortho proton, which itself is fixed by the two aryl groups of the catalyst, leading to a well-defined binding pocket. The dissociation energy is negative at 298 °C ($-0.5\,\text{kcal mol}^{-1}$) but positive at −78 °C ($+12.6\,\text{kcal mol}^{-1}$; $+5.2\,\text{kcal mol}^{-1}$ in toluene). These mechanistic studies using a combination of experimental as well as computational studies emphasize the high relevance of NCIs in anion-binding catalysis for the formation of a well-defined binding pocket that can furnish reactions with high stereoinduction [393].

1.2.5 Anion-Binding in Lewis Acid Enhancement Catalysis

In 2011, Schreiner's group utilized silicon–thiourea Lewis acid **260** in the House–Meinwald rearrangement of tri-substituted epoxides **261** and obtained the corresponding quaternary aldehydes **262** in yields of 43–88% (Scheme 1.60) [189]. Catalyst **260** forms by deprotonation of **46** and addition of $SiCl_4$ as evident from IR, NMR, and MS experiments. In blind experiments utilizing either **46** or $SiCl_4$, the authors did not observe product formation, which confirmed

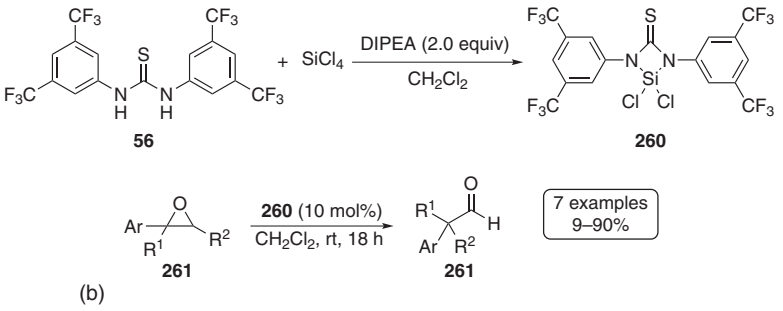

Scheme 1.60 (a) Synthesis of silicon-thiourea Lewis acid through deprotonation of **56** and (b) House–Meinwald rearrangement utilizing tri-substituted epoxides.

the increased Lewis acidity of **260**. When utilizing enantioenriched epoxides, synthesized by Shi epoxidation [395], the authors observed increased enantiopurity for the starting material as well as the product. They performed a negative control experiment spiking the reaction mixture with enantioenriched product. However, a corresponding autocatalytic process could be excluded as no chirality enhancement for the product was observed.

Schreiner and coworkers proposed that an epoxide coordinates the silicon first and forms the active catalyst species. Binding by another epoxide would consequently lead to diastereomeric transition structures and to diastereomeric matched and mismatched combinations. Therefore, the reaction was described as "*similar to a kinetic resolution of non-racemic starting materials*" [396]. This reaction utilized a thiourea-based complex that increased the silicon's Lewis acidity by covalent bond formation and not through anion binding. Nevertheless, this was a proof-of-concept study for Lewis acid enhancement utilizing (thio)ureas.

In 2017, Jacobsen's group took up this concept in the activation of triflates for the generation of oxocarbenium ions [344]. Using **263** as a model substrate in Mukaiyama aldol reactions, the authors screened various (thio)ureas and squaramides and observed that only squaramides catalyzed the aldol reaction, which was explained by squaramides' dual functionality [197–199]. Jacobsen's group employed squaramides with various dispersion energy donors and found 1-pyrenyl-substituted derivate **266** as the most active one (100% conversion, 88% *ee*, Scheme 1.61); it displays a structure similar to that of thiourea **217** (cf. Scheme 1.50). The importance of catalysts hydrogen-bonding donor motif was validated through the *N,N′*-dimethylated analog of **266** that promoted the aldol reaction only little and nearly without selectivity (43% conversion, 2% *ee*) [344].

Subsequently, Jacobsen's group utilized the **266**-silyl-triflate system in [4+3] cycloadditions of oxyallyl cations and furan derivatives **268** and obtained bicyclic **269** in yields of 55–98% and 66–96% *ee* as single diastereomers (Scheme 1.62) [344]. The authors performed kinetic analysis and found zero-order kinetics for furan derivatives **268**, first-order kinetics for the oxyallyl cation precursor **267** as well as squaramide catalyst **266**, and saturation kinetics for trialkyl silyl triflate (TESOTf). The kinetic data are consistent with a pre-equilibrium between **266** and TESOTf, and rate-limiting oxyallyl cation formation. To prove the formation of a

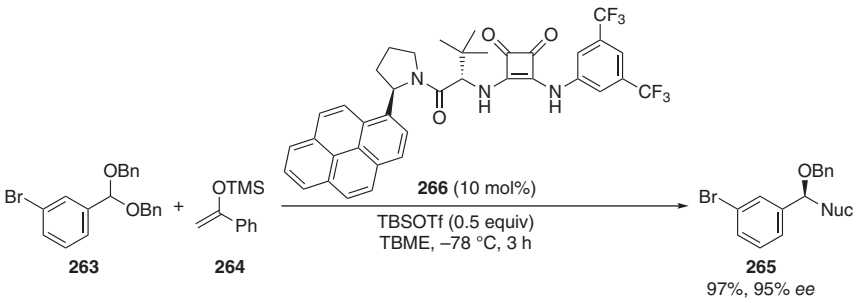

Scheme 1.61 Representative example of enantioselective aldol reaction utilizing TBSOTf as Lewis acid and catalyst **266**.

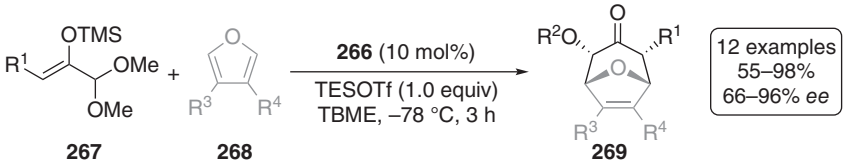

Scheme 1.62 Enantioselective [4+3] cycloaddition catalyzed with **266** and TESOTf.

pre-equilibrium, the authors preformed ^{1}H NMR experiments with NBu_4OTf and TESOTf and observed stable complexes with both triflate species. However, TESOTf was found to bind 4000 times as strongly as NBu_4OTf and forms simultaneous hydrogen bonds to the squaramides' N–Hs. While monitoring TESOTf addition to the squaramide catalyst utilizing IR spectroscopy, Jacobsen's group observed the disappearance of the absorbance attributed to the squaramide carbonyl groups. The authors proposed that complexation of **266** and trialkyl silyl triflates (R_3SiOTf) is more Lewis acid than (R_3SiOTf) alone because of the stabilization of the triflate anion through hydrogen-bonding interactions [344].

The authors suggested a catalytic cycle that starts with the resting state formation of the catalytically active enhanced Lewis acid **270** [344]. After the rate-determining ionization and generation of the oxyallyl cation, ion pair **271** forms. In a stepwise and enantiodetermining cycloaddition, the desired product forms and free enhanced Lewis acid **270** ensues (Scheme 1.63). Furthermore, the authors performed DFT studies (at the uncorrected M06-2X/6-31+G(d,p)//B3LYP/6-31G(d) level of theory) and identified transition structures leading to the formation of the major and minor products. Jacobsen's group described that the furan position near the catalyst's aromatic substituent leads to a stabilization of the major enantiomer trough NCIs, whereas the transition structure for the minor enantiomer lacks this stabilization [344].

1.2.6 Anion-Binding in Phase Transfer Catalysis

Fluorine incorporation in organic molecules leads to modified properties, such as lowering the pK_a of the neighboring groups and changing molecules' dipole moments. In particular, sp^3 C–F bonds have a large influence on metabolic

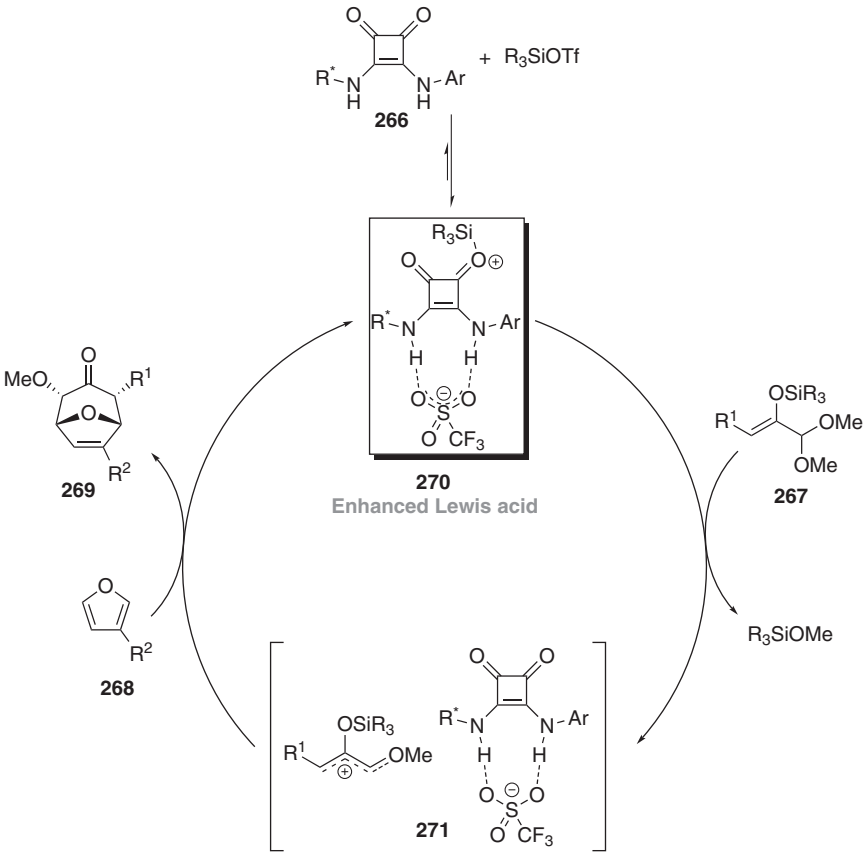

Scheme 1.63 Pre-equilibrium leading to the formation of the enhanced Lewis acid 268 and the proposed catalytic cycle for the enantioselective [4+3] cycloaddition.

stability, lipophilicity, and bioavailability – characteristics that are highly important in pharmaceutical science [397–402]. Gouverneur's group utilized urea-based phase transfer catalysts (PTC) [403–405] for the asymmetric nucleophilic fluorine incorporation [346–348] and utilized the well-known potent ability of ureas' fluoride recognition [384, 406–408]. Generally, fluorination is dominated by methods utilizing electrophilic fluorine species [409, 410] such as selectfluor [411]. Additionally, asymmetric PTC using organic electrophilic fluorine species are known [412, 413], whereas the anion-binding-mediated fluorination approach of Gouverneur's group based on cheap alkali-metal fluorides, such as cesium fluoride [346, 347] or potassium fluoride [348], mimic the nucleophilic enzymatic fluorination of *S*-adenosyl-L-methionine [414–416]. In 2016, Gouverneur and coworkers obtained single crystals by refluxing *N,N′*-bis(4-chloro)phenylurea and tetrabutylammonium fluoride (TBAF) in *n*-hexane. An X-ray crystal structure analysis of this complex revealed two different complexes with both urea moieties forming hydrogen bonds to the fluoride. The main difference of the two complexes is the twisted geometries as expressed through the interplanar angles of 40.6° and 76.3°. Gouverneur and coworkers synthesized tridentate and tetradentate catalysts

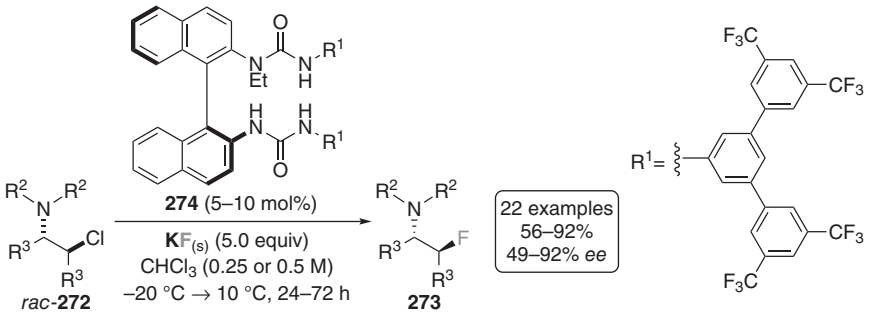

Scheme 1.64 Generation of β-fluoroamines obtained by asymmetric PTC fluorination with bis-urea **274**.

with two urea units, the privileged 3,5-bis(trifluoromethyl)phenyl motif [190], and 1,1′-binaphthalene-2,2′-diamine (BINAM) as the chiral backbone. The authors observed higher enantioinduction using tridentate derivatives as monoalkyl incorporation into one urea resulted in a preferred *anti-syn* conformation and formation of a well-defined binding pocket [346]. In 2019 [347], the same group utilized anion-binding-mediated PTC for the enantioselective synthesis of β-fluoroamines **273** that are a highly relevant substance class in medicinal chemistry [417–420]. The idea was the *in situ* formation of a prochiral aziridinium species **276** (Scheme 1.65) that subsequently underwent ring opening by the fluoride. The authors optimized the catalyst and identified **274** as the most active catalyst incorporating additional 3,5-bis(trifluoromethyl)phenyl substituents (cf. Scheme 1.64). Utilizing 5–10 mol% of bis-urea **274**, β-fluoroamines were obtained in yields of 63–92% and 49–92% *ee* [348].

The authors utilized molecular dynamics (MD) simulations and DFT computations (ΔG values at ωB97X-D3/(ma)-def2-TZVPP/COSMO($CHCl_3$)//M06-2X/def2-SVP(TZVPPD)/CPCM($CHCl_3$)) to gain insights into the reaction mechanism [348]. The MD simulations reveal a preferred *anti-syn* conformation of the catalysts. Utilizing DFT computations, 15 optimized transition structures for ring-opening of bisaryl-based aziridinium species were found, with the lowest lying transition structure leading to the major product being favored by 1.6 kcal mol^{-1}. The most favorable transition structure for both major and minor enantiomer reveals that the aziridinium ion N-substituents are pointing away from the catalytic pocket into the solvent, thereby helping to rationalize the indifference to this substituent (Scheme 1.64). Furthermore, Gouverneur and coworkers found cation–π interactions between the naphthyl ring and the aziridinium Cα–H protons. The authors described stronger cation–π interactions for transition structure leading to the major enantiomer since the distance compared with the transition structure for the minor enantiomer was shorter (2.26 Å vs. 2.41 Å, respectively). Additionally, unfavorable geometric distortions due to steric crowding contribute with about 1.0 kcal mol^{-1}. The authors proposed a mechanism that starts with the formation of the soluble and chiral fluoride from inorganic and insoluble potassium fluoride. Additionally, Gouverneur and coworkers suggested an equilibrium of the racemic β-chloroamines **272** and the reactive aziridinium chloride ion pair **276**. Ion pairs **275** and **276** underwent

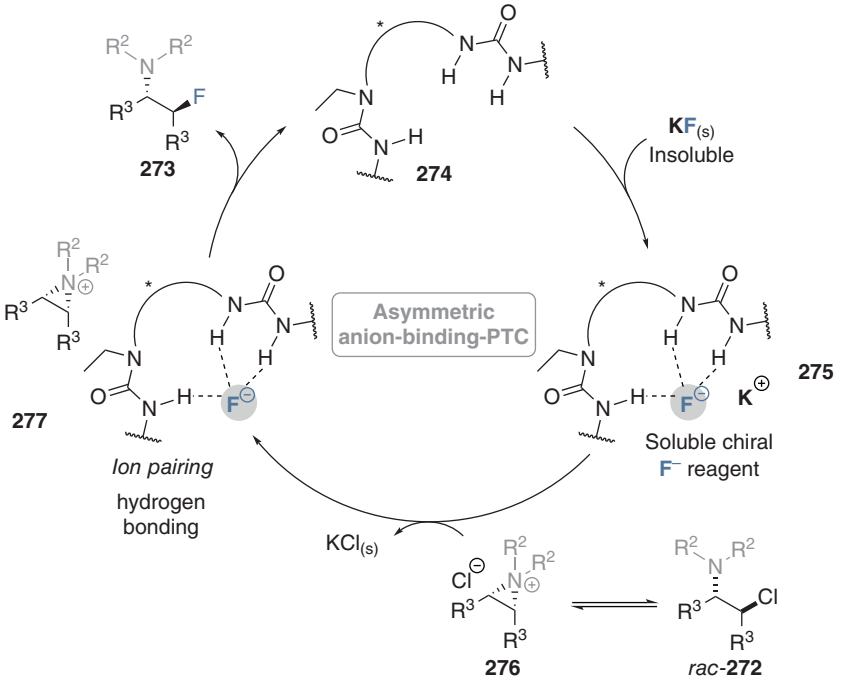

Scheme 1.65 Proposed mechanism of the asymmetric hydrogen-bonding PTC to furnish enantioenriched β-fluoroamines, utilizing KF, racemic β-chloroamines, and bis-urea **274**.

an ion-change process leading to the formation of insoluble potassium chloride and supramolecular anion pair **277**. Nucleophilic addition to the aziridinium ion furnishes the desired product **273** and free catalyst **274** (Scheme 1.65) [348].

1.3 Summary and Outlook

This chapter reviews the long evolution in anion-binding chemistry starting with the first observations in the 1940s and 1950s and ending today with highly efficient organocatalysts that activate and direct reactions through anion binding. Starting with unselective (thio)ureas that show low TOF values ($<1\ h^{-1}$), in the last years, organic chemist designed highly active anion-binding organocatalysts for asymmetric induction with TOF values up to $4000\ h^{-1}$, thereby underlining the success story of anion-binding catalysts – after initial ignorance and skepticism in the early years. After the foundational work in the late 1990s and early 2000s, the growing interest in this research field has been exponential, as demonstrated by the milestone achievements and guidelines for (thio)urea catalyst design summarized and presented here. The evident success of these design principles for anion-binding catalysts also triggered the development of novel catalyst classes over the past few years, such as those binding through C–H hydrogen bonds and σ-holes and incorporating anion-binding motifs into switchable catalysts. One crucial design element in asymmetric

anion-binding catalysis is NCIs, including hydrogen-bonding, π–π as well as cation–π stacking, and dipole interactions. What is missing is the appreciation of London dispersion interactions (*via* dispersion energy donors, DEDs) as a design element. The inclusion of these interactions will finally complete all supposedly "weak" interactions that are at the heart of transition-state stabilization in a catalytic event.

The preferred use of non-polar solvents supports contact ion pair formation in intermediates and transition structures. In previous reviews, the authors divided organocatalysts in bound anion species, such as halide, enolate, and so on. In this chapter, we presented the five general activation modes in anion-binding catalysis utilizing selected representative examples, describing catalyst design principles, and presenting mechanistic proposals that go along with them:

(1) Recognition of the nucleophile in addition reactions and NCIs between the catalyst and the electrophile.
(2) Abstraction of the leaving group in S_N1-type reactions and formation of a chiral contact ion pair.
(3) Cooperative catalysis with an additional Brønsted acid forming a well-defined binding pocket to interact with the substrate.
(4) Lewis acid enhancement through activation by a Lewis base.
(5) Nucleophile delivery in phase transfer catalysis by nucleophile-binding and subsequent transfer into the organic medium.

Some important conceptual and practical points to be considered in future anion-binding-catalyzed reactions (and not only these) may include the following:

(1) To make catalyst reactivities and stereoselectivities more comparable, TOF values should be used and uncatalyzed reference reactions should always be reported.
(2) Typically, reactions are performed on a very small scale (0.1–0.2 mmol). To show the practicability of a new reaction, scale-up experiments (5–10 mmol) should be carried out to leave the "proof-of-concept" phase toward the challenging phase in which research should focus on broader, even large-scale applications.
(3) The product yields should be given and not just conversion of the starting materials because any side reaction also consumes the starting material. Furthermore – as we all know all too well – the work-up process is crucial for the isolation of a pure product. Only the yield determined for a sizeable amount of pure product matters when, for instance, it is to be used for (bio)medical applications.
(4) Novel applications in anion-binding catalysis should be investigated using experimental and theoretical studies to elucidate catalyst activation modes and principle mechanistic hypotheses.

Acknowledgment

We gratefully acknowledge the financial support by the German Research Foundation (Deutsche Forschungsgemeinschaft) and the State of Hesse for the many years

of continuing support. We thank Raffael C. Wende and Bastian Bernhardt for valuable discussions.

References

1 Schreiner, P.R. (2003). *Chem. Soc. Rev.* 32: 289–296.
2 Zhang, Z. and Schreiner, P.R. (2009). *Chem. Soc. Rev.* 38: 1187–1198.
3 Pihko, P.M. (2004). *Angew. Chem. Int. Ed.* 43: 2062–2064.
4 Takemoto, Y. (2005). *Org. Biomol. Chem.* 3: 4299–4306.
5 Connon, S.J. (2006). *Chem. Eur. J.* 12: 5418–5427.
6 Taylor, M.S. and Jacobsen, E.N. (2006). *Angew. Chem. Int. Ed.* 45: 1520–1543.
7 Akiyama, T., Itoh, J., and Fuchibe, K. (2006). *Adv. Synth. Chem.* 348: 999–1010.
8 Doyle, A.G. and Jacobsen, E.N. (2007). *Chem. Rev.* 107: 5713–5743.
9 Brak, K. and Jacobsen, E.N. (2013). *Angew. Chem. Int. Ed.* 52: 534–561.
10 Beckendorf, S., Asmus, S., and García Mancheño, O. (2012). *ChemCatChem* 4: 926–936.
11 Pihko, P.M. (2009). *Hydrogen Bonding in Organic Synthesis*. Weinheim: Wiley VCH.
12 Mahlau, M. and List, B. (2013). *Angew. Chem. Int. Ed.* 52: 518–533.
13 Auvil, T.J., Schafer, A.G., and Mattson, A.E. (2014). *Eur. J. Org. Chem.* 2014: 2633–2646.
14 Phipps, R.J., Hamilton, G.L., and Toste, F.D. (2012). *Nat. Chem.* 4: 603–614.
15 Schramm, V.L. (2006). *Chem. Rev.* 106: 3029–3030.
16 Watson, J.D. and Crick, F.H.C. (1953). *Nature* 171: 737–738.
17 Jeffrey, G.A. and Saenger, W. (1994). *The Role of Hydrogen Bonding in the Structure and Function of the Nucleic Acids*. Berlin: Springer.
18 Fonseca Guerra, C., Bickelhaupt, F.M., Snijders, J.G., and Baerends, E.J. (2000). *J. Am. Chem. Soc.* 122: 4117–4128.
19 Fersht, A. (1999). *Structure and Mechanism in Protein Science*. New York: Macmillan Education.
20 Gao, J., Ma, S., Major, D.T. *et al*. (2006). *Chem. Rev.* 106: 3188–3209.
21 Carey, P.R. (2006). *Chem. Rev.* 106: 3043–3054.
22 Boehr, D.D., Dyson, H.J., and Wright, P.E. (2006). *Chem. Rev.* 106: 3055–3079.
23 Bruice, T.C. (2006). *Chem. Rev.* 106: 3119–3139.
24 Antoniou, D., Basner, J., Núñez, S., and Schwartz, S.D. (2006). *Chem. Rev.* 106: 3170–3187.
25 Kirby, A.J. (1996). *Angew. Chem. Int. Ed.* 35: 706–724.
26 Kohen, A. and Klinman, J.P. (1998). *Acc. Chem. Res.* 31: 397–404.
27 Lindskog, S. (1997). *Pharmacol. Ther.* 74: 1–20.
28 Bruice, T.C. and Benkovic, S.J. (2000). *Biochemistry* 39: 6267–6274.
29 Williams, D.H., Stephens, E., O'Brien, D.P., and Zhou, M. (2004). *Angew. Chem. Int. Ed.* 43: 6596–6616.
30 Evans, M.J. and Cravatt, B.F. (2006). *Chem. Rev.* 106: 3279–3301.
31 Christianson, D.W. (2006). *Chem. Rev.* 106: 3412–3442.

32 Pauling, L. (1960). *The Nature of the Chemical Bond*. Ithaca, NY: Cornell University Press.

33 Pimentel, G.C. and McClellan, A.L. (1960). *The Hydrogen Bond*. San Francisco: W. H. Freemann.

34 Jeffrey, G.A. and Jeffrey, G.A. (1997). *An Introduction to Hydrogen Bonding*. New York: Oxford University Press.

35 Prins, L.J., Reinhoudt, D.N., and Timmerman, P. (2001). *Angew. Chem. Int. Ed.* 40: 2382–2426.

36 Steiner, T. (2002). *Angew. Chem. Int. Ed.* 41: 48–76.

37 Hunter, C.A. (2004). *Angew. Chem. Int. Ed.* 43: 5310–5324.

38 Riordan, J., McElvany, K., and Borders, C. (1977). *Science* 195: 884–886.

39 Riordan, J.F. (1979). *Mol. Cell. Biochem.* 26: 71–92.

40 Riley, K.E. and Hobza, P. (2013). *Acc. Chem. Res.* 46: 927–936.

41 Meyer, E.A., Castellano, R.K., and Diederich, F. (2003). *Angew. Chem. Int. Ed.* 42: 1210–1250.

42 Dessent, C.E.H. and Müller-Dethlefs, K. (2000). *Chem. Rev.* 100: 3999–4022.

43 Wear, M.A., Kan, D., Rabu, A., and Walkinshaw, M.D. (2007). *Angew. Chem. Int. Ed.* 46: 6453–6456.

44 Warshel, A., Sharma, P.K., Kato, M. *et al*. (2006). *Chem. Rev.* 106: 3210–3235.

45 Kraut, D.A., Sigala, P.A., Pybus, B. *et al*. (2006). *PLoS Biol.* 4: 201–519.

46 Lau, E.Y., Newby, Z.E., and Bruice, T.C. (2001). *J. Am. Chem. Soc.* 123: 3350–3357.

47 Hopmann, K.H. and Himo, F. (2006). *Chem. Eur. J.* 12: 6898–6909.

48 Hopmann, K.H. and Himo, F. (2006). *J. Phys. Chem. B* 110: 21299–21310.

49 de Vries, E.J. and Janssen, D.B. (2003). *Curr. Opin. Biochem.* 14: 414–420.

50 Jormakka, M., Törnroth, S., Abramson, J. *et al*. (2002). *Acta Crystallogr. D* 58: 160–162.

51 Hedstrom, L. (2002). *Chem. Rev.* 102: 4501–4524.

52 Product inhibition and substrate inhibition are effects also known in enzyme catalysis that can reduce catalytic efficiency. Generally, catalytic systems (natural or artificial) based on covalent interactions are more sensitive towards inhibitions than non-covalent systems utilizing weak interactions:Garcia-Junceda, E. (2008). *Multi-Step Enzyme Catalysis*. Weinheim: Wiley-VCH.

53 Vigny, M., Bon, S., Massoulié, J., and Leterrier, F. (1978). *Eur. J. Biochem.* 85: 317–323.

54 Blackmond, D.G., Armstrong, A., Coombe, V., and Wells, A. (2007). *Angew. Chem. Int. Ed.* 46: 3798–3800.

55 Sheldon, R.A. (2008). *Chem. Commun.* 44: 3352–3365.

56 Murakami, Y., Kikuchi, J.-i., Hisaeda, Y., and Hayashida, O. (1996). *Chem. Rev.* 96: 721–758.

57 Kirby, A.J. and Hollfelder, F. (2009). *From Enzyme Models to Model Enzymes*. Cambridge: Royal Society of Chemistry.

58 Breslow, R. (2005). Artificial Enzymes. In: *Artificial Enzymes* (ed. R. Breslow), 1–35. Weinheim: Wiley-VCH.

59 Breslow, R. (1982). *Science* 218: 532–537.

60 Breslow, R. (1995). *Acc. Chem. Res.* 28: 146–153.
61 Pascal, R. (2003). *Eur. J. Org. Chem.* 2003: 1813–1824.
62 Egorova, K.S. and Ananikov, V.P. (2017). *Organometallics* 36: 4071–4090.
63 Pauling, L. (1948). *Nature* 161: 707–709.
64 Pauling, L. (1946). *Chem. Eng. News* 24: 1375–1377.
65 Zhang, X. and Houk, K.N. (2005). *Acc. Chem. Res.* 38: 379–385.
66 Jencks, W.P. (1980). *Acc. Chem. Res.* 13: 161–169.
67 Jencks, W.P. (1976). *Acc. Chem. Res.* 9: 425–432.
68 Warshel, A. (1981). *Biochemistry* 20: 3167–3177.
69 Johnson, K.A. and Goody, R.S. (2011). *Biochemistry* 50: 8264–8269.
70 Michaelis, L. and Menten, M. (1913). *Biochem. Z.* 49: 333–369.
71 Bruice, T.C. (2002). *Acc. Chem. Res.* 35: 139–148.
72 Fox, K.M. and Karplus, P.A. (1994). *Structure* 2: 1089–1105.
73 Kawai, Y., Inaba, Y., and Tokitoh, N. (2001). *Tetrahedron: Asymmetry* 12: 309–318.
74 Kawai, Y., Inaba, Y., Hayashi, M., and Tokitoh, N. (2001). *Tetrahedron Lett.* 42: 3367–3368.
75 Meah, Y. and Massey, V. (2000). *Proc. Natl. Acad. Sci. U.S.A.* 97: 10733–10738.
76 Bartlett, P.D. and Dauben, H.J. Jr., (1940). *J. Am. Chem. Soc.* 62: 1339–1344.
77 Swain, C.G. (1948). *J. Am. Chem. Soc.* 70: 1119–1128.
78 Lund, H. (1958). *Acta Chem. Scand.* 12: 298–302.
79 Bufalini, J. and Stern, K.H. (1961). *J. Am. Chem. Soc.* 83: 4362–4366.
80 Tsuboi, M. (1952). *Bull. Chem. Soc. Jpn.* 25: 60–66.
81 Tsubomura, H. (1955). *J. Chem. Phys.* 23: 2130–2133.
82 Allerhand, A. and v. R. Schleyer, P. (1963). *J. Am. Chem. Soc.* 85: 1233–1237.
83 Simmons, H.E. and Park, C.H. (1968). *J. Am. Chem. Soc.* 90: 2428–2429.
84 Park, C.H. and Simmons, H.E. (1968). *J. Am. Chem. Soc.* 90: 2429–2431.
85 Park, C.H. and Simmons, H.E. (1968). *J. Am. Chem. Soc.* 90: 2431–2432.
86 Bell, R.A., Christoph, G.G., Fronczek, F.R., and Marsh, R.E. (1975). *Science* 190: 151–152.
87 Busschaert, N., Caltagirone, C., Van Rossom, W., and Gale, P.A. (2015). *Chem. Rev.* 115: 8038–8155.
88 Molina, P., Zapata, F., and Caballero, A. (2017). *Chem. Rev.* 117: 9907–9972.
89 He, Q., Vargas-Zúñiga, G.I., Kim, S.H. *et al*. (2019). *Chem. Rev.* 119: 9753–9835.
90 Schmidtchen, F.P. and Berger, M. (1997). *Chem. Rev.* 97: 1609–1646.
91 Kim, S.K. and Sessler, J.L. (2010). *Chem. Soc. Rev.* 39: 3784–3809.
92 Park, I.-W., Yoo, J., Adhikari, S. *et al*. (2012). *Chem. Eur. J.* 18: 15073–15078.
93 Gunnlaugsson, T., Glynn, M., Tocci, G.M. *et al*. (2006). *Coord. Chem. Rev.* 250: 3094–3117.
94 Mutihac, L., Lee, J.H., Kim, J.S., and Vicens, J. (2011). *Chem. Soc. Rev.* 40: 2777–2796.
95 Teresa Albelda, M., Frías, J.C., García-España, E., and Schneider, H.-J. (2012). *Chem. Soc. Rev.* 41: 3859–3877.
96 Wichmann, K., Antonioli, B., Söhnel, T. *et al*. (2006). *Coord. Chem. Rev.* 250: 2987–3003.

97 Moyer, B.A. (2013). *Ion Exchange and Solvent Extraction: Volume 21, Supramolecular Aspects of Solvent Extraction*. Boca Raton: CRC Press.

98 Davis, A.P. (2006). *Coord. Chem. Rev.* 250: 2939–2951.

99 Davis, A.P., Sheppard, D.N., and Smith, B.D. (2007). *Chem. Soc. Rev.* 36: 348–357.

100 Matile, S., Vargas Jentzsch, A., Montenegro, J., and Fin, A. (2011). *Chem. Soc. Rev.* 40: 2453–2474.

101 Davis, J.T., Okunola, O., and Quesada, R. (2010). *Chem. Soc. Rev.* 39: 3843–3862.

102 Gale, P.A. (2011). *Acc. Chem. Res.* 44: 216–226.

103 Behera, H. and Madhavan, N. (2017). *J. Am. Chem. Soc.* 139: 12919–12922.

104 Busschaert, N. and Gale, P.A. (2013). *Angew. Chem. Int. Ed.* 52: 1374–1382.

105 Gokel, G.W. and Barkey, N. (2009). *New J. Chem.* 33: 947–963.

106 Lankshear, M.D. and Beer, P.D. (2006). *Coord. Chem. Rev.* 250: 3142–3160.

107 Gimeno, N. and Vilar, R. (2006). *Coord. Chem. Rev.* 250: 3161–3189.

108 Custelcean, R. (2014). *Chem. Soc. Rev.* 43: 1813–1824.

109 Vilar, R. (2003). *Angew. Chem. Int. Ed.* 42: 1460–1477.

110 Galbraith, E. and James, T.D. (2010). *Chem. Soc. Rev.* 39: 3831–3842.

111 Nishiyabu, R., Kubo, Y., James, T.D., and Fossey, J.S. (2011). *Chem. Commun.* 47: 1106–1123.

112 Hudnall, T.W., Chiu, C.-W., and Gabbaï, F.P. (2009). *Acc. Chem. Res.* 42: 388–397.

113 Izzo, I., Licen, S., Maulucci, N. *et al.* (2008). *Chem. Commun.* 44: 2986–2988.

114 Caballero, A., Zapata, F., White, N.G. *et al.* (2012). *Angew. Chem. Int. Ed.* 51: 1876–1880.

115 Hine, J., Ahn, K., Gallucci, J.C., and Linden, S.M. (1984). *J. Am. Chem. Soc.* 106: 7980–7981.

116 Hine, J., Linden, S.M., and Kanagasabapathy, V.M. (1985). *J. Am. Chem. Soc.* 107: 1082–1083.

117 Hine, J., Linden, S.M., and Kanagasabapathy, V.M. (1985). *J. Org. Chem.* 50: 5096–5099.

118 Errera, J. and Mollet, P. (1936). *Nature* 138: 882–882.

119 Wolf, K.L., Prahm, H., and Harms, H. (1937). *Z. Phys. Chem.* 36B: 237.

120 Sidgwick, N.V. (1927). *Electronic Theory of Valency*. New York: Oxford University Press.

121 Hine, J., Hahn, S., and Miles, D.E. (1986). *J. Org. Chem.* 51: 577–584.

122 Hine, J. and Ahn, K. (1987). *J. Org. Chem.* 52: 2083–2086.

123 Hine, J., Hahn, S., Miles, D.E., and Ahn, K. (1985). *J. Org. Chem.* 50: 5092–5096.

124 Hine, J. and Ahn, K. (1987). *J. Org. Chem.* 52: 2089–2091.

125 Kelly, T.R., Meghani, P., and Ekkundi, V.S. (1990). *Tetrahedron Lett.* 31: 3381–3384.

126 Blake, J.F. and Jorgensen, W.L. (1991). *J. Am. Chem. Soc.* 113: 7430–7432.

127 Blake, J.F., Lim, D., and Jorgensen, W.L. (1994). *J. Org. Chem.* 59: 803–805.

128 Severance, D.L. and Jorgensen, W.L. (1992). *J. Am. Chem. Soc.* 114: 10966–10968.

129 Etter, M.C. and Baures, P.W. (1988). *J. Am. Chem. Soc.* 110: 639–640.

130 Etter, M.C. and Panunto, T.W. (1988). *J. Am. Chem. Soc.* 110: 5896–5897.
131 Etter, M.C. and Reutzel, S.M. (1991). *J. Am. Chem. Soc.* 113: 2586–2598.
132 Dannecker, W. and Kopf, J. (1979). *Acta Cryst.* 8: 429–432.
133 Taylor, R. and Kennard, O. (1982). *J. Am. Chem. Soc.* 104: 5063–5070.
134 Etter, M.C. (1991). *J. Phys. Chem. A* 95: 4601–4610.
135 Smith, P.J., Reddington, M.V., and Wilcox, C.S. (1992). *Tetrahedron Lett.* 33: 6085–6088.
136 Wilcox, C.S., Adrian, J.C. Jr.,, Webb, T.H., and Zawacki, F.J. (1992). *J. Am. Chem. Soc.* 114: 10189–10197.
137 Wilcox, C.S., Kim, E.-i., Romano, D. *et al*. (1995). *Tetrahedron* 51: 621–634.
138 Fan, E., Van Arman, S.A., Kincaid, S., and Hamilton, A.D. (1993). *J. Am. Chem. Soc.* 115: 369–370.
139 Curran, D.P. and Kuo, L.H. (1995). *Tetrahedron Lett.* 36: 6647–6650.
140 Curran, D.P. and Kuo, L.H. (1994). *J. Org. Chem.* 59: 3259–3261.
141 Wittkopp, A. (1997). Wasserstoffbrückenbindungen als dirigierendeWechselwirkung in der organischen Synthese: Thioharnstoffe als Katalysatoren. Diploma Thesis. University of Göttingen, Germany.
142 Kotke, M. and Schreiner, P.R. (2009). (Thio)urea Organocatalysts. In: *Hydrogen Bonding in Organic Synthesis* (ed. P.M. Pihko), 141–351. Weinheim: Wiley VCH.
143 Jakab, G., Tancon, C., Zhang, Z. *et al*. (2012). *Org. Lett.* 14: 1724–1727.
144 Busschaert, N., Karagiannidis, L.E., Wenzel, M. *et al*. (2014). *Chem. Sci.* 5: 1118–1127.
145 Minami, T., Liu, Y., Akdeniz, A. *et al*. (2014). *J. Am. Chem. Soc.* 136: 11396–11401.
146 Gómez, D.E., Fabbrizzi, L., Licchelli, M., and Monzani, E. (2005). *Org. Biomol. Chem.* 3: 1495–1500.
147 Bonizzoni, M., Fabbrizzi, L., Taglietti, A., and Tiengo, F. (2006). *Eur. J. Org. Chem.* 2006: 3567–3574.
148 Jiménez Blanco, J.L., Bootello, P., Benito, J.M. *et al*. (2006). *J. Org. Chem.* 71: 5136–5143.
149 Custelcean, R. (2008). *Chem. Commun.* 44: 295–307.
150 Succaw, G.L., Weakley, T.J.R., Han, F., and Doxsee, K.M. (2005). *Cryst. Growth Des.* 5: 2288–2298.
151 Yonova, P.A. and Stoilkova, G.M. (2004). *J. Plant Growth Regul.* 23: 280–291.
152 Richter, C.P. (1945). *JAMA* 129: 927–931.
153 Bhogala, B.R., Captain, B., Parthasarathy, A., and Ramamurthy, V. (2010). *J. Am. Chem. Soc.* 132: 13434–13442.
154 Harris, K.D.M. (1997). *Chem. Soc. Rev.* 26: 279–289.
155 Harris, K.D.M. (2007). *Supramol. Chem.* 19: 47–53.
156 Wittkopp, A. and Schreiner, P.R. (2000). *The Chemistry of Dienes and Polyenes*, vol. 2. New York: John Wiley & Sons.
157 Wittkopp, A. and Schreiner, P.R. (2003). *Chem. Eur. J.* 9: 407–414.
158 Schreiner, P.R. and Wittkopp, A. (2002). *Org. Lett.* 4: 217–220.
159 Jai-Nhuknan, J., Karipides, A., Hughes, J., and Cantrell, J. (1997). *Acta Crystallogr. C* 53: 455–457.

160 Kotke, M. (2010). Hydrogen-Bonding (Thio)urea Organocatalysts in Organic Synthesis: State of the Art and Practical Methods for Acetalization, Tetrahydropyranylation, and Cooperative Epoxide Alcoholysis. Dissertation, Universitätsbibliothek Gießen (University of Gießen, Germany, published online).
161 Okino, T., Hoashi, Y., and Takemoto, Y. (2003). *J. Am. Chem. Soc.* 125: 12672–12673.
162 Ooi, T., Miki, T., Taniguchi, M. *et al*. (2003). *Angew. Chem. Int. Ed.* 42: 3796–3798.
163 Sohtome, Y., Tanatani, A., Hashimoto, Y., and Nagasawa, K. (2004). *Tetrahedron Lett.* 45: 5589–5592.
164 Herrera, R.P., Sgarzani, V., Bernardi, L., and Ricci, A. (2005). *Angew. Chem. Int. Ed.* 44: 6576–6579.
165 Honjo, T., Sano, S., Shiro, M., and Nagao, Y. (2005). *Angew. Chem. Int. Ed.* 44: 5838–5841.
166 Wang, J., Li, H., Yu, X. *et al*. (2005). *Org. Lett.* 7: 4293–4296.
167 Vakulya, B., Varga, S., Csámpai, A., and Soós, T. (2005). *Org. Lett.* 7: 1967–1969.
168 Lan, Q., Wang, X., and Maruoka, K. (2007). *Tetrahedron Lett.* 48: 4675–4678.
169 Klausen, R.S. and Jacobsen, E.N. (2009). *Org. Lett.* 11: 887–890.
170 Zhang, Z., Lippert, K.M., Hausmann, H. *et al*. (2011). *J. Org. Chem.* 76: 9764–9776.
171 Hayashi, Y., Gotoh, H., Hayashi, T., and Shoji, M. (2005). *Angew. Chem. Int. Ed.* 44: 4212–4215.
172 Marigo, M., Wabnitz, T.C., Fielenbach, D., and Jørgensen, K.A. (2005). *Angew. Chem. Int. Ed.* 44: 794–797.
173 Akiyama, T., Morita, H., Itoh, J., and Fuchibe, K. (2005). *Org. Lett.* 7: 2583–2585.
174 Sigman, M.S. and Jacobsen, E.N. (1998). *J. Am. Chem. Soc.* 120: 4901–4902.
175 Okino, T., Hoashi, Y., Furukawa, T. *et al*. (2005). *J. Am. Chem. Soc.* 127: 119–125.
176 Kotke, M. and Schreiner, P.R. (2006). *Tetrahedron* 62: 434–439.
177 Karimi, B., Hazarkhani, H., and Maleki, J. (2005). *Synthesis*: 279–285.
178 Ranu, B.C., Jana, R., and Samanta, S. (2004). *Adv. Synth. Chem.* 346: 446–450.
179 Mayr, H., Bug, T., Gotta, M.F. *et al*. (2001). *J. Am. Chem. Soc.* 123: 9500–9512.
180 Tantillo, D.J. and Houk, K.N. (2002). *J. Comput. Chem.* 23: 84–95.
181 Pauling, L. (1935). *J. Am. Chem. Soc.* 57: 2680–2684.
182 Kotke, M. and Schreiner, P.R. (2007). *Synthesis* 2007: 779–790.
183 Li, H., Wang, Y., Tang, L., and Deng, L. (2004). *J. Am. Chem. Soc.* 126: 9906–9907.
184 Zuend, S.J. and Jacobsen, E.N. (2009). *J. Am. Chem. Soc.* 131: 15358–15374.
185 Madarász, Á., Dósa, Z., Varga, S. *et al*. (2016). *ACS Catal.* 6: 4379–4387.
186 Bradshaw, G.A., Colgan, A.C., Allen, N.P. *et al*. (2019). *Chem. Sci.* 10: 508–514.
187 Balmond, E.I., Coe, D.M., Galan, M.C., and McGarrigle, E.M. (2012). *Angew. Chem. Int. Ed.* 51: 9152–9155.
188 Rossini, E., Bochevarov, A.D., and Knapp, E.W. (2018). *ACS Omega* 3: 1653–1662.

189 Hrdina, R., Müller, C.E., Wende, R.C. *et al*. (2011). *J. Am. Chem. Soc.* 133: 7624–7627.
190 Lippert, K.M., Hof, K., Gerbig, D. *et al*. (2012). *Eur. J. Org. Chem.* 2012: 5919–5927.
191 Malerich, J.P., Hagihara, K., and Rawal, V.H. (2008). *J. Am. Chem. Soc.* 130: 14416–14417.
192 Alemán, J., Parra, A., Jiang, H., and Jørgensen, K.A. (2011). *Chem. Eur. J.* 17: 6890–6899.
193 Chauhan, P., Mahajan, S., Kaya, U. *et al*. (2015). *Adv. Synth. Chem.* 357: 253–281.
194 Storer, R.I., Aciro, C., and Jones, L.H. (2011). *Chem. Soc. Rev.* 40: 2330–2346.
195 Ni, X., Li, X., Wang, Z., and Cheng, J.-P. (2014). *Org. Lett.* 16: 1786–1789.
196 Prohens, R., Tomàs, S., Morey, J. *et al*. (1998). *Tetrahedron Lett.* 39: 1063–1066.
197 Tomàs, S., Prohens, R., Vega, M. *et al*. (1996). *J. Org. Chem.* 61: 9394–9401.
198 Davis, P.A., Draper, S., M., Dunne, G., and Ashton, P. (1999). *Chem. Commun.* 35: 2265–2266.
199 Quiñonero, D., Prohens, R., Garau, C. *et al*. (2002). *Chem. Phys. Lett.* 351: 115–120.
200 Zhao, B.-L., Li, J.-H., and Du, D.-M. (2017). *Chem. Rec.* 17: 994–1018.
201 Rombola, M., Sumaria, C.S., Montgomery, T.D., and Rawal, V.H. (2017). *J. Am. Chem. Soc.* 139: 5297–5300.
202 Busschaert, N., Elmes, R.B.P., Czech, D.D. *et al*. (2014). *Chem. Sci.* 5: 3617–3626.
203 Elmes, R.B.P., Busschaert, N., Czech, D.D. *et al*. (2015). *Chem. Commun.* 51: 10107–10110.
204 Ho, J., Zwicker, V.E., Yuen, K.K.Y., and Jolliffe, K.A. (2017). *J. Org. Chem.* 82: 10732–10736.
205 Jeppesen, A., Nielsen, B.E., Larsen, D. *et al*. (2017). *Org. Biomol. Chem.* 15: 2784–2790.
206 Zwicker, V.E., Yuen, K.K.Y., Smith, D.G. *et al*. (2018). *Chem. Eur. J.* 24: 1140–1150.
207 Kumler, W.D. (1935). *J. Am. Chem. Soc.* 57: 600–605.
208 Li, Y. and Flood, A.H. (2008). *Angew. Chem. Int. Ed.* 47: 2649–2652.
209 Sutor, D.J. (1960). *Nature* 188: 47–48.
210 Sutor, D.J. (1963). *Acta Crystallogr. A* 16: 97–104.
211 Sutor, D.J. (1963). *J. Chem. Soc.*: 1105–1110.
212 Zhu, S.S., Staats, H., Brandhorst, K. *et al*. (2008). *Angew. Chem. Int. Ed.* 47: 788–792.
213 Li, Y. and Flood, A.H. (2008). *J. Am. Chem. Soc.* 130: 12111–12122.
214 Juwarker, H., Lenhardt, J.M., Pham, D.M., and Craig, S.L. (2008). *Angew. Chem. Int. Ed.* 47: 3740–3743.
215 Meudtner, R.M. and Hecht, S. (2008). *Angew. Chem. Int. Ed.* 47: 4926–4930.
216 Yoon, D.-W., Gross, D.E., Lynch, V.M. *et al*. (2008). *Angew. Chem. Int. Ed.* 47: 5038–5042.
217 Maeda, H., Mihashi, Y., and Haketa, Y. (2008). *Org. Lett.* 10: 3179–3182.

218 Berryman, O.B., Sather, A.C., Hay, B.P. *et al*. (2008). *J. Am. Chem. Soc.* 130: 10895–10897.
219 Nishio, M., Umezawa, Y., Fantini, J. *et al*. (2014). *Phys. Chem. Chem. Phys.* 16: 12648–12683.
220 Desiraju, G.R. (1996). *Acc. Chem. Res.* 29: 441–449.
221 Nishio, M., Umezawa, Y., Hirota, M., and Takeuchi, Y. (1995). *Tetrahedron* 51: 8665–8701.
222 Nishio, M. (2004). *CrystEngComm* 6: 130–158.
223 Nishio, M., Umezawa, Y., Honda, K. *et al*. (2009). *CrystEngComm* 11: 1757–1788.
224 Takahashi, O., Kohno, Y., and Nishio, M. (2010). *Chem. Rev.* 110: 6049–6076.
225 Nishio, M. (2011). *Phys. Chem. Chem. Phys.* 13: 13873–13900.
226 Hua, Y. and Flood, A.H. (2010). *Chem. Soc. Rev.* 39: 1262–1271.
227 McDonald, K.P., Hua, Y., Lee, S., and Flood, A.H. (2012). *Chem. Commun.* 48: 5065–5075.
228 Zurro, M. and García Mancheño, O. (2017). *Chem. Rec.* 17: 485–498.
229 Beckendorf, S., Asmus, S., Mück-Lichtenfeld, C., and García Mancheño, O. (2013). *Chem. Eur. J.* 19: 1581–1585.
230 Asmus, S., Beckendorf, S., Zurro, M. *et al*. (2014). *Chem. Asian J.* 9: 2178–2186.
231 Zurro, M., Asmus, S., Beckendorf, S. *et al*. (2014). *J. Am. Chem. Soc.* 136: 13999–14002.
232 García Mancheño, O., Asmus, S., Zurro, M., and Fischer, T. (2015). *Angew. Chem. Int. Ed.* 54: 8823–8827.
233 Fischer, T., Bamberger, J., and García Mancheño, O. (2016). *Org. Biomol. Chem.* 14: 5794–5802.
234 Fischer, T., Duong, Q.-N., and García Mancheño, O. (2017). *Chem. Eur. J.* 23: 5983–5987.
235 Duong, Q.-N., Schifferer, L., and García Mancheño, O. (2019). *Eur. J. Org. Chem.* 2019: 5452–5461.
236 Zurro, M., Asmus, S., Bamberger, J. *et al*. (2016). *Chem. Eur. J.* 22: 3785–3793.
237 Fischer, T., Bamberger, J., Gómez-Martínez, M. *et al*. (2019). *Angew. Chem. Int. Ed.* 58: 3217–3221.
238 Eichstaedt, K., Jaramillo-Garcia, J., Leigh, D.A. *et al*. (2017). *J. Am. Chem. Soc.* 139: 9376–9381.
239 Dorel, R. and Feringa, B.L. (2020). *Angew. Chem. Int. Ed.* 59: 785–789.
240 Koumura, N., Zijlstra, R.W.J., van Delden, R.A. *et al*. (1999). *Nature* 401: 152–155.
241 Lehnherr, D., Ford, D.D., Bendelsmith, A.J. *et al*. (2016). *Org. Lett.* 18: 3214–3217.
242 Reisman, S.E., Doyle, A.G., and Jacobsen, E.N. (2008). *J. Am. Chem. Soc.* 130: 7198–7199.
243 Wang, H., Wang, W., and Jin, W.J. (2016). *Chem. Rev.* 116: 5072–5104.
244 Colin, M. (1814). *Ann. Chim.* 91: 252–272.
245 Bineau, M.A. (1844). *C. R. Acad. Sci.* 55: 762–767.
246 Guthrie, F. (1863). *J. Am. Chem. Soc.* 16: 239–244.

247 Mulliken, R.S. (1950). *J. Am. Chem. Soc.* 72: 600–608.
248 Mulliken, R.S. (1952). *J. Phys. Chem. A* 56: 801–822.
249 Benesi, H.A. and Hildebrand, J.H. (1949). *J. Am. Chem. Soc.* 71: 2703–2707.
250 Hassel, O. and Hvoslef, J. (1954). *Acta Chem. Scand.* 8: 873–873.
251 Hassel, O. and Stromme, K. (1958). *Acta Chem. Scand.* 12: 1146–1147.
252 Hassel, O. and Stromme, K. (1959). *Acta Chem. Scand.* 13: 1781–1786.
253 Hassel, O. and Strømme, K. (1959). *Acta Chem. Scand.* 13: 275–280.
254 Hassel, O. and Rømming, C. (1962). *Q. Rev. Chem. Soc.* 16: 1–18.
255 Paolo, T.D. and Sandorfy, C. (1974). *Can. J. Chem.* 52: 3612–3622.
256 Dumas, J.M., Peurichard, H., and Gomel, M. (1978). *J. Chem. Res.*: 54–55.
257 Dumas, J.M., Gomel, M., and Guerin, M. (1983). Molecular Interactions Involving Organic Halides. In: *Halides, Pseudo-Halides and Azides* (eds. S. Patai and Z. Rappoport), 985–1020. Weinheim: Wiley VCH.
258 Lim, J.Y.C. and Beer, P.D. (2018). *Chem* 4: 731–783.
259 Clark, T. (2013). *WIREs Comput. Mol. Sci.* 3: 13–20.
260 Bauzá, A. and Frontera, A. (2015). *Angew. Chem. Int. Ed.* 54: 7340–7343.
261 Scholfield, M.R., Zanden, C.M.V., Carter, M., and Ho, P.S. (2013). *Protein Sci.* 22: 139–152.
262 Politzer, P., Lane, P., Concha, M.C. *et al*. (2007). *J. Mol. Model.* 13: 305–311.
263 Politzer, P. and Murray, J.S. (2013). *ChemPhysChem* 14: 278–294.
264 Erdélyi, M. (2012). *Chem. Soc. Rev.* 41: 3547–3557.
265 Wolters, L.P., Schyman, P., Pavan, M.J. *et al*. (2014). *WIREs Comput. Mol. Sci.* 4: 523–540.
266 Beale, T.M., Chudzinski, M.G., Sarwar, M.G., and Taylor, M.S. (2013). *Chem. Soc. Rev.* 42: 1667–1680.
267 Metrangolo, P., Neukirch, H., Pilati, T., and Resnati, G. (2005). *Acc. Chem. Res.* 38: 386–395.
268 Clark, T., Hennemann, M., Murray, J.S., and Politzer, P. (2007). *J. Mol. Model.* 13: 291–296.
269 Clark, T. (2017). *Faraday Discuss.* 203: 9–27.
270 Politzer, P., Murray, J.S., Clark, T., and Resnati, G. (2017). *Phys. Chem. Chem. Phys.* 19: 32166–32178.
271 Breugst, M. and Koenig, J.J. (2020). *Eur. J. Org. Chem.* 2020: 5473–5487.
272 Walter, S.M., Kniep, F., Herdtweck, E., and Huber, S.M. (2011). *Angew. Chem. Int. Ed.* 50: 7187–7191.
273 Walter, S.M., Kniep, F., Rout, L. *et al*. (2012). *J. Am. Chem. Soc.* 134: 8507–8512.
274 Kniep, F., Jungbauer, S.H., Zhang, Q. *et al*. (2013). *Angew. Chem. Int. Ed.* 52: 7028–7032.
275 Schottel, B.L., Chifotides, H.T., and Dunbar, K.R. (2008). *Chem. Soc. Rev.* 37: 68–83.
276 Frontera, A., Gamez, P., Mascal, M. *et al*. (2011). *Angew. Chem. Int. Ed.* 50: 9564–9583.
277 Frontera, A., Quiñonero, D., and Deyà, P.M. (2011). *WIREs Comput. Mol. Sci.* 1: 440–459.

278 Quiñonero, D., Garau, C., Rotger, C. *et al*. (2002). *Angew. Chem. Int. Ed.* 41: 3389–3392.
279 Alkorta, I., Rozas, I., and Elguero, J. (2002). *J. Am. Chem. Soc.* 124: 8593–8598.
280 Mascal, M., Armstrong, A., and Bartberger, M.D. (2002). *J. Am. Chem. Soc.* 124: 6274–6276.
281 Zhao, Y., Domoto, Y., Orentas, E. *et al*. (2013). *Angew. Chem. Int. Ed.* 52: 9940–9943.
282 Zhao, Y., Beuchat, C., Domoto, Y. *et al*. (2014). *J. Am. Chem. Soc.* 136: 2101–2111.
283 Lu, T. and Wheeler, S.E. (2014). *Org. Lett.* 16: 3268–3271.
284 Zhao, Y., Cotelle, Y., Liu, L. *et al*. (2018). *Acc. Chem. Res.* 51: 2255–2263.
285 Neel, A.J., Hilton, M.J., Sigman, M.S., and Toste, F.D. (2017). *Nature* 543: 637–646.
286 Berkessel, A., Das, S., Pekel, D., and Neudörfl, J.-M. (2014). *Angew. Chem. Int. Ed.* 53: 11660–11664.
287 Schafer, A.G., Wieting, J.M., Fisher, T.J., and Mattson, A.E. (2013). *Angew. Chem. Int. Ed.* 52: 11321–11324.
288 Wieting, J.M., Fisher, T.J., Schafer, A.G. *et al*. (2015). *Eur. J. Org. Chem.* 2015: 525–533.
289 Attard, J.W., Osawa, K., Guan, Y. *et al*. (2019). *Synthesis* 51: 2107–2115.
290 Borovika, A., Tang, P.-I., Klapman, S., and Nagorny, P. (2013). *Angew. Chem. Int. Ed.* 52: 13424–13428.
291 Weil, T., Kotke, M., Kleiner, C.M., and Schreiner, P.R. (2008). *Org. Lett.* 10: 1513–1516.
292 Lee, J.H., Kim, W.H., and Danishefsky, S.J. (2010). *Tetrahedron Lett.* 51: 1252–1253.
293 Wöhler, F. and v. Liebig, J. (1832). *Liebigs Ann.* 3: 249–282.
294 Langenbeck, W. (1927). *Ber. Dtsch. Chem. Ges.* 60: 930–934.
295 Langenbeck, W. (1928). *Angew. Chem.* 41: 740–745.
296 Langenbeck, W. (1929). *Liebigs Ann.* 469: 16–25.
297 Langenbeck, W. (1932). *Angew. Chem.* 45: 97–99.
298 Langenbeck, W. (1949). *Die organischen Katalysatoren und ihre Beziehungen zu den Fermenten (Organic Catalysts and their Relation to the Enzymes)*. Berlin: Springer.
299 Langenbeck, W. (1958). *Tetrahedron* 3: 185–196.
300 v. Liebig, J. (1860). *Liebigs Ann.* 113: 246–247.
301 v. Liebig, J. (1870). *Liebigs Ann.* 153: 1–47.
302 Seebach, D. (1990). *Angew. Chem. Int. Ed.* 29: 1320–1367.
303 Morrill, L.A., Susick, R.B., Chari, J.V., and Garg, N.K. (2019). *J. Am. Chem. Soc.* 141: 12423–12443.
304 Simons, J.P. (1987). *J. Phys. Chem. A* 91: 5378–5387.
305 Aldegunde, J., de Miranda, M.P., Haigh, J.M. *et al*. (2005). *J. Phys. Chem. A* 109: 6200–6217.
306 Zhan, C.-G., Bentley, J., and Chipman, D.M. (1998). *J. Chem. Phys.* 108: 177–192.

307 Ostwald, W. (1894). *Z. Phys. Chem.* 15: 705–707.
308 Roberts, M.W. (2000). *Catal. Lett.* 67: 1–4.
309 Palmer, T. and Bonner, P.L. (2011). The Chemical Nature of Enzyme Catalysis. In: *Enzymes*, 2e (eds. T. Palmer and P. L. Bonner), 189–221. Sawston: Horwood Publishing Ltd.
310 List, B. (2007). *Chem. Rev.* 107: 5413–5883. special issue on organocatalysis.
311 Abbasov, M.E. and Romo, D. (2014). *Nat. Prod. Rep.* 31: 1318–1327.
312 Wende, R.C. and Schreiner, P.R. (2012). *Green Chem.* 14: 1821–1849.
313 Seayad, J. and List, B. (2005). *Org. Biomol. Chem.* 3: 719–724.
314 Berkessel, A. and Gröger, H. (2006). *Asymmetric Organocatalysis: From Biomimetic Concepts to Applications in Asymmetric Synthesis*. Weinheim: Wiley VCH.
315 Marcia de Figueiredo, R. and Christmann, M. (2007). *Eur. J. Org. Chem.* 2007: 2575–2600.
316 Marqués-López, E., Herrera, R.P., and Christmann, M. (2010). *Nat. Prod. Rep.* 27: 1138–1167.
317 MacMillan, D.W.C. (2008). *Nature* 455: 304–308.
318 Dalko, P.I. and Moisan, L. (2001). *Angew. Chem. Int. Ed.* 40: 3726–3748.
319 Dalko, P.I. and Moisan, L. (2004). *Angew. Chem. Int. Ed.* 43: 5138–5175.
320 Szwarc, M. (1969). *Acc. Chem. Res.* 2: 87–96.
321 Bjerrum, N. (1926). *K. Dan. Vidensk. Selsk. Mat.-Fys. Medd.* 7: 3–48.
322 Anslyn, E.V. and Dougherty, D.A. (2006). *Modern Physical Organic Chemistry*. Sausalito: University Science Books.
323 Einstein, A. (1905). *Ann. Phys.* 322: 549–560.
324 Marcus, Y. (1985). Solvation of Ion Pairs. In: *Ion Solvation* (ed. Y. Marcus), 218–244. Chichester: Wiley.
325 Marcus, Y. and Hefter, G. (2006). *Chem. Rev.* 106: 4585–4621.
326 Sadek, H. and Fuoss, R.M. (1954). *J. Am. Chem. Soc.* 76: 5897–5901.
327 Winstein, S., Clippinger, E., Fainberg, A.H., and Robinson, G.C. (1954). *J. Am. Chem. Soc.* 76: 2597–2598.
328 Erkkilä, A., Majander, I., and Pihko, P.M. (2007). *Chem. Rev.* 107: 5416–5470.
329 Huang, Y., Walji, A.M., Larsen, C.H., and MacMillan, D.W.C. (2005). *J. Am. Chem. Soc.* 127: 15051–15053.
330 Yamashita, Y., Yasukawa, T., Yoo, W.-J. *et al*. (2018). *Chem. Soc. Rev.* 47: 4388–4480.
331 Romea, P. and Urpi, F. (2013). Stereoselective Acetate Aldol Reactions. In: *Modern Methods in Stereoselective Aldol Reactions* (ed. R. Mahrwald), 1–81. Weinheim: Wiley-VCH.
332 Mayer, S. and List, B. (2006). *Angew. Chem. Int. Ed.* 45: 4193–4195.
333 Corey, E.J. and Grogan, M.J. (1999). *Org. Lett.* 1: 157–160.
334 Li, J., Jiang, W.-Y., Han, K.-L. *et al*. (2003). *J. Org. Chem.* 68: 8786–8789.
335 Goerigk, L., Kruse, H., and Grimme, S. (2011). *ChemPhysChem* 12: 3421–3433.
336 Wagner, J.P. and Schreiner, P.R. (2015). *Angew. Chem. Int. Ed.* 54: 12274–12296.
337 Birrell, J.A., Desrosiers, J.-N., and Jacobsen, E.N. (2011). *J. Am. Chem. Soc.* 133: 13872–13875.

338 Taylor, M.S. and Jacobsen, E.N. (2004). *J. Am. Chem. Soc.* 126: 10558–10559.
339 Knowles, R.R., Lin, S., and Jacobsen, E.N. (2010). *J. Am. Chem. Soc.* 132: 5030–5032.
340 Kutateladze, D.A., Strassfeld, D.A., and Jacobsen, E.N. (2020). *J. Am. Chem. Soc.* 142: 6951–6956.
341 Seidel, D. (2014). *Synlett* 25: 783–794.
342 De, C.K., Klauber, E.G., and Seidel, D. (2009). *J. Am. Chem. Soc.* 131: 17060–17061.
343 De, C.K., Mittal, N., and Seidel, D. (2011). *J. Am. Chem. Soc.* 133: 16802–16805.
344 Banik, S.M., Levina, A., Hyde, A.M., and Jacobsen, E.N. (2017). *Science* 358: 761–764.
345 Wendlandt, A.E., Vangal, P., and Jacobsen, E.N. (2018). *Nature* 556: 447–451.
346 Pupo, G., Ibba, F., Ascough, D.M.H. *et al.* (2018). *Science* 360: 638–642.
347 Roagna, G., Ascough, D.M.H., Ibba, F. *et al.* (2020). *J. Am. Chem. Soc.* 142: 14045–14051.
348 Pupo, G., Vicini, A.C., Ascough, D.M.H. *et al.* (2019). *J. Am. Chem. Soc.* 141: 2878–2883.
349 Sigman, M.S., Vachal, P., and Jacobsen, E.N. (2000). *Angew. Chem. Int. Ed.* 39: 1279–1281.
350 HCN was generated by the method of Ziegler. Alternatively, generation of HCN in situ by reaction of TMSCN and MeOH afforded identical results: Ziegler, K. (1932). In: *Organic Syntheses Collective*, Volume 1 (eds. H. Gilman and H. Blatt), p. 314. New York: Wiley
351 Vachal, P. and Jacobsen, E.N. (2002). *J. Am. Chem. Soc.* 124: 10012–10014.
352 Wittkopp, A. (2001). Organokatalyse von Diels–Alder-Reaktionen durch neutrale Wasserstoffbrückendonoren in organischen und wässrigen Lösungsmitteln. Dissertation, University of Göttingen, Germany, published online (Germany).
353 Tárkányi, G., Király, P., Varga, S. *et al.* (2008). *Chem. Eur. J.* 14: 6078–6086.
354 Oh, S.H., Rho, H.S., Lee, J.W. *et al.* (2008). *Angew. Chem. Int. Ed.* 47: 7872–7875.
355 Zuend, S.J., Coughlin, M.P., Lalonde, M.P., and Jacobsen, E.N. (2009). *Nature* 461: 968–970.
356 Wadhwa, P., Kharbanda, A., and Sharma, A. (2018). *Asian J. Org. Chem.* 7: 634–661.
357 Enders, D., Lüttgen, K., and Narine, A.A. (2007). *Synthesis* 2007: 959–980.
358 Enders, D., Wang, C., and Liebich, J.X. (2009). *Chem. Eur. J.* 15: 11058–11076.
359 Zhu, R., Zhang, D., Wu, J., and Liu, C. (2006). *Tetrahedron: Asymmetry* 17: 1611–1616.
360 Hoashi, Y., Yabuta, T., and Takemoto, Y. (2004). *Tetrahedron Lett.* 45: 9185–9188.
361 Hoashi, Y., Yabuta, T., Yuan, P. *et al.* (2006). *Tetrahedron* 62: 365–374.
362 Takemoto, Y. (2010). *Chem. Pharm. Bull.* 58: 593–601.
363 An overview of numerous application is discussed in Kotke, M., Schreiner, P. R. (2009). (Thio)urea Organocatalysts. In: *Hydrogen Bonding in Organic Synthesis* (ed. P. M. Pihko), 141–351. Weinheim: Wiley VCH.

364 Hamza, A., Schubert, G., Soós, T., and Pápai, I. (2006). *J. Am. Chem. Soc.* 128: 13151–13160.
365 Izzo, J.A., Myshchuk, Y., Hirschi, J.S., and Vetticatt, M.J. (2019). *Org. Biomol. Chem.* 17: 3934–3939.
366 Tan, B., Lu, Y., Zeng, X. *et al*. (2010). *Org. Lett.* 12: 2682–2685.
367 Nishizawa, S., Bühlmann, P., Iwao, M., and Umezawa, Y. (1995). *Tetrahedron Lett.* 36: 6483–6486.
368 Wenzel, A.G. and Jacobsen, E.N. (2002). *J. Am. Chem. Soc.* 124: 12964–12965.
369 Bentley, K.W. (2004). *Nat. Prod. Rep.* 21: 395–424.
370 Bentley, K.W. (2006). *Nat. Prod. Rep.* 23: 444–463.
371 Taylor, M.S., Tokunaga, N., and Jacobsen, E.N. (2005). *Angew. Chem. Int. Ed.* 44: 6700–6704.
372 Bose, A.K., Spiegelman, G., and Manhas, M.S. (1971). *Tetrahedron Lett.* 12: 3167–3170.
373 Raheem, I.T., Thiara, P.S., Peterson, E.A., and Jacobsen, E.N. (2007). *J. Am. Chem. Soc.* 129: 13404–13405.
374 Dijkink, J. and Speckamp, W.N. (1977). *Tetrahedron Lett.* 18: 935–938.
375 Dijkink, J. and Speckamp, W.N. (1978). *Tetrahedron* 34: 173–178.
376 Ford, D.D., Lehnherr, D., Kennedy, C.R., and Jacobsen, E.N. (2016). *J. Am. Chem. Soc.* 138: 7860–7863.
377 Ford, D.D., Lehnherr, D., Kennedy, C.R., and Jacobsen, E.N. (2016). *ACS Catal.* 6: 4616–4620.
378 Kennedy, C.R., Lehnherr, D., Rajapaksa, N.S. *et al*. (2016). *J. Am. Chem. Soc.* 138: 13525–13528.
379 Park, Y., Harper, K.C., Kuhl, N. *et al*. (2017). *Science* 355: 162–166.
380 Lairson, L.L., Henrissat, B., Davies, G.J., and Withers, S.G. (2008). *Annu. Rev. Biochem.* 77: 521–555.
381 Nigudkar, S.S. and Demchenko, A.V. (2015). *Chem. Sci.* 6: 2687–2704.
382 Albert, J.S. and Hamilton, A.D. (1993). *Tetrahedron Lett.* 34: 7363–7366.
383 Kelly, T.R. and Kim, M.H. (1994). *J. Am. Chem. Soc.* 116: 7072–7080.
384 Boiocchi, M., Del Boca, L., Gómez, D.E. *et al*. (2004). *J. Am. Chem. Soc.* 126: 16507–16514.
385 Amendola, V., Esteban-Gómez, D., Fabbrizzi, L., and Licchelli, M. (2006). *Acc. Chem. Res.* 39: 343–353.
386 Lee, Y., Klausen, R.S., and Jacobsen, E.N. (2011). *Org. Lett.* 13: 5564–5567.
387 Klausen, R.S., Kennedy, C.R., Hyde, A.M., and Jacobsen, E.N. (2017). *J. Am. Chem. Soc.* 139: 12299–12309.
388 Burns, N.Z., Witten, M.R., and Jacobsen, E.N. (2011). *J. Am. Chem. Soc.* 133: 14578–14581.
389 Klauber, E.G., De, C.K., Shah, T.K., and Seidel, D. (2010). *J. Am. Chem. Soc.* 132: 13624–13626.
390 Klauber, E.G., Mittal, N., Shah, T.K., and Seidel, D. (2011). *Org. Lett.* 13: 2464–2467.
391 Min, C., Mittal, N., De, C.K., and Seidel, D. (2012). *Chem. Commun.* 48: 10853–10855.
392 Mittal, N., Sun, D.X., and Seidel, D. (2012). *Org. Lett.* 14: 3084–3087.

393 Mittal, N., Lippert, K.M., De, C.K. *et al.* (2015). *J. Am. Chem. Soc.* 137: 5748–5758.

394 Lutz, V., Glatthaar, J., Würtele, C. *et al.* (2009). *Chem. Eur. J.* 15: 8548–8557.

395 Wang, Z.-X., Tu, Y., Frohn, M. *et al.* (1997). *J. Am. Chem. Soc.* 119: 11224–11235.

396 Kagan, H. and Fiaud, J. (1988). *Top. Stereochem.* 18: 21.

397 Müller, K., Faeh, C., and Diederich, F. (2007). *Science* 317: 1881–1886.

398 Purser, S., Moore, P.R., Swallow, S., and Gouverneur, V. (2008). *Chem. Soc. Rev.* 37: 320–330.

399 Ojima, I. (2009). *Fluorine in Medicinal Chemistry and Chemical Biology*. New York: John Wiley & Sons.

400 Gouverneur, V. and Müller, K. (2012). *Fluorine in Pharmaceutical and Medicinal Chemistry: From Biophysical Aspects to Clinical Applications*. Singapur: World Scientific.

401 Jeschke, P. (2004). *ChemBioChem* 5: 570–589.

402 Gillis, E.P., Eastman, K.J., Hill, M.D. *et al.* (2015). *J. Med. Chem.* 58: 8315–8359.

403 Nelson, A. (1999). *Angew. Chem. Int. Ed.* 38: 1583–1585.

404 Ooi, T. and Maruoka, K. (2007). *Angew. Chem. Int. Ed.* 46: 4222–4266.

405 Maruoka, K. (2008). *Asymmetric Phase Transfer Catalysis*. Weinheim: Wiley VCH.

406 Esteban-Gómez, D., Fabbrizzi, L., and Licchelli, M. (2005). *J. Org. Chem.* 70: 5717–5720.

407 Jose, D.A., Kumar, D.K., Ganguly, B., and Das, A. (2004). *Org. Lett.* 6: 3445–3448.

408 Pfeifer, L., Engle, K.M., Pidgeon, G.W. *et al.* (2016). *J. Am. Chem. Soc.* 138: 13314–13325.

409 Yang, X., Wu, T., Phipps, R.J., and Toste, F.D. (2015). *Chem. Rev.* 115: 826–870.

410 Auria-Luna, F., Mohammadi, S., Divar, M. *et al.* (2020). *Adv. Synth. Chem.* 362: 5275–5300.

411 Nyffeler, P.T., Durón, S.G., Burkart, M.D. *et al.* (2005). *Angew. Chem. Int. Ed.* 44: 192–212.

412 Wang, X., Lan, Q., Shirakawa, S., and Maruoka, K. (2010). *Chem. Commun.* 46: 321–323.

413 Rauniyar, V., Lackner, A.D., Hamilton, G.L., and Toste, F.D. (2011). *Science* 334: 1681–1684.

414 O'Hagan, D., Schaffrath, C., Cobb, S.L. *et al.* (2002). *Nature* 416: 279–279.

415 Zhu, X., Robinson, D.A., McEwan, A.R. *et al.* (2007). *J. Am. Chem. Soc.* 129: 14597–14604.

416 O'Hagan, D. and Deng, H. (2015). *Chem. Rev.* 115: 634–649.

417 Morgenthaler, M., Schweizer, E., Hoffmann-Röder, A. *et al.* (2007). *ChemMedChem* 2: 1100–1115.

418 Briggs, C.R.S., O'Hagan, D., Howard, J.A.K., and Yufit, D.S. (2003). *J. Fluor. Chem.* 119: 9–13.

419 Sofia, M.J., Bao, D., Chang, W. *et al.* (2010). *J. Med. Chem.* 53: 7202–7218.

420 Sato, K., Hoshino, K., Tanaka, M. *et al.* (1992). *Antimicrob. Agents Chemother.* 36: 1491–1498.